University of Szeged
Faculty of Pharmacy
Department of Pharmaceutical Technology
Head: Prof. Dr. Habil. Piroska Szabó-Révész D.Sc.

Ph.D. Thesis

Preparation and investigation of cross-linked hyaluronic acid nanoparticle systems

By
Mónika Maroda

Supervisor:
Dr. Erzsébet Csányi Ph.D.

Szeged
2013

CONTENTS

LIST OF PUBLICATIONS

I. M. Maroda, M. Bodnár, Sz. Berkó, J. Bakó, G. Erős, E. Csányi, P. Szabó- Révész, JF. Hartmann, L. Kemény, J. Borbély: Preparation and investigation of a cross-linked hyaluronan nanoparticles system. Carbohydr. Polymer (2011); 83: 1322-1329.
IF: 3.628

II. Csizmazia E., Berkó Sz., Maroda M., Szabó-Révész P., Csányi E.: A bőrön keresztüli hatóanyag permeáció modellezése és penetrációfokozók hatásának vizsgálata. Acta Pharmaceutica Hungarica (2012); 82: 15-22.
IF: -

III. Sz. Berkó, M. Maroda; M. Bodnár, G. Erős, P. Hartmann, K. Szentner; P. Szabó-Révész, L. Kemény, J. Borbély, E. Csányi: Advantages of cross-linked versus linear hyaluronic acid for semisolid skin delivery systems Eur. Polym. J. (2013), 49: 2511-2517
IF: 2.739

ABBREVIATIONS

API	active pharmaceutical ingredient
CDI	(dimethylamino)propyl-3-ethylcarbodiimide methiodide
CLHA	cross-linked hyaluronic acid
DLS	dynamic light scattering
GPC	gel permeation chromatography
HA	hyaluronic acid
HD	hydrodynamic diameter
NDP	number distribution profile
NMR	nuclear magnetic resonance
PBS	phosphate-buffered saline solution
PSD	particle size distribution
SC	stratum corneum
TEM	transmission electron microscopy
TEWL	transepidermal water loss

1 Introduction

Nanoparticles and nanomedicines are increasingly applied in the manufacture of pharmaceuticals and cosmetic products. Nanocarrier-based nanomedicines are comprised of polymers, liposomes, dendrimers, quantum dots, nanotubes and their combinations. These systems form the basis for the introduction of personalized medicine and are powerful tools for the detection of diseases and diagnoses coupled with highly-effective targeted therapy.
Some major biopolymers are also used in medicine, such as alginic acid, hyaluronic acid (HA), chitosan and polyglutamic acid, and nanosystems prepared from these biopolymers. Biopolymers are characterized by favourable biological properties, pharmaceutical technology and nanotechnological applications. The applied and intended pharmaceutical formulations will be described. One of the challenging aims of research at present is to achieve targeted drug delivery with minimum side-effects. The physical, chemical and pharmacokinetic properties of the active pharmaceutical ingredient can be changed through the use of nanotechnology. Combination therapy can be developed with nanotechnology systems. Nanotechnology is able to wrap up giant molecules via the covalent cross-linking of valuable groups. Certain nanoparticles are below 100 nm size and their original properties are not lost. The body does not handle them as foreign molecules and the nanomolecules display self-organizing ability to enhance stable and effective use.
This work describes and discusses the successful preparation and characterization of stable nanoparticulate systems based on HA. The effects of the concentration of the HA, the cross-linking ratio and the applied medium were investigated. A stable cross-linked HA-based nanoparticulate semisolid preparation was also investigated in comparison with a hydrogel containing linear HA.

1.1 Nanoparticles

Nanoscience is a rapidly developing field of science, and increasing attention is being devoted to nanomaterials and nanotechnology. Different areas of our lives have been greatly affected by achievements made by nanomaterials scientific research, e.g. information technology, medicine, the pharmaceutical and the food industry.

There is no general international definition of a nanoparticle. A few decades ago, particles in the colloidal size range (1-500 nm) were called nanoparticles. Nowadays, particles are referred to as nanoparticles if at least one of their dimensions is below 100 nm. Novel properties of nanoparticles are observed under a critical size of about 100 nm. Differences between nano- and not nanoparticles are not well defined.

Richard Feynman predicted the future of nanotechnology in 1959. Since then a number of nanomaterials have been developed for medical use, and have been used for detection, and prevention purposes, and also applied successfully in oncology [1, 2].

The fundamental aims of biopolymer research are to develop nanosystems suitable for use for targeted drug and gene delivery, controlled drug release or tissue regeneration.

1.2 Hyaluronic acid (HA) and hyaluronic acid derivatives

HA, also known as hyaluronan, is a non-sulfated glycosaminoglycan comprising a long unbranched linear polysaccharide consisting of repeating disaccharide units. This negatively charged, high-molecular weight polysaccharide is found in all tissues and body fluids of superior animals and most abundantly in the soft connective tissues. The total amount in an adult human has been estimated to be 11–17 g [3]. A nanofibrous HA scaffold has been successfully fabricated to mimic the architecture of the natural extracellular matrix [4, 5].

HA occurs *in vivo* primarily as the sodium salt. The acid form is unstable, and it is usually extracted and refined as the sodium salt. It is a biodegradable, biocompatible, non-toxic, non-immunogenic and non-inflammatory substance, which has been used for various medical applications.

It is a pharmaceutical raw material used as an excipient and an active agent. It can be applied as an active agent in dermal semi-solid dosage forms, ophthalmic preparation and injections.

The excellent water-holding capacity of HA makes it capable of retaining moisture in the eyes, joints and skin tissues [6]. The solution of the sodium salt is highly viscous, with unique viscoelastic properties, which enable its use in orthopaedics [7]. Many studies have been conducted with HA in injectable form [8], administered to treat osteoarthritis of the knee [9]. Ophthalmology mainly uses it as eye solutions and drops [10]. The oral use of HA has recently been suggested, although its effectiveness needs to be demonstrated. HA is a potential biodegradable carrier that has also been investigated as a transdermal drug delivery system [11]. Slightly modified HA derivatives have been used for the target-specific

intracellular delivery of nucleotide therapeutics, and highly modified HA derivatives have been utilized for the long-acting conjugation of peptide and protein therapeutics. HA has also been used as a novel depot system [12] in the forms of physically and chemically cross-linked hydrogels [13, 14, 15] or nano- and micro- particulate systems [16, 17] for the delivery of various proteins and drugs [18], peptides [19] or genes [20, 21].

1.3 Hyaluronic acid conjugates (cross-linked or modified)

Various methods have been developed for the production of cross-linked HA (CLHA) systems for potential use in hydrogels [22, 23], films [24, 25] or particulate systems [26]. Several attempts have also been made to produce CLHA particles through a carbodiimide (CDI) technique in aqueous medium [12, 16, 27,]. As an alternative to HA conjugation onto particles, some authors have described the synthesis of HA derivatives as particles or other drug delivery systems themselves, e.g. HA modification with hydrophobic 5-cholanic acid via an aminoethyl-amide linker in dimethylformamide [28]. The resulting amphiphilic derivative formed nanoparticles under physiological conditions and exhibited prolonged blood circulation and a high affinity for tumour cells *in vitro*. These nanoparticles are therefore promising drug carriers for tumour-targeted drugs. HA nanogels have been developed for siRNA delivery [20]. Thiol–HA was first prepared by using the CDI method with cystamine, followed by dithiothreitol treatment to cleave the disulfide bonds. CLHA nanogels were then generated by an inverse emulsion method from the thiol–HA solution containing siRNA, during which the disulfide bonds were formed. The encapsulation method induced no damage to the siRNA and the uptake by CD44-expressing cells. Microspheres prepared from HA esters, obtained using alkyl halides, have been used as drug delivery systems for drugs such as hydrocortisone [29]. It was observed that hydrocortisone was released faster when encapsulated into HA microspheres than when covalently conjugated to HA. Microspheres were formed from HA esters by using either spray-drying or inverse emulsion technology. [30]. In the former case, the drug was dissolved in a solution containing HA and spray-dried. In the latter case, a water-in-oil emulsion was formed containing the HA and drug solution in the water droplets emulsified in oil with a surfactant (sorbitan trioleate, Span® 85) and further centrifuged to isolate the HA microspheres. A process of making HA microspheres by using inverse emulsification was patented [31]. Later, the preparation of HA microspheres was

reported by using CDI and adipic hydrazide combined with the inverse emulsion method [32]. Plasmid DNA was incorporated into the microspheres when mixed into the HA solution prior to the addition of the cross-linking reagents. The microspheres obtained were shown to deliver structurally intact plasmid DNA and to transfect cells *in vitro* and *in vivo*.

CDI CLHA hydrogels were recently reported for potential use as cell sheet delivery systems [33]. Better ocular biocompatibility was displayed in comparison with that of HA discs cross-linked with glutaraldehyde. This appears to be a promising approach since cell sheet engineering is an emerging technique for tissue regeneration. The preparation of drug-loaded CLHA films has been reported for the sustained release of drugs at wound sites [34].The formation of HA composites has also been reported by covalently linking HA to other polymers, such as carboxymethylcellulose [35], poly(vinyl alcohol) or poly(acrylic acid) [36]. A recent example involved the use of poly(l-lactic acid) macroporous hybrid scaffolds coated with HA [37]. The preformed scaffolds were immersed in an HA solution which was then cross-linked with glutaraldehyde in water/acetone. Applications for this type of material generally concern bone tissue engineering.

Cross-linked Hyaluronan nanoparticles were patented by Borbely et al. [38] following a report by Bodnar et al. using a CDI method [39] . The structure of HA used for the synthesis and the obtained cross-linked nanosystems (Fig. 1) were characterized by nuclear magnetic resonance (NMR) spectroscopy.

Transparent or opalescent stable colloid systems were fabricated in aqueous medium at room temperature. The results of characterization revealed that the size of the particles in the dried state by transmission electron microscopy (TEM) and in solution by dynamic light scattering (DLS) and also the rheological properties depended on the molecular weight of the HA. Both the TEM and the DLS data supported the formation of particles. The average hydrodynamic diameters of the individual particles ranged from 30 to 140 nm. The CLHA nanoparticles had much lower viscosity than that of the parent linear biopolymer, because of the contraction of the linear chains in connection with the intrachain cross-linking and the absence of entanglement coupling. At high biopolymer molecular weight, an interplay between inter- and intramolecular cross-linking was found. The low viscosity and the nano size of the separated CLHA nanoparticles could lead to the development of new methods or products in medicine, pharmaceutics, and cosmetics [39].

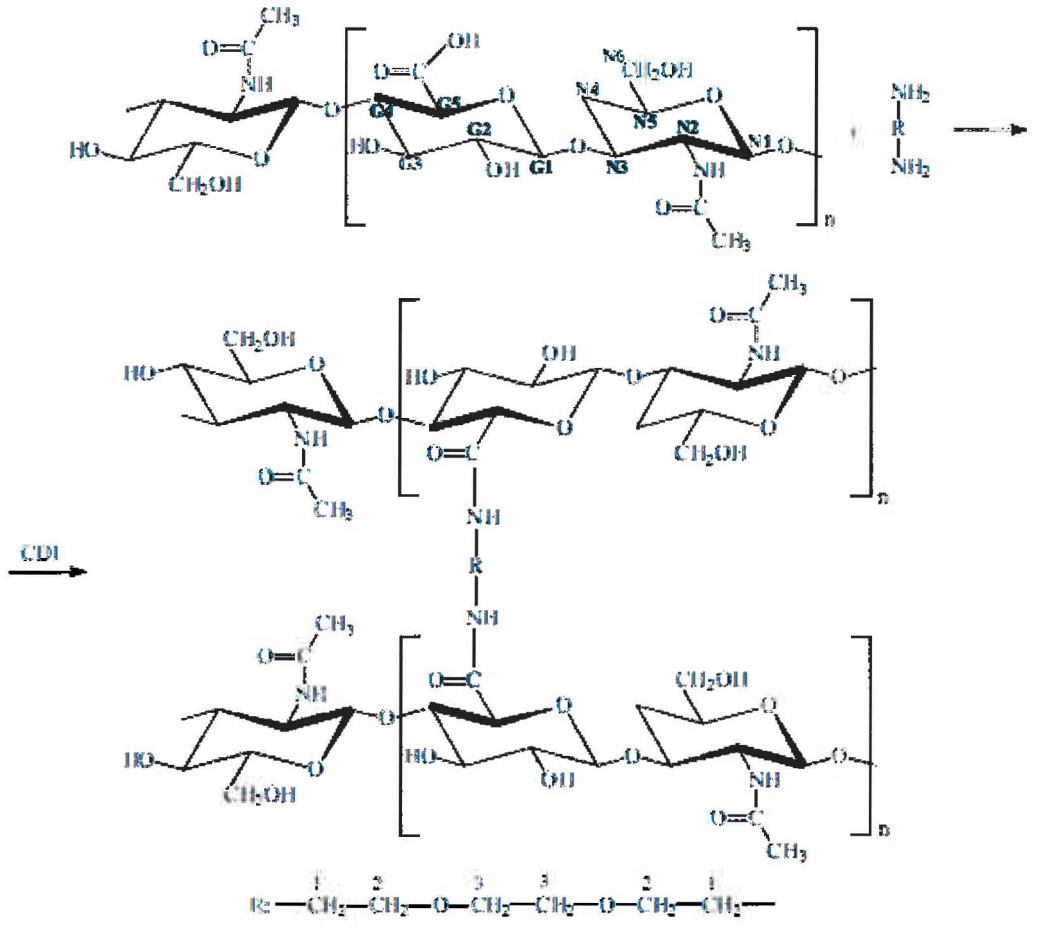

Figure 1. Reaction between HA and 2,2'(ethylenedioxy) bis(ethylamine) with the use of CDI as condensation agent [39]

The assignments and chemical shifts of the ^{1}H and ^{13}C NMR signals of HA 3 h (HA subjected to acidic decomposition for 3 h) and the cross-linked nanoparticles based on HA 3 h were determined. The chemical shifts were in accordance with published results [40, 41]. Proton chemical shifts are given in Figure 2a, which illustrates the difference between the signals of the original HA 3 h material **(I)** and the cross-linked nanoparticles based on HA 3 h at a stoichiometric ratio of 50% **(II)**.

The assignments and chemical shifts of the ^{1}H signals are as follows: HA for 3 h: ^{1}H NMR (D_2O): δ=4.51 (G1), δ=4.61 (N1), δ=3.40 (G2), δ=3.92 (N2), δ=3.63 (G3), δ=3.74–3.85 (N3, N6, G4, G5), δ=3.51–3.62 (N4, N5), and δ=2.07 ($NCOCH_3$); HA 3 h cross-linked with diamine at 50%: ^{1}H NMR (D_2O): δ=4.51 (G1), δ=4.62 (N1), δ=3.39 (G2), δ=3.96 (N2), δ=3.63 (G3), δ=3.70–3.84 (N3, N6, G4, G5, C1, C2), δ=3.49–3.60 (N4, N5), δ=2.07

($NCOCH_3$), and δ=3.33 (C3). The ^{13}C assignments were made on the basis of ^{13}C projection. Figure 2b demonstrates the difference between the signals of the original HA 3 h material **(III)** and the hyaluronan nanoparticles based on HA 3 h cross-linked at a stoichiometric ratio of 50% **(IV)**. The assignments and chemical shifts of the ^{13}C signals are given as follows: HA 3 h: ^{13}C NMR (D_2O): δ=103.71 (G1), δ=101.05 (N1), δ=73.08 (G2), δ=54.82 (N2), δ=74.17 (G3), δ=83.28 (N3), δ=80.48 (G4), δ=69.07 (N4), δ=76.88 (G5), δ=75.91 (N5), δ=61.10 (N6),δ=174.58 (COO−), and δ=23.04 ($NCOCH_3$); HA 3 h cross-linked with diamine at 50%: 13C NMR (D_2O): δ=103.63 (G1), δ=101.02 (N1), δ=73.01 (G2), δ=54.83 (N2), δ=74.14 (G3), δ=80.10 (N3), δ=80.47 (G4), δ=69.02 (N4), δ=76.77 (G5), δ=75.92 (N5), δ=61.10 (N6), δ=174.52 (COO−), δ=23.03 ($NCOCH_3$), and the signals of the cross-linker δ=66.93 (C1), δ=70.18 (C2), and δ=38.75 (C3).

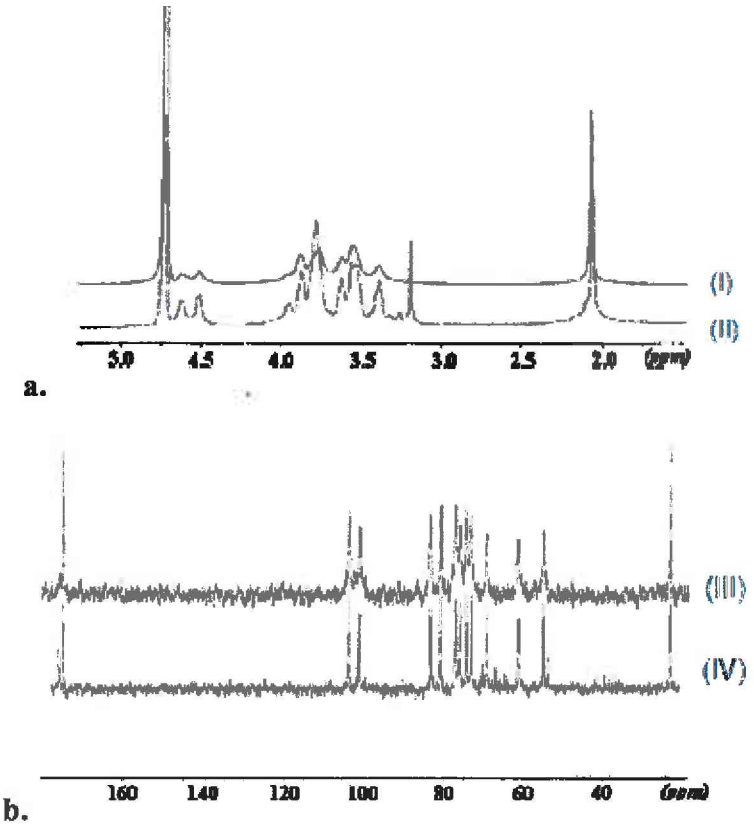

Figure 2. a. 500 MHz ^1H NMR spectra of hyaluronic acid (HA) 3 h **(I)** and hyaluronan nanoparticles based on HA 3 h cross-linked with diami at 50% **(II)** [39]

b. 500 MHz ^{13}C NMR spectra of HA 3 h **(III)** and nanoparticles based on HA 3 h cross-linked with diamine at 50% **(IV)** [39]

1.4 HA-based nanoparticles as an effective carrier in transdermal API delivery

It is planned to use HA, a naturally occurring polymer composed of unbranched repeating units of glucuronic acid and N-acetyl glucosamine linked by β1–3 and β1–4 glycosidic bonds [42], as a carrier of APIs through the skin.

The major function of the skin, the largest organ in the body, is to protect the body from dehydration and unwanted effects from the external environment [43]. Although the protective and impermeable qualities of the skin protect the organism from loosing water, minerals and dissolved proteins, the advantages of the percutaneous delivery system as a topical delivery system have been utilized in the pharmaceutical or cosmetic industries. In contrast with the traditional API administration routes, transdermal administration is a non-invasive procedure which eliminates side-effects, increases patient compliance and offer a possibility for continuous and controlled API absorption [44]. Besides being a vital organ, the skin must be nourished by means of cosmetic formulations [45]. The stratum corneum (SC), the outermost non-viable layer of the epidermis, comprises flattened, stacked, and cornified cells (corneocytes or horny cells) anchored in a mortar of highly organized intercellular lipids, described as a 'brick and mortar' model [46]. The corneocytes are surrounded by hydrophobic lipid bilayers aligned approximately parallel to the surface of the corneocytes, while the intercellular spaces are abundant in SC lipids [47]. The particular structure is regarded as the rate-controlling barrier in the transdermal absorption of substances, and this is directly related to the lipophilicity of the substances [48]. However, a lipophilic molecule does not favourably partition out of the SC into the more aqueous viable epidermis [49], hindering deeper diffusion and further capillary uptake into the circulation. In comparison, hydrophilic substances penetrate through the skin with more difficulty than lipophilic penetrants; 10–4-fold differences in flux may be observed [50].

In order to overcome the SC barrier so as to increase transdermal transport, various transdermal carrier systems have been developed. As the permeability of a substance through the skin is inversely related to its size under certain conditions [48], investigations of nanoparticulate systems such as solid lipid nanoparticles, nanostructured lipid carriers, liposomes, microemulsions and hexagonal phase nanodispersions are promising [51]. In addition to the benefits of the transdermal delivery system, which may allow desirable amounts of API to overcome the skin barrier, the material has to be biocompatible,

preferentially biodegradable, or at least able to be excreted [52], ensure non-irritancy to the skin and sustain the activity of the ingredients on the skin surface or during the permeation process [53]. Among those transdermal carrier systems, nanoemulsions and nanoparticle appear to be attractive and competitive.

The skin contains slightly more than 50% of the total HA content present within the human body [54]. After the age of 20 years, the amount of HA continuously decreases.

Thanks to its versatile properties, such as its biocompatibility, non-immunogenicity, biodegradability and viscoelasticity, HA is an ideal biomaterial for cosmetic, medical and pharmaceutical applications. It is widely utilized for the treatment of osteoarthritis, vesicourethral reflux and urinary incontinence. HA is incorporated in many moisturizing creams and wound-healing dressings, and it is also applied in ophthalmology [55, 56, 6, 57, 58]. However, with the exception of the vitreous body, where its half-life is 20-70 days, the turnover of HA in most tissues in the body is surprisingly rapid. The typical half-life in the human skin is 2-5 days, in the joints and pleura it is 0.5-1 day, and in the anterior chamber of the eye it is merely 1-2 h. A novel approach is the use of HA-based nanoparticles as an effective carrier in transdermal API delivery [59 -63].

In view of the problem of the enzymatic degradation of HA, a number of research studies have been made with the aim of elongating the presence of HA in the body [64]. In order to increase the resistance of HA to enzymatic digestion, N-alanyl-hyaluronamide derivatives have been prepared. Molecular modelling based on crystallographic studies indicated that the recognition sites of the Hyal-2 enzymes and CD44 receptors are the carboxylate groups of HA [65]. Its chemical modification may therefore diminish enzymatic recognition and enhance the stability of HA against hyaluronidase-mediated hydrolysis. The N-alanyl-hyaluronamides present enhanced resistance to enzymatic digestion while forming solutions with similar viscosities to those of solutions of HAs of similar lengths [64].

Another problem in the application of HA is the administration route. In most cases, HA is injected, which is a painful application procedure and sometimes causes inflammatory complications and bacterial infections. HA exhibits good gelling properties and leads to a hydration effect in the uppermost layer of the SC following dermal application, which in most cases promotes penetration of the drug. The water may cause the compact structure of the horny layer to swell and open up, leading to an increase in the extent of penetration. However,

the penetration of HA into the deeper layers of the skin is very slow or may be inhibited, depending on the molecular weight of the HA [66]. Cross-linking of the HA molecule may be a possible mode of chemical modification with the aims of preventing the degradation and improving the penetration of HA.

1.5 API permeation through the skin

The skin, the largest body organ, weighs approximately 5 kg and has a surface area of about 2 m^2 in adult humans [43, 67, 68]. This multilayered organ has the essential function of protecting the body from the surrounding environment, by being an efficient permeation obstacle for exogenous molecules. The barrier properties of the skin lie mainly within its uppermost stratum, the SC. This highly hydrophobic layer is composed of differentiated non-nucleated cells, corneocytes, which are filled with keratins and embedded in the lipid domain. Since the rate-limiting step for the skin absorption of most molecules is considered to involve this non-viable layer, the percutaneous permeation of molecules is believed to be governed by diffusion laws. The extent of skin permeation of a compound may depend on the route of absorption. There are three pathways which can be involved in the transdermal permeation of chemicals: (1) through the intercellular lipid domains in the SC; (2) through the skin appendages; and (3) through the keratin bundles in the SC [69].

The lack of a correlation in the transdermal permeation of molecules across species or from different application sites in the same animal model is due mainly to variations in skin (or SC) thickness, in the composition of intercellular SC lipids and in the number of skin shafts. Netzlaff et al. [70] have shown that the amounts of free fatty acids and triglycerides and the density of hair follicles are important factors causing differences between the skin barriers in the different species. As the majority of molecules applied onto the skin permeate along the SC lipid domain, the organization of these regions is very important as concerns the barrier function of the skin. The SC lipid composition and organization differ from those of other biological membranes, with long-chain ceramides, free fatty acids, cholesterol and cholesteryl esters being the main lipid classes [71, 72].

To evaluate the transdermal absorption of a molecule, the most relevant membrane is the human skin. Skin from various sources, including cosmetic surgery and amputations, has been

used for the *ex vivo* assessment of percutaneous penetration [73]. However, its availability is limited and animal skin is therefore frequently used. A wide range of animal models have been suggested as suitable replacements for human skin and have been used to evaluate the percutaneous permeation of molecules. These include primate, porcine, mouse, rat, guinea pig and snake models.

Since the use of primates in research is highly restricted, the most relevant animal model for human skin is the pig. Porcine skin is readily obtainable from abattoirs and its histological and biochemical properties have been repeatedly shown to be similar to those of human skin [74]. Porcine ear skin is particularly well-suited for permeation studies and gives comparable results to those with human skin. Studies examining the thickness of various skin layers have shown that the SC thickness in pigs is 21–26 μm [75] which is comparable with that of human skin [76]. The viable epidermis in porcine ear skin is 66–72 μm thick, which is very similar to the human epidermal thickness of 70 μm (shoulder) [77]. The follicular structure of porcine skin also resembles that of humans, with hairs and infundibula extending deep into the dermis. An average of 20 hairs are present per 1 cm^2 of porcine ear skin, as compared with 14–32 hairs (except the forehead area) in humans. Moreover, the vascular anatomy and collagen fibre arrangement in the dermis, and also the contents of SC glycosphingolipids and ceramides, are similar in man and the domestic pig [78]. Due to its availability, the skin of rodents (mice, rats and guinea pigs) is the most commonly used in *in vitro* and *in vivo* percutaneous permeation studies. The advantages of these animals are their small size, uncomplicated handling and relatively low cost. There are a number of hairless species (nude mice and hairless rats), in which the absence of a hair coat mimics the human skin better than does hairy skin [79]. In these animals, there is no need for hair removal (clipping or shaving) prior to the experiment, and this avoids the risk of injury to the cutaneous tissue. Other models have the disadvantage of an extremely high density of hair follicles and require hair removal. Since both issues may affect the percutaneous absorption of molecules, hairy rodent skin is usually not used in *in vitro* permeation studies, although *in vivo* studies are still performed on these species. Among rodents, rat skin exhibits more structural similarities to human tissue (Table 1).

Table 1. Thickness of skin strata in rats, mice and humans [80]

	SC (μm)	Epidermis (μm)	Whole skin (mm)
Rat	18	32	2.09
Mouse	9	29	0.70
Human	17	47	2.97

With the exception of the rat skin, rodent skin generally displays a higher permeation rate than that of human skin [81]. As regards rat skin, the permeation kinetic parameters are frequently comparable with those of human skin. Snake skin has also been proposed as a membrane in skin permeation experiments. Differential scanning calorimetry thermograms and infrared spectra have revealed certain similarities in structure and components of the SC of snake, porcine and human skins [82]. The distinguishing feature of the shed snake membrane is its lack of follicles.

The human skin is one of the best biological barriers. The SC or horny layer the outermost, very thin (~17 μm) layer of the epidermis, contributes over 80% to the skin permeability resistance.

Due to the special and strictly ordered structure of the SC and its excellent diffusional resistance, it makes the transdermal permeation of APIs difficult or frequently impossible. The permeation of drugs through the skin includes the diffusion through the intact epidermis and through the skin appendages, i.e. hair follicles and sweat glands, which form shunt pathways through the intact epidermis. However, these skin appendages occupy only 0.1% of the total human skin surface and the contribution of this pathway is usually considered to be small. The physicochemical properties of the compound, and also the formulation used, are the main factors influencing the choice of pathway. Originating from the structure of the SC, two permeation pathways are possible through the intact SC: the transcellular route crossing through the corneocytes and the intervening lipids, and the intercellular lipid route between the corneocytes (Figure 3).

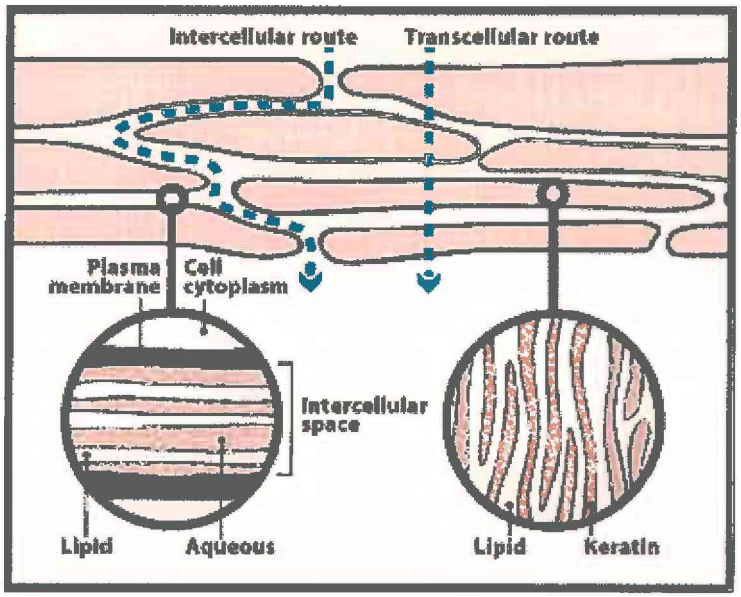

Figure 3. The ordered structure of the SC and the penetration routes [83 - 85]

Under normal conditions, the transcellular route is not considered to be the preferred way of dermal invasion, the reason being the very low permeability through the corneocytes and the obligation to partition several times from the more hydrophilic corneocytes into the lipid intercellular layers in the SC and *vice versa*. The transcellular pathway can gain in importance when a penetration enhancer is used, which increases the permeability of the corneocytes by altering the keratin structure [86].

The intercellular microroute is considered to be the predominantly used pathway in most cases. Resulting from the bilayer structure, the intercellular pathway provides hydrophilic and lipophilic regions, allowing the more hydrophilic substances to use the hydrophilic route and the more lipophilic substances the lipophilic route. In addition, it is possible to influence this pathway by including certain excipients in the formulation. Many enhancing techniques aim to disrupt or bypass this special molecular architecture.

The water content of the SC is around 15-20% of the dry weight, but can vary with the humidity of the external environment. Increasing the skin hydration is the most widely used and safest method to increase the skin penetration of both hydrophilic and lipophilic permeants. Water within the SC may alter the permeant solubility and thereby modify the partitioning from the vehicle into the membrane. In addition, increased skin hydration may

swell and open up the compact structure of the horny layer, leading to an increase in penetration. Hence it is required to develop well-moisturizing transdermal delivery systems.

1.6 Models for penetration

The vertical Franz diffusion cells model is regarded as the most valid *in vitro* model for evaluating API penetration from semisolid preparations [87]. Basically, a donor and an acceptor compartment are separated by a membrane (of animal, human or artificial origin). The most widely used skin permeation model membranes are listed in Table 2.

Table 2. Model membranes for permeation examinations

Ex vivo	Human skin equivalent
	Excised animal skin
	SC
	Heat-separated epidermis
	Dermatomed skin
	Human full-thickness skin
In vitro	Synthetic membrane
In vivo	Animal skin

Although *ex vivo* tests are frequently used and approved methods [88] and their application is strongly encouraged in order to reduce the need for both animal and human studies, they show some imperfections. The majority of *ex vivo* models are not able to test the metabolism of API molecules in the skin [89]. Thus, *in vivo* examinations cannot be avoided in pharmacological and dermatological studies. Many different types of *in vivo* methods have been developed. Nevertheless, in contrast with the Franz diffusion cell, these techniques do not provide a possibility for the exact quantitative measurement of penetration.

Accordingly, there appears to be a need for broadening the toolbox of models available for permeation studies. The dorsal skin-fold chamber is an accepted and sophisticated

experimental model to study the microcirculation under different conditions, to test the biocompatibility of different materials [90] and to examine angiogenesis [91] and wound healing [92]. A novel modified version of this experimental set-up seems to provide an effective means for the *in vivo* examination of transdermal permeation. Two holding stitches are inserted in the dorsal midline and a moderate tension is exerted in order to form a skin-fold. Two symmetrical titanium frames (IROLA GmbH, Schonach, Germany) are then implanted to sandwich the extended double layer of the skin (Figure 4a). A circular full dermal thickness wound is formed on one side of the skin-fold (Figure 4b).

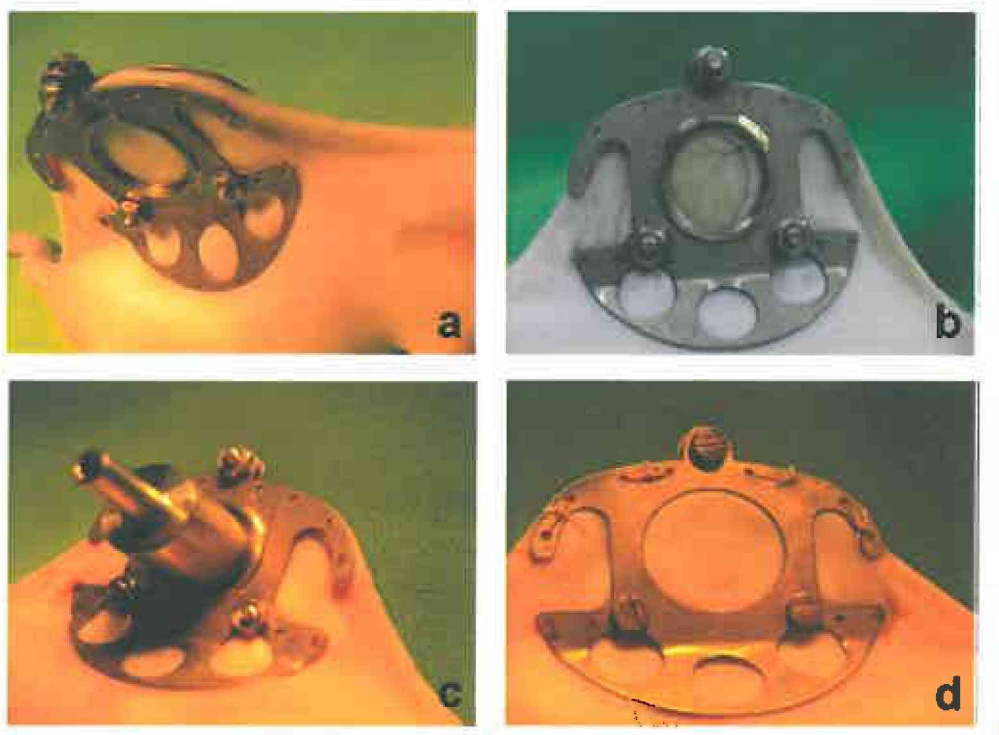

Figure 4. The novel mouse model [93]

A stainless steel cylinder with a volume of 1 ml is fixed into the window of the titanium frame on the wounded site (Figure 4c). The opposite, non-wounded site (Figure 4d) serves for the application of the study formulation. In our model, the creation of the circular wound makes the double-layered skin fold one-layered on the area of the cylinder with the acceptor phase. Thus, the API placed onto the non-wounded site has to penetrate via one layer of epidermis, dermis and a thin layer of striated muscle, respectively, prior to entering the acceptor buffer [93].

2 Aims

The aim of my work was to prepare and investigate a cross-linking nanoparticle system produced through the reaction between HA and 2,2'(ethylenedioxy)bis(ethylamine), using a water-soluble CDI as condensation agent in aqueous medium.

In the first part of the investigation, the matrix form was synthetized in order to know the common effects caused by the different variables.
The main steps in our experiments were as follows.

- Parallel reactions under the same conditions and with the same parameters. In this case, the variables were the medium, the concentration of HA and the amount of the diamine and CDI. The standard parameters were the volume of the medium (50 ml), the dissolved HA was adjusted to the same pH, the preparation of the diamine solution, the mixing and stirring times, the temperatures applied, the dialysis and freeze-drying methods.
- Confirmation of the existence of HA nanoparticles by TEM.

In the second part of the investigation, the manufacturing process was studied, as follows.

- Comparison of the particle sizes, particle size distributions (PSDs), molecule weight distributions and rheological measurements at different phases of the technology.
- Determination of the effects of the salt concentration on the size of the particles.
- Determination of the stability of these nanoparticle systems in different media and at different feed ratios.

In the third part of the investigation, HA-based nanoparticulate semisolid preparations were compared with a hydrogel containing linear HA.

- Measurements were made of the rheological properties, and hydration, and irritation effects.
- Skin penetration abilities were determined by using *in vitro, ex vivo* and *in vivo* skin models.

3 Experimental section

3.1 Materials

- HA (M_W = 4350 kDa) was obtained from Gedeon Richter Ltd. (Budapest, Hungary) in sodium salt form. Its quality met the Ph. Eur. 6th requirements.
- 2,2'-(Ethylenedioxy)bis(ethylamine) was purchased from Sigma-Aldrich Ltd. (Budapest, Hungary).
- 1-[3-(dimethylamino)propyl]-3-ethylcarbodiimide methiodide, was purchased from Sigma-Aldrich Ltd. (Budapest, Hungary) (Figure. 5).

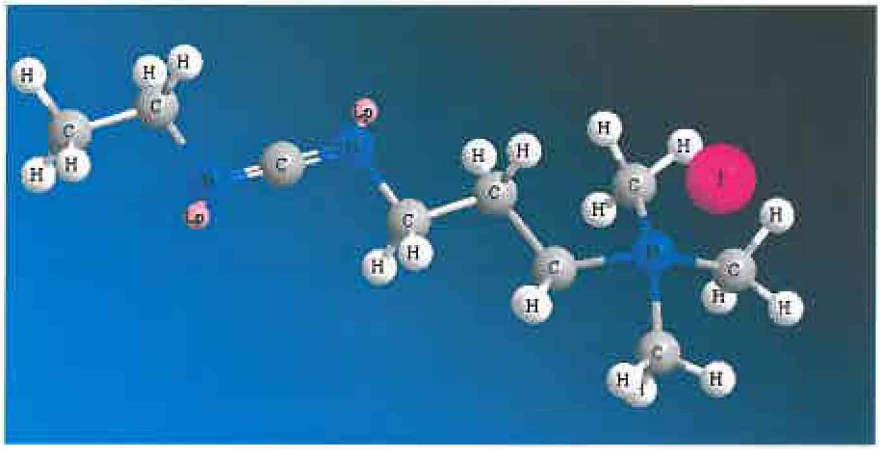

Figure 5. The CDI structure

- The pH was adjusted with NaOH and HCl solutions.
- Millipore water was used throughout the study.
- Transcutol® (diethylene glycol monoethyl ether) was from S&D Chemicals Ltd. (Budapest, Hungary).
- Labrasol® (caprylocaproyl macrogol-8 glycerides) was from S&D Chemicals Ltd. (Budapest, Hungary).
- Glycerol 85% was from Molar Chemicals Ltd. (Budapest, Hungary).
- Semisolid gel formulation: glycerol 85% and purified water as solvents, with Transcutol® and Labrasol® as penetration enhancers, comprised the hydrophilic base of the gel. 1% of either the CLHA or the linear HA was dispersed into this base. The gels were stirred at intervals until complete dissolution was attained.

  The chemicals were all of analytical grade.

3.2 Preparation of cross-linked hyaluronic acid (CLHA)

In our study CLHA nanoparticles (Figure 6) were prepared by literature [38, 39] with modifications of the medium and with the use of different amounts of reactants. HA was dissolved in water to produce a 1 mg/mL solution, which was adjusted to pH 5.5 with 0.1 M NaOH solution. The diamine was dissolved in water to produce a 1.0 v/v% solution and similarly pH-adjusted to 5.5 with 0.1 M NaOH solution. The diamine solution was added to the HA solution and the mixture was stirred for 30 min at room temperature. Subsequently, after the addition of the water-soluble CDI solution dropwise, the reaction mixture was stirred at room temperature for 24 h.

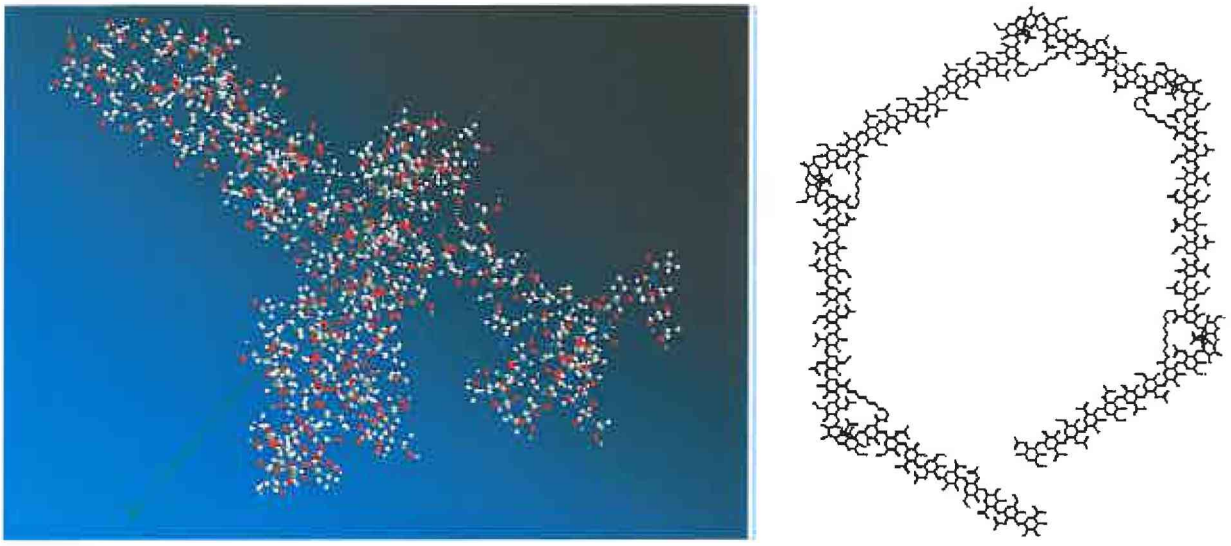

Figure 6. HA nanoparticle (5 times intra-cross-linked 32-disaccharide units of HA)

The solution containing the dissolved HA nanoparticles was purified by dialysis for 7 days against distilled water and freeze-dried. The scheme of synthesis reaction between HA and 2,2'-(ethylenedioxy)bis(ethylamine) with the CDI as condensation agent was unchanged. (Figure 7).

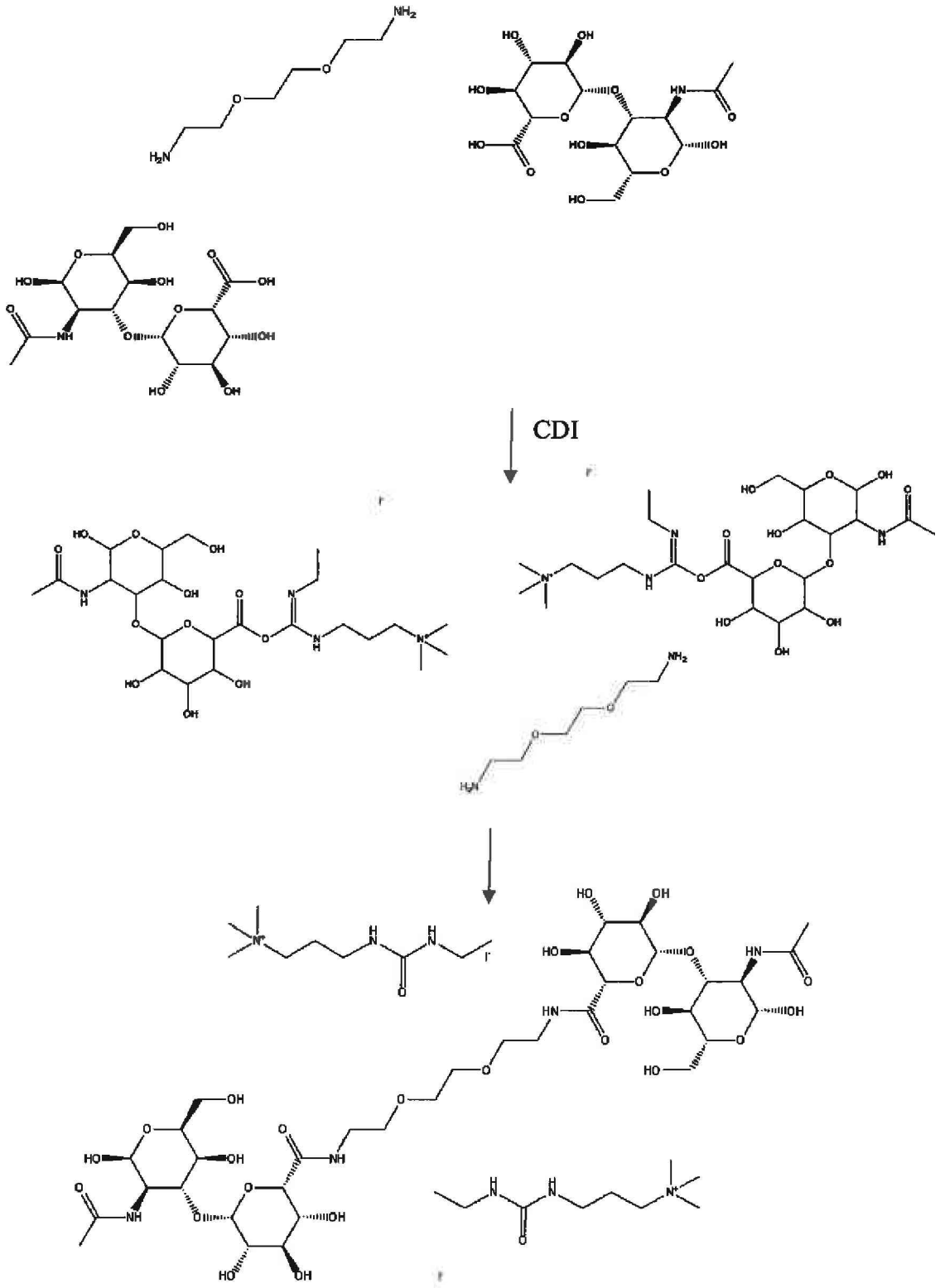

Figure 7. Scheme of synthesis reaction between HA and 2,2'-(ethylenedioxy) bis(ethylamine) with the CDI as condensation agent

The cross-linking reaction of HA was carried out in three different media (Table 3).

Table 3. The notations applied for the media throughout the study

Medium	water	NaCl (0.09% w/w)	NaCl (0.9% w/w)
Notation	A	B	C

The matrix end-products of the reactions were synthetized under different reaction conditions as concerns the medium applied, the concentration of HA and the cross-linking ratio. The nanoparticles obtained were identified by a three-notation system as follows: the initial letter refers to the medium and is followed by a number indicating the concentration of HA (mg/ml), and the final number indicating stoichiometric cross-linking ratio (feed ratio). As an example, the notation A_1_25 means that: the medium is water, concentration of HA is 1 mg/ml and the cross-linking ratio is 25%.

The HA nanoparticles that were prepared in water, with their notations, are detailed in Table 4.

Table 4. Matrix products of parallel reactions in water

A_1_25	A_2_25	A_3_25
A_1_12	A_2_12	A_3_12
A_1_7	A_2_7	A_3_7

The reaction conditions applied for the preparation of some matrix products are presented in Table 5.

Table 5. The reaction conditions applied for some matrix products

Notation	Medium	HA (mg)	Concentration of HA(as sodium salt) (mg/ml)	Stoichiometric cross-linking ratio (%)	Quantity of 1.0 % w/w diamine (µl)	Quantity of CDI (mg)
A_1_25	Water	50	1	25	228	9.3
A_2_25	Water	100	2	25	456	18.5
A_3_25	Water	150	3	25	684	27.8
A_3_12	Water	150	3	12	328	13.3
A_3_7	Water	150	3	7	191	7.8

The pH of the reaction mixture for the matrix products was adjusted from 4 to 8 by the addition of 0.1 M NaOH or 0.1 M HCl solutions.

3.3 Characterization of the nanoparticle products, the semisolid linear HA and CLHA preparations

3.3.1 Dynamic light scattering (DLS)

The hydrodynamic diameter and size distribution of the CLHA nanosystems were measured with a Malvern–Zetasizer NanoZS90 instrument (Malvern Instruments Ltd., Worcestershire, UK).

The reaction mixture and different pH-adjusted samples were placed into the optically homogeneous polystyrene cell of the Malvern–Zetasizer NanoZS90 laser diffraction particle size analyser. The freeze-dried samples were suspended in distilled water, sonicated for at least 1 min and then placed into the cell. The determinations of the particle size distribution for the HA nanoparticle systems were repeated 5 times per sample and average serial data were calculated. The measurements were made by photon correlation spectroscopy at a fixed angle of 173° at 25 °C.

3.3.2 Ultraviolet spectrophotometry

Transmittances of CLHA nanosystems were analysed with an HP-8453 Ultraviolet Spectrophotometer, at 500 nm in optically homogeneous quartz cells at 25 °C.

3.3.3 Transmission electron microscopy (TEM)

The size and morphology of the dried HA nanoparticles were determined with a JEOL2000 FX-II transmission electron microscope.

Samples for TEM were prepared as follows: The reaction mixture of CLHA was diluted to 0.2 mg/ml solution, and the pH of the diluted colloid system was then adjusted to pH 10. 10 μl solution was dropped onto the carbon film-coated copper grid. The sample was dried at room temperature.

3.3.4 Gel permeation chromatography (GPC)

GPC is a type of size exclusion chromatography that separates analystes on the basis of size. The GPC column applied was the BioSuite 450 HR SEC. Samples were dissolved in water, and the solution was injected onto the column after 5 μm filtering. The eluent used was 0.05

M NaOAc + 0.2 M NaCl : MeOH = 8:2. The measurements were performed at a flow rate of 0.7 ml/min with detection at 210 nm.

Semisolid gels were characterized on a Waters HPLC system with an Ultrahydrogel-Linear column. Samples were dissolved in phosphate-buffered saline solution (PBS), and filtered through a 5 μm pre-column sieve. The mobile phase was a mixture of 140 mM NaCl, 7.5 mM Na_2HPO_4, 2 mM NaH_2PO_4 and 2.7 mM KCl, pH 7.4 (PBS); the flow rate was 1 ml/min. The eluent was monitored at 220 nm. The analysis time was 20 min/sample.

3.3.5 Rheometry involving characterization of nanoparticle test products

Rheological measurements were carried out with a Physica MCR101 rheometer (Anton Paar, Austria). A cone-plate measuring device was used in which the cone angle was 1°, and the thickness of the sample in the middle of the cone was 0.046 mm. The measurements were performed at 25 C. The pH was adjusted to 6.3±0.2. The flow curves of the different samples were also determined. The shear rate was increased from 0.1 to 150 1/s (up-curve), and then decreased from 150 to 0.1 1/s (down curve) in the CR mode. For both segments, the shearing time was 300 s. In the case of semisolid gels, the measurements were made at 32 °C. The flow curves of the different samples were also determined. The shear rate was increased from 0.1 to 100 1/s (up-curve), and then decreased from 100 to 0.1 1/s (down-curve) in the CR mode. The shearing time in both segments was 300 s. Oscillation measurements were used to analyse both the storage modulus *(G')* and the loss modulus *(G")* for frequencies between 0.01 and 100 Hz in the linear viscoelastic region. The measurements were performed at 32 °C.

3.3.6 Hydration and irritation tests

The Corneometer® CM 825 (Courage and Khazaka Electronic GmbH, Cologne, Germany) is the instrument commonly used worldwide to determine the level of hydration of the skin surface, and mainly the SC. The investigation is based on measurement of the capacitance of a dielectric medium. The Tewameter® TM 300 (Courage and Khazaka Electronic GmbH, Cologne, Germany) is the most generally accepted measuring device for the assessment of transepidermal water loss (TEWL). This is the most important parameter for evaluation of the barrier function of the SC. High TEWL values indicate a greater loss of water and are consistent with increased damage to the barrier function of the SC, such as may occur during

irritant exposure. The probe indirectly measures the density gradient of water evaporation from the skin via the two pairs of sensors inside the hollow cylinder.

Six hairless mouse without any dermatological disease or allergy were used in the experiment. All interventions were in full accordance with the NIH guidelines relating to experimentation with animals. The procedures and protocols of all animal experiments in the present study were approved in advance by the Ethical Committee for the Protection of Animals in Scientific Research at the University of Szeged. To promote the attainment of standard circumstances, all the skin tests were performed after the adaptation of the animals to room conditions (30 min at 23–25 °C and 40–50% relative humidity). During the experiment, test samples were applied to the skin of the dorsal region in all animals. The measured values were compared with those on the non-treated skin. The changes in moisturizing and TEWL levels were expressed as percentages.

3.3.7 *In vitro* API release and skin penetration measurements

Membrane diffusion and permeability studies were performed with a vertical Franz diffusion cell system (Hanson Microette TM Topical & Transdermal Diffusion Cell System, Hanson Research Corporation, Chatsworth, CA, USA). 0.30 g of sample was placed as a donor phase on a Porafil membrane filter (cellulose acetate; pore diameter 0.45 μm) or on human epidermis supported on a Porafil membrane filter. The effective diffusion surface area was 1.767 cm^2. PBS (pH=7.4) was used as an acceptor phase to ensure sink conditions. The rotation of the magnetic stirbar was set to 450 rpm. Experiments were performed at 37±0.5 °C for 24 h in the case of the synthetic membrane, and for 48 h with the human epidermis. Samples of 0.8 ml were taken from the acceptor phase by the autosampler (Hanson Microette Autosampling System, Hanson Research Corporation, Chatsworth, CA, USA) and replaced with fresh receiving medium. The quantitative measurements of linear HA and CLHA were made by means of GPC.

3.3.8 Preparation of human epidermis by a heat-separation technique

Excised human skin from female patients who had undergone abdominal plastic surgery was used. This was approved by the Ethical Committee of the University of Szeged, Albert Szent-Györgyi Clinical Centre (Human Investigation Review Board). Immediately after excision, the subcutaneous fatty tissue was removed and the skin was stored frozen at

-20 °C. For the permeation study, the skin was thawed, and the epidermis was separated from the underlying dermis through use of a heat-separation technique based on a procedure reported by Kligman and Christophers [94]. Individual portions were immersed in water at 60 °C for 90 s. Following removal of skin from the water, it was placed SC side up on a filter paper. The dermis was discarded and the epidermal membrane was floated on the surface of PBS (pH=7.4) for at least 20 min, after which it was placed on a supporting Porafil membrane.

3.3.9 *In vivo* animal study

The modified skinfold chamber model was used. The experiments were performed on 15-week-old male hairless mice. The full skin was removed from one side of the skinfold. On the other side of the skinfold, the skin comprised complete epidermis, dermis and skin muscle. The gel (0.1 g) was applied to the intact site, and the stainless steel cylinder with 1 ml of acceptor phase (PBS, pH=7.4) was fixed into the wounded site of the skinfold. The effective diffusion surface area was 1.539 cm^2. Experiments were performed for 6 h. The total acceptor phase was changed every hour. HA was determined by GPC.

3.3.10 Statistical analysis

The results were evaluated and analysed statistically with Student's t-test. The data are the averages of the results of six parallel experiments ± SD ($p < 0.05$*).

4 Results and discussion

4.1 Results on the nanoparticle products

4.1.1 DLS results

The cross-linking process of HA can result in intramolecular and intermolecular cross-linking. A proportion of the CLHA nanoparticles were formed as small, individual particles; however, large particles were also produced. The large particles can be aggregates, associations caused by secondary interactions or intermolecular cross-linked particles. The hydrodynamic diameter of the nanoparticles from the reaction mixtures was therefore not monomodal, so the *Z*-average size was used to compare hydrodynamic size.

4.1.1.1 **Particle size distribution (PSD)**

The end-point of Number Distribution Profile (NDP) for the reaction mixture of the matrix products shifts to smaller particles with increase of the concentration of HA at the same feed ratio (25%). (Figure 8a-c) Figure 8 shows the variation in size of the CLHA, with a higher concentration of native HA forming smaller nanoparticles. The explanation is that a higher concentration of HA leads to an increasing possibility of intermolecular cross-linking, thereby leading to more and more compact CLHA. This tendency indicates that the intermolecular forces between the nanoparticles are very low. Further, TEM showed that the HA nanoparticles were well dispersed with a spherical shape. At fixed pH, the PSD for the reaction mixture changed less for A_2_25 than for A_1_25, and less for A_3_25 than for A_2_25, which confirms the fact that a small particle size (~10 nm) was reached and the compaction was more perfect.

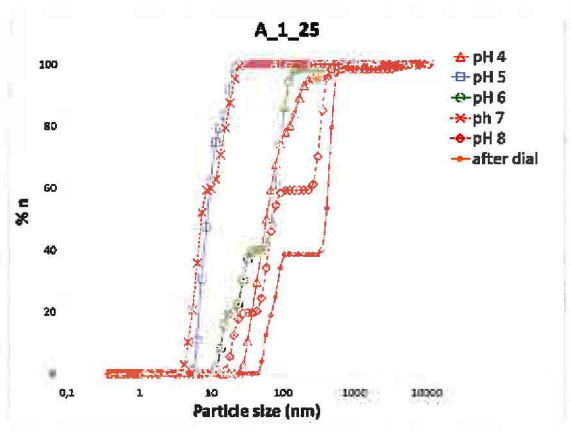

a

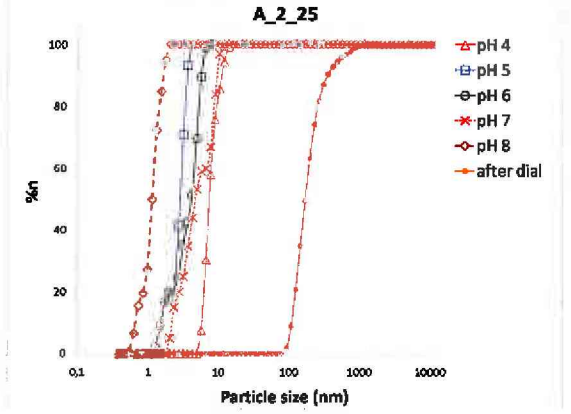

b

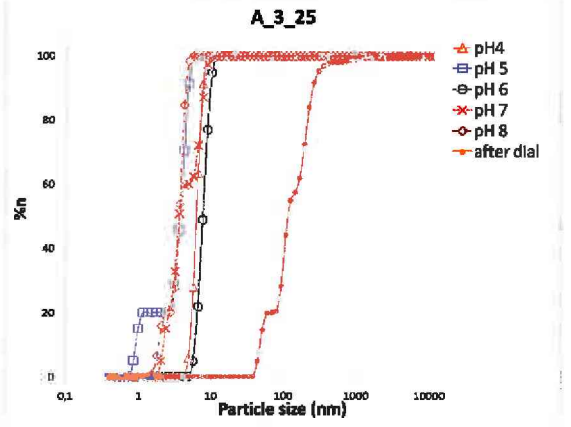

c

Figure 8. Effects of concentration of HA, pH and purification on the PSD of CLHA particles under the indicated reaction conditions: **a:** c_{HA} = 1 mg/ml, cross-linking ratio: 25%, prepared in water; **b:** c_{HA} = 2 mg/ml, cross-linking ratio: 25%, prepared in water; **c:** c_{HA} = 3 mg/ml, cross-linking ratio: 25%, prepared in water

Figures 8c and 9a,b indicated that applied smaller feed ratio (12% or 7%) is sufficient to create an appropriate amount of intermolecular binding when an adequate concentration of HA is used. This is probably caused by the decrease in the feed ratio from 25% to 7%, and the setting of the pH for reaction mixtures does not significantly influence the cross-linked systems.

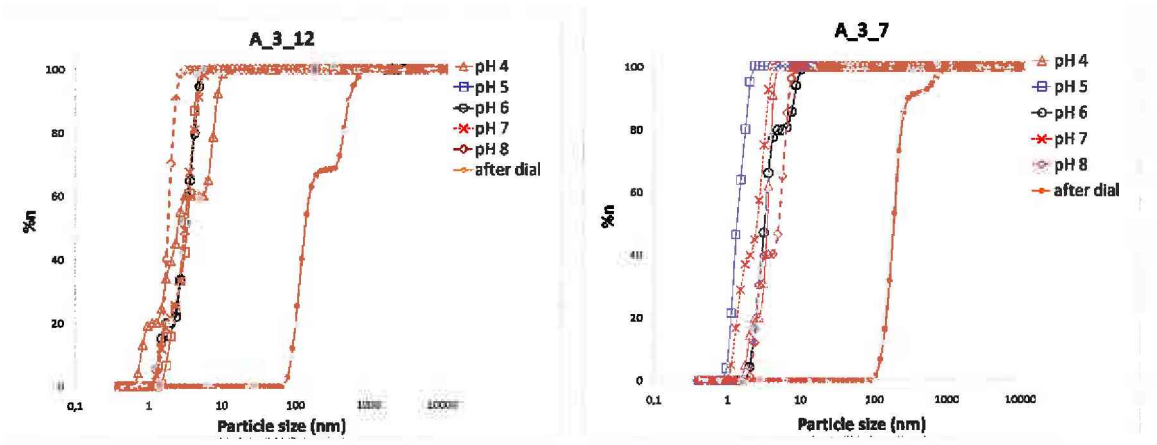

a **b**

Figure 9. Effects of a smaller feed ratio of HA, pH and purification on the PSD of CLHA particles under the indicated reaction conditions: **a:** c_{HA} = 3 mg/ml, cross-linking ratio: 12%, prepared in water; **b:** c_{HA} = 3 mg/ml, cross-linking ratio: 7%, prepared in water

We also determined the effect of the salt concentration on the size of the particles (Figures 8a and 10a,b). We observed a higher gradient of NDP at higher salinity, narrower particle size range systems being formed, which were not changed significantly when the pH was modified. The overall charge of the CLHA is negative. The overall charge of the CLHA nanoparticles could be modified by adjusting the pH, but mutual repulsive forces and electric double layer were decreased by higher salinity.

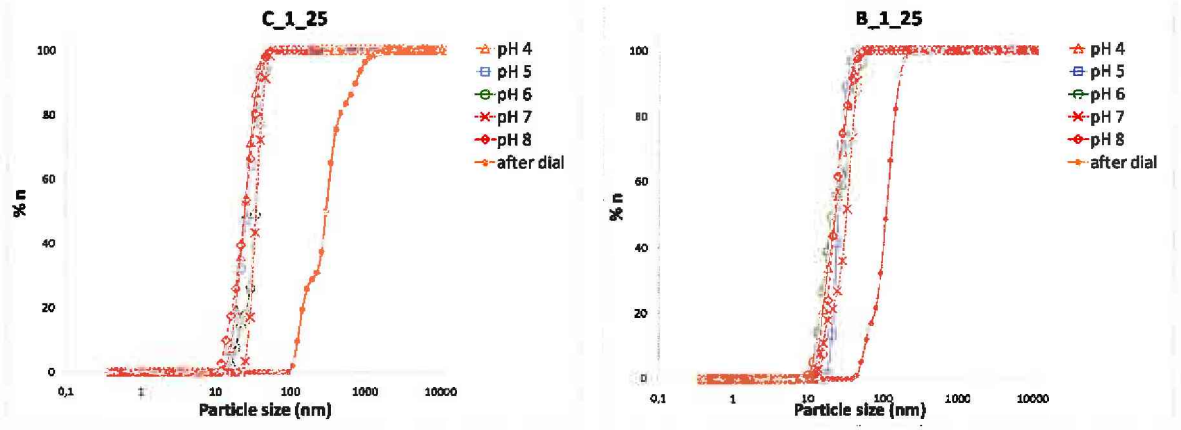

Figure 10. Effects of salt concentration, pH and purification on the PSD of CLHA particles under the indicated reaction conditions: **a:** c_{HA} = 1 mg/ml, cross-linking ratio: 25%, c_{NaCl} = 0.9 m/m%; **b:** c_{HA} = 1 mg/ml, cross-linking ratio: 25%, c_{NaCl} = 0.09 m/m%

Nevertheless, no significant correlations were established between the hydrodynamic diameters of swelled particles and the physico-chemical parameters of the reactions; the size and size distribution by number of all CLHA particles were below 20 nm.

However, we did observe differences between the PSDs of the reaction mixture and the dialysed samples. The latter-mentioned profiles are indicated 'after dial' in Figures 6-8. Since the PSDs of all of the tested dialysed matrix products were similar and shifted towards larger particle sizes, it was clear that the smaller particles were lost when the reaction mixtures were dialyzed. This phenomenon was confirmed by GPC and rheology measurements. The tested reaction mixtures contained larger particles in low amount, which comprised the 100% of the PSD after dialysis.

4.1.1.2 **Hydrodynamic diameter (HD)**

The reaction mixtures are not monomodal, so the *Z*-average size can only be used to compare results with samples measured via matrix products by the same technique. The HD was measured with DLS. The size of a particle was calculated from the translational diffusion coefficient by using the Stokes-Einstein equation: **HD** $= kT/3\pi\mu D$ ***(1)***

where: HD = hydrodynamic diameter, D = translational diffusion coefficient, k = Boltzmann's constant, T = absolute temperature, and μ = viscosity.

A tendency of HD to increase was observed when the pH was elevated because the increasing total ion concentration also affected the particle diffusion speed by changing the thickness of the electric double layer. The DLS (Figure 11) shows that, at a higher concentration of native HA, the CLHA forms smaller and more compacted nanoparticles, which leads to increasing HD through the wider electric double layer. The using of higher conductivity media (B and C) suppresses the electrical double layer and the measured HD.

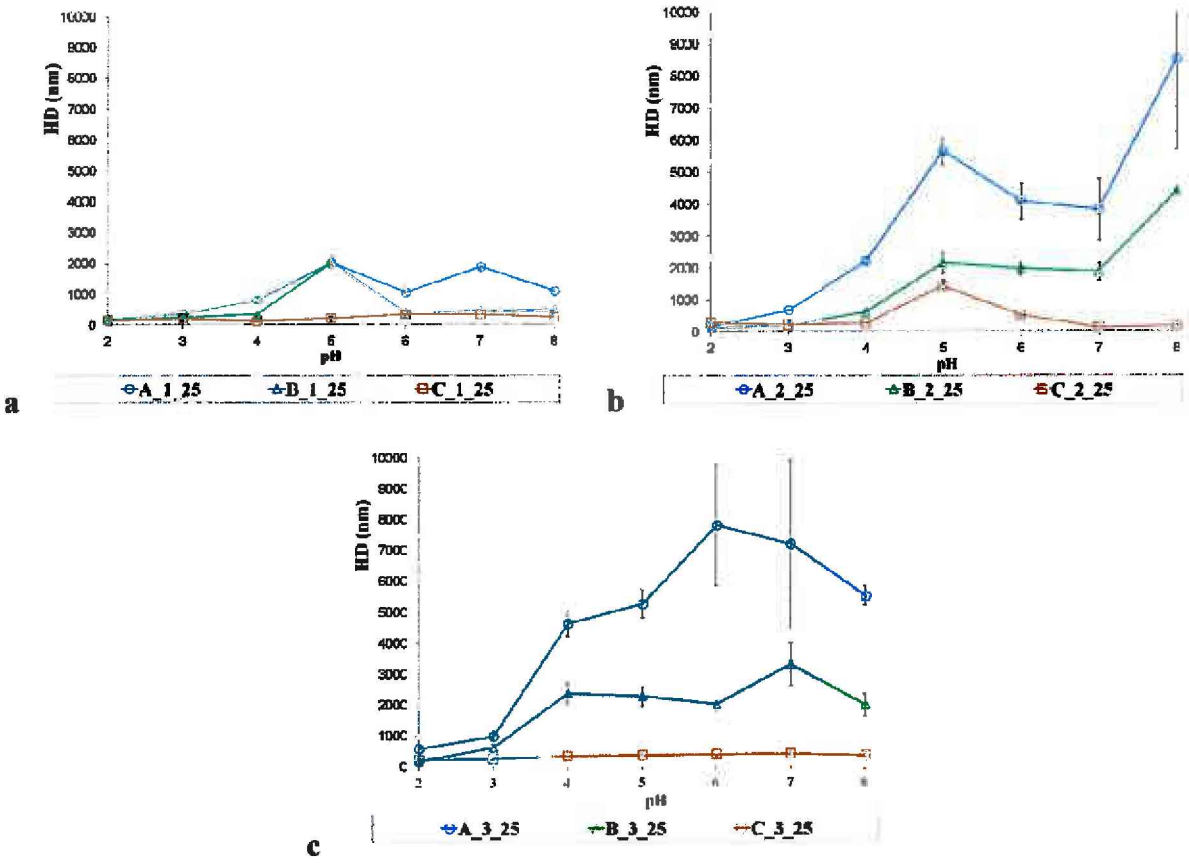

Figure 11. Effects of the pH and salt concentration of the medium on the *Z*-average HD of HA nanoparticles cross-linked at 25%, at the indicated HA concentration. **a:** c_{HA} = 1 mg/ml; **b:** c_{HA} = 2 mg/ml; **c:** c_{HA} = 3 mg/ml

The translational diffusion coefficient *D* depends not only on the size of the particle "core", but also the surface structure, and on the concentration and type of ions in the medium. A comparison of the A_1_25, A_2_25 and A_3_25 matrix products with the other matrix products reveals that the low conductivity medium water produces an extended double layer of ions around the particle, reducing the diffusion speed and resulting in a larger, apparent HD than in other media (Figure 11).

4.1.2 TEM results

The TEM micrographs (Figure 12) show that the CLHA nanoparticles are separated into spherical particles. TEM confirmed the existence of small nanoparticles (~10 nm) not only in the A_1_25 reaction mixture, but also in the A_3_7 mixture, where the HA concentration was higher and the feed ratio was lower. The histograms demonstrate that the concentration of the native HA affects the size of the nanoparticles. Increasing concentration of the native HA reduced the size of the dried particles to below 110 nm.

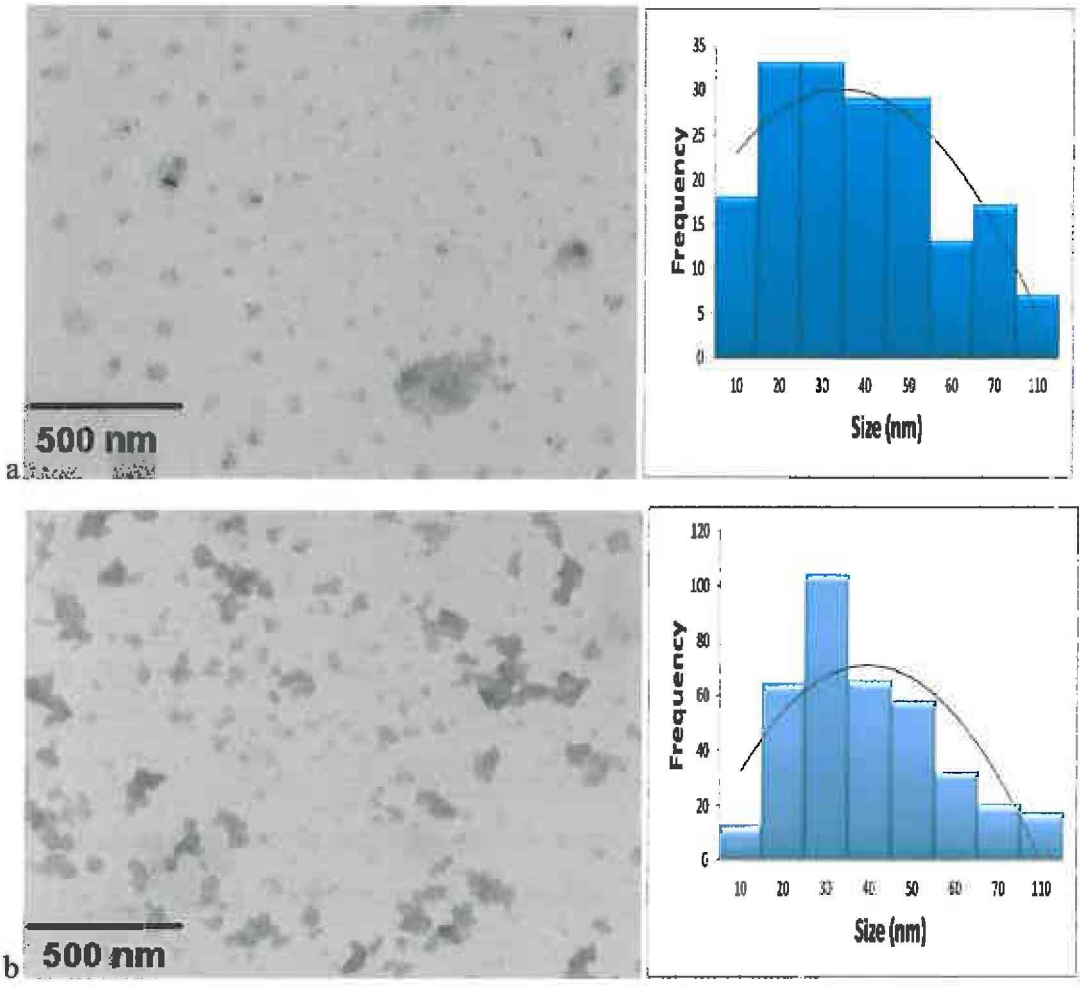

Figure 12. TEM images and size distributions of CLHA particles. **a:** A_1_25 (c_{HA} = 1 mg/ml, at a stoichiometric cross-linking ratio of 25%, prepared in water). **b:** A_3_7 (c_{HA} = 3 mg/ml, at a stoichiometric cross-linking ratio of 7%, prepared in water)

4.1.3 GPC results

Figure 13 shows a GPC trace of HA with the broad size distribution of the linear biopolymer.

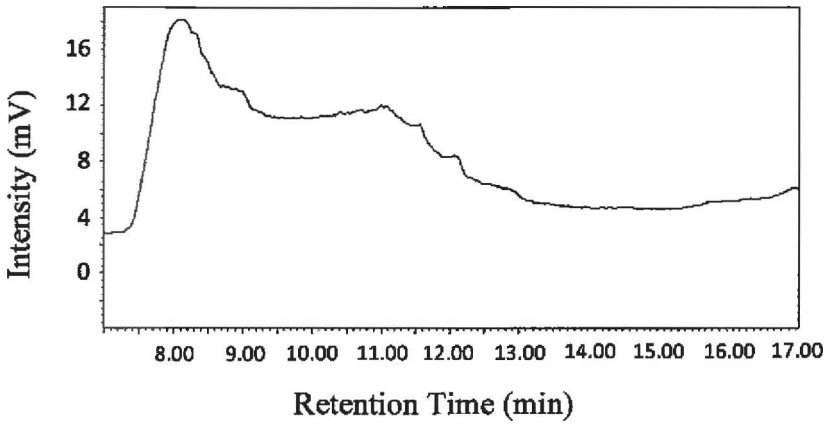

Figure 13. GPC chromatograms of HA (c_{HA} = 3 mg/ml);

Cross-linking produces nanoparticles. Figures 14 and 15 present GPC chromatograms of HA nanoparticles before and after dialysis. Before dialysis (Figure 14), the unimodal nanoparticulate system displayed a broad size distribution. The retention time for the nanoparticles increased; smaller particles were formed during the cross-linking reaction.

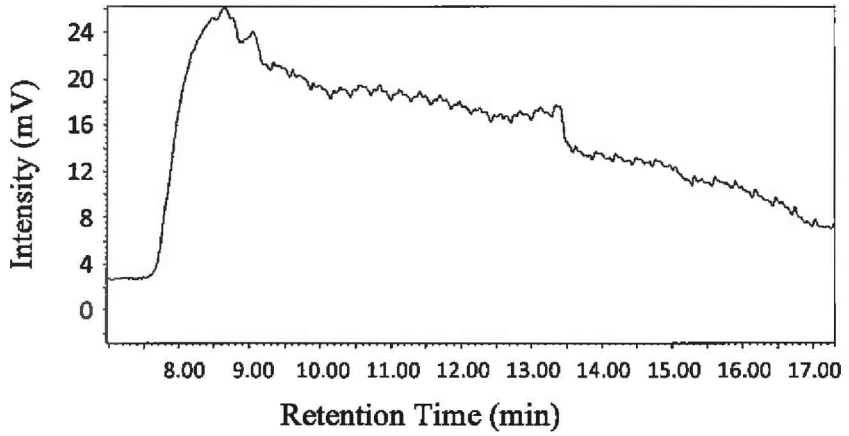

Figure 14. GPC chromatograms of the A_3_7 reaction mixture (c_{HA} = 3 mg/ml, at a stoichiometric cross-linking ratio of 7%, prepared in water)

Following dialysis with cellulose dialysis tubes (molecular weight cut-off = 12 000 Da), the intensity of the GPC chromatogram of the purified reaction mixture was reduced at higher retention times (Figure 15). This suggests that smaller particles were formed during the cross-linking reaction, diffused through the membrane tube and were lost during the dialysis.

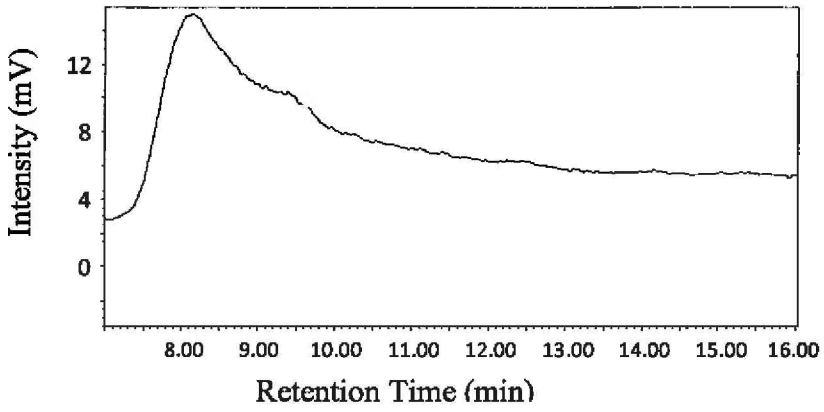

Figure 15. GPC chromatograms of the purified A_3_7 reaction mixture (c_{HA} = 3 mg/ml, at a stoichiometric cross-linking ratio of 7%, prepared in water)

4.1.4 Transmittance results

We can infer the stability of colloidal aqueous systems containing nanoparticles from the transmittance values. The transmittance values were measured for the reaction mixtures of the different CLHA matrix products. These colloid dispersions are transparent or mildly opalescent systems. The transmittance values ranged between 91% and 99%. The transmittance of A_2_25 was lower than that of A_1_25, and that of A_3_25 was lower than that of A_2_25 (Figure 16).

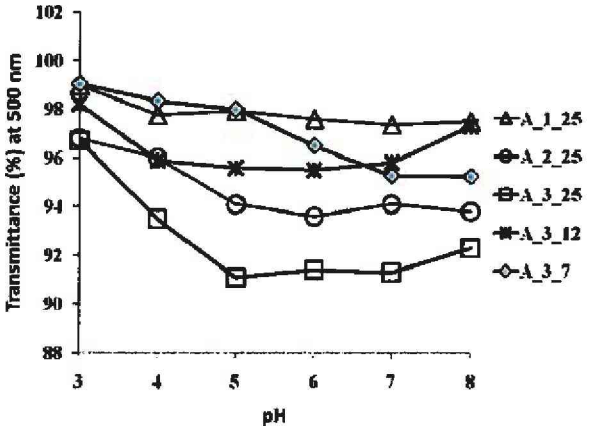

Figure 16. Transmittance of CLHA nanoparticles and effect of pH

A_1_25: c_{HA} = 1 mg/ml, at a stoichiometric cross-linking ratio of 25%, prepared in water;

A_2_25: c_{HA} = 2 mg/ml, at a stoichiometric cross-linking ratio of 25%, prepared in water;

A_3_25: c_{HA} = 3 mg/ml, at a stoichiometric cross-linking ratio of 25%, prepared in water;

A_3_12: c_{HA} = 3 mg/ml, at a stoichiometric cross-linking ratio of 12%, prepared in water;

A_3_7: c_{HA} = 3 mg/ml, at a stoichiometric cross-linking ratio of 7%, prepared in water

These results correspond with the Bouguer-Lambert-Beer law that transmittance values can be reduced due to increased concentration. The transmittance values were very high in the pH range 3–8 because of the solvation of the CLHA nanoparticles in the aqueous medium. Stable colloid particles were formed over a wide pH range of pH 3–8 in the different media (Figure 17) during 3 weeks. The stability of these nanoparticles was not dependent on the medium or the feed ratio (from 7 to 25): no aggregation was found after several weeks.

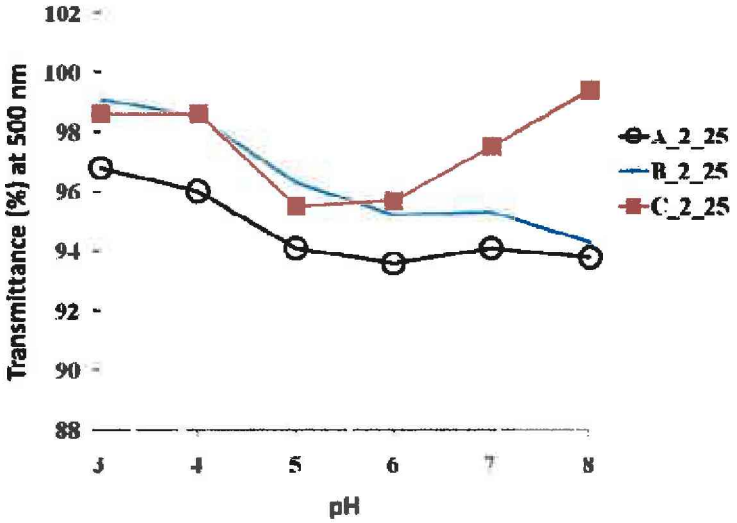

Figure 17. Effects of pH and medium on the transmittance values of CLHA nanoparticles A_2_25: c_{HA} = 2 mg/ml, at a stoichiometric cross-linking ratio of 25%, prepared in water; B_2_25: c_{HA} = 2 mg/ml, at a stoichiometric cross-linking ratio of 25%, c_{NaCl} = 0.09 m/m%; C_2_25: c_{HA} = 2 mg/ml, at a stoichiometric cross-linking ratio of 25%, c_{NaCl} = 0.9 m/m%;

4.1.5 Rheological measurements

Viscosity, an important property of colloid systems, is related to the nature and the extent of the intermolecular interactions, and the entanglements of the polymer chains. The shear rate dependence of the shear stress (Figure 18) is shown for HA and CLHA nanoparticles.

The shear stress vs. shear rate graphs ("flow curves") indicate shear thinning, reflecting the fact that the macromolecular systems behave as pseudoplastic materials. This form becomes more and more linear as the cross-linking reactions result in smaller and smaller particles. This result indicates that no interconnected network structures were formed. The flow curves of the purified nanoparticle system run lower than that for the native HA, which proves that the successful cross-linking method resulted in small particles.

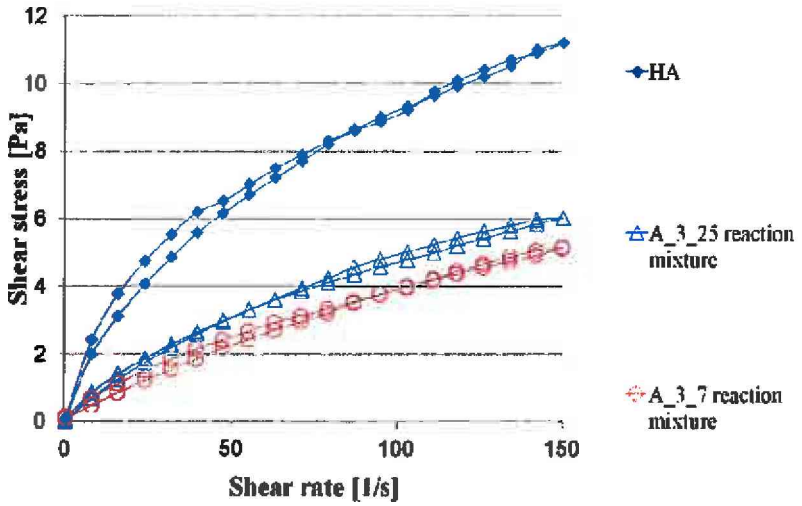

Figure 18. Shear rate dependence of the shear stress for the systems of HA and its cross-linked derivatives at the indicated cross-linking ratios: A_3_25 c_{HA} = 3 mg/ml, cross-linking ratio: 25%, prepared in water, A_3_7 c_{HA} = 3 mg/ml, cross-linking ratio: 7%, prepared in water

The comparison of the curve for the purified nanoparticle system ('after dial') and that for the unpurified nanoparticle system ('reaction mixture') (Figure 19) reveals that the curve for the reaction mixture runs lower than that for the dialysed sample, and the unpurified nanoparticle system contains small particles, which are missing from the purified sample. The DLS and GPC results suggested the diffusion of smaller CLHA particles through the wall of the dialysis membrane. The applied pore size of the wall was 12 000 Da.

The rheology properties are connected with the composition of the polydisperse system, i.e. the sizes of the nanoparticles and their PSD.

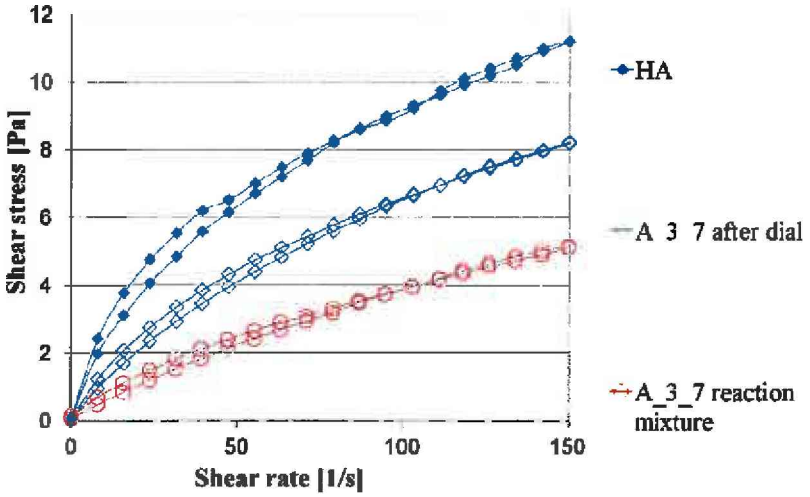

Figure 19. Effect of purification on the rheological properties of CLHA nanoparticles (c_{HA}=3 mg/ml, pH=6.3±0.2)

A_3_7 reaction mixture: c_{HA} = 3 mg/ml, cross-linking ratio: 7%, prepared in water, without purification;

A_3_7 after dial: c_{HA} = 3 mg/ml, cross-linking ratio: 7%, prepared in water, after purification

The small particles produced in the applied cross-linking process can be lost during the purification, while the larger nanoparticles can remain in the purified system. The properties of these purified systems were determined by the larger particles.

4.2 Results on the semisolid linear HA and CLHA preparations

4.2.1 Results of rheological measurements

The produced CLHA nanoparticles have lower viscosity than that of the parent linear biopolymer because of the contraction of linear chains in connection with the intrachain cross-linking and the absence of entanglement coupling (Bodnar et al.). Figure 20 shows the flow curves of CLHA and linear HA. Both gels exhibited slight thixotropy. The shear stress of the CLHA was a little lower than that of the linear HA, which confirmed the successful cross-linking and the formation of smaller particles.

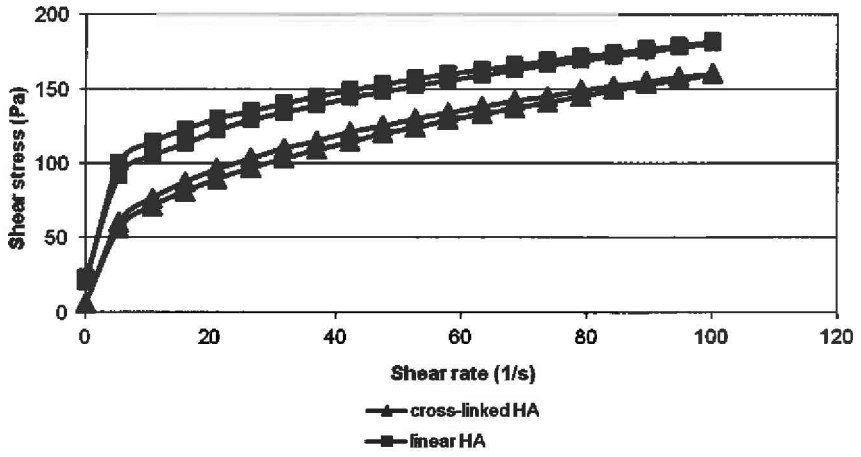

Figure 20. Flow curves of semisolid preparations containing linear HA or CLHA

The elastoviscous nature of linear HA has been studied quite extensively. At lower frequencies the HA gel behaves as a viscous solution, while at higher frequencies it behaves elastically [95-96]. These properties are shown by the changes in the elastic storage modulus (*G'*), and the viscous loss modulus (*G''*) as a function of frequency (Figure 21).

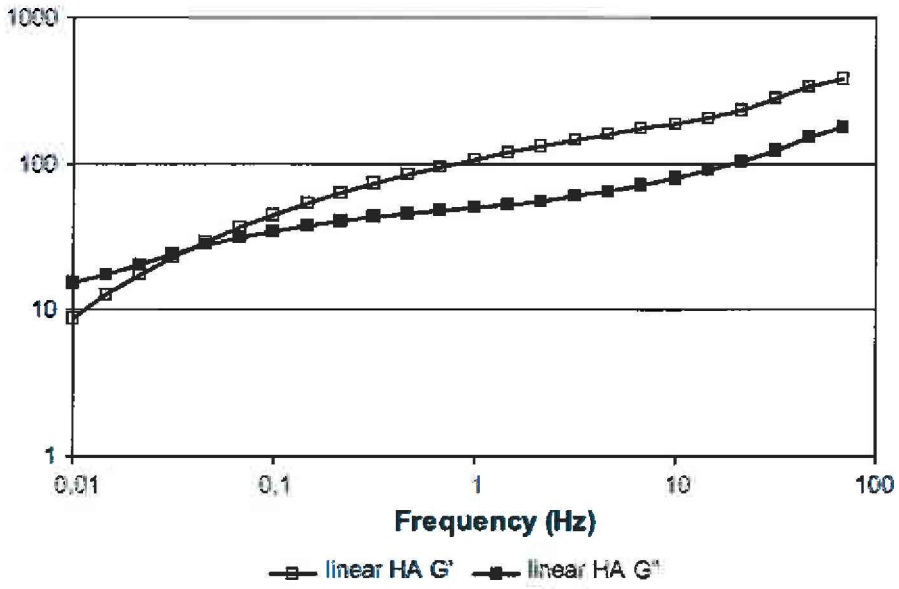

Figure 21. Storage modulus (*G'*) and loss modulus (*G''*) of linear HA.

The transition from viscous to elastic behaviour is marked by the cross-over point of the two curves. This specific elastoviscous property appears in the CLHA curves too (Figure 22).

However, it requires a higher frequency to reach the cross-over point, which results in the elastic property of the preparation containing CLHA. The elasticity (*G'* values) of the gel is decreased, thanks to the modification of the molecule.

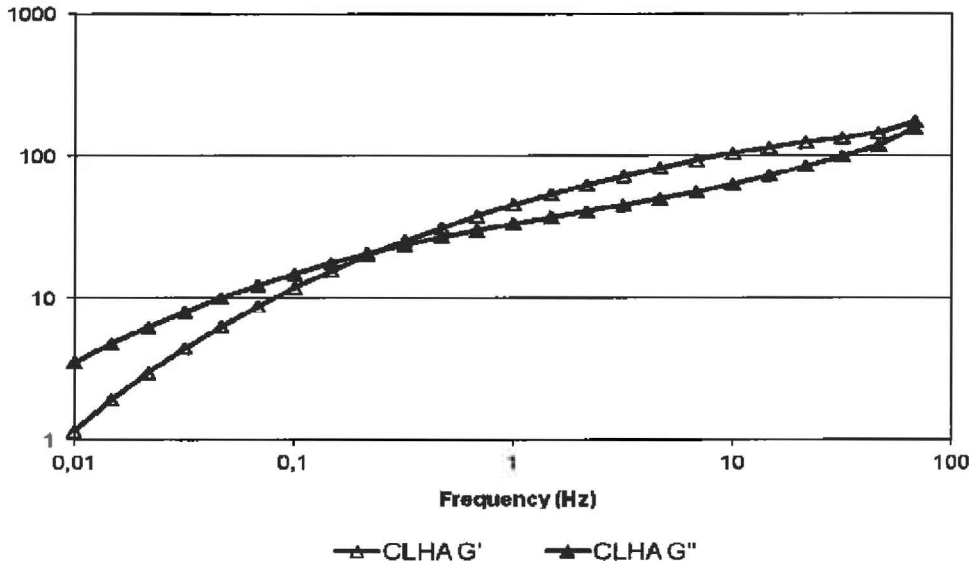

Figure 22. Storage modulus (*G'*) and loss modulus (*G"*) of CLHA.

4.2.2 Results of hydration and irritation tests

Corneometry determines the water content of the SC. It was found that there were no differences in the hydration effects of the CLHA and the linear HA. Linear HA is known to hydrate the skin surface; after the chemical modification, the CLHA retained the hydration effect (Figure 23).

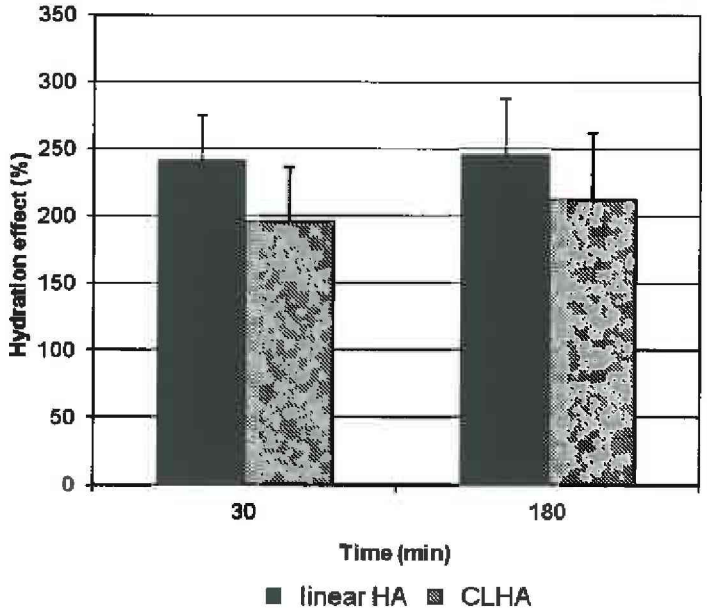

Figure 23. Hydration effects of linear HA and CLHA

In this study the cross-linking ratio was 25%. TEWL proved to be decreased after the application of the CLHA gel, which means that it undergoes longer hydration with no irritation effect on the skin (Figure 24).

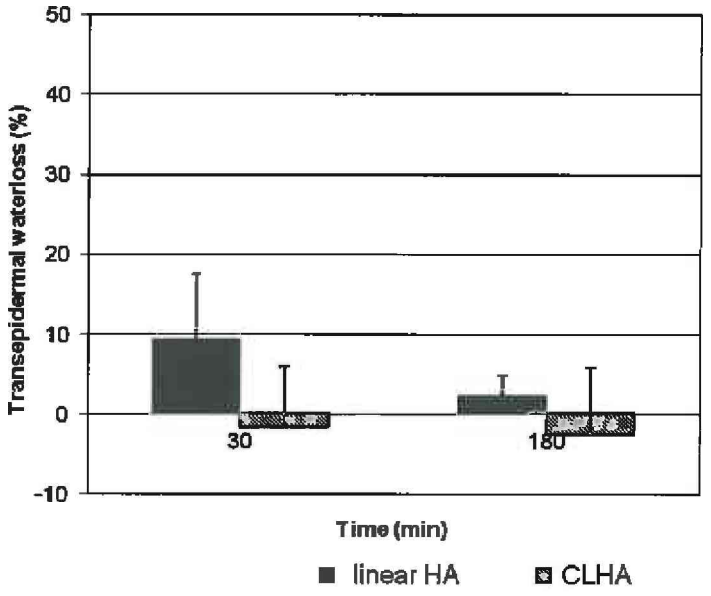

Figure 24. Transepidermal water loss of linear HA and CLHA

4.2.3 Diffusion, penetration and *in vivo* studies

Figure 25 depicts the rate of cumulation per unit area of linear HA and CLHA that diffused through the synthetic membrane.

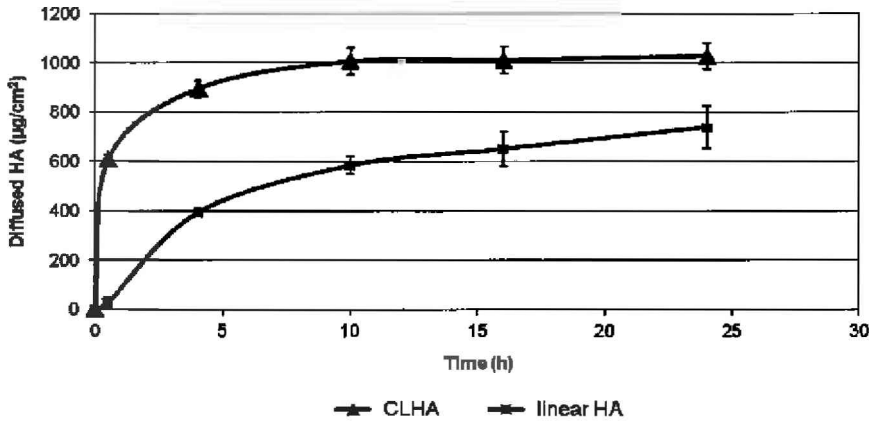

Figure 25. Cumulative amount of HA that diffused through a synthetic membrane

It is clear that the diffusion of the CLHA was more intensive. After 10 h, a steady state was seen. The calculated results after 24 h: 1028 µg/cm^2. The linear HA also diffused through the synthetic membrane, but more slowly, and the amount diffused was significantly less, at 739 µg/cm^2 (after 24 h). The better diffusion of the CLHA may be explained by the lower viscosity and the smaller particle size. The penetration through the human epidermis is illustrated in Figure 26.

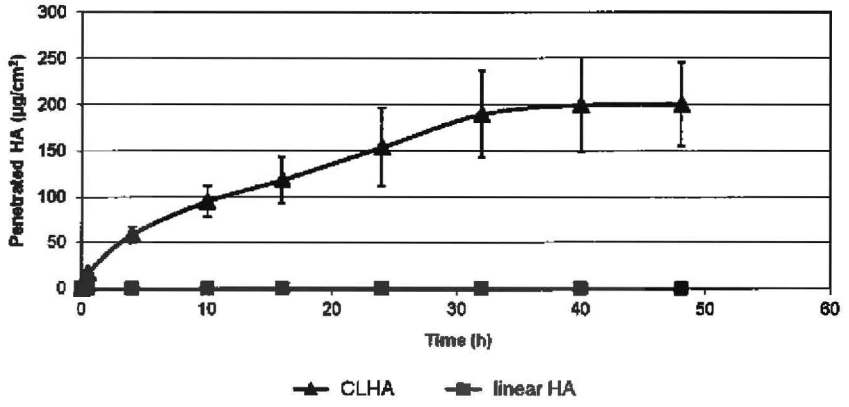

Figure 26. Cumulative amount of HA that penetrated through the human epidermis

There was no detectable penetration of linear HA during the observation period, whereas the level of penetration of CLHA was 200 μg/cm^2 (after more than 45 hours).
Figure 27 demonstrates the penetration of the CLHA and the linear HA as a function of time through living animal skin.

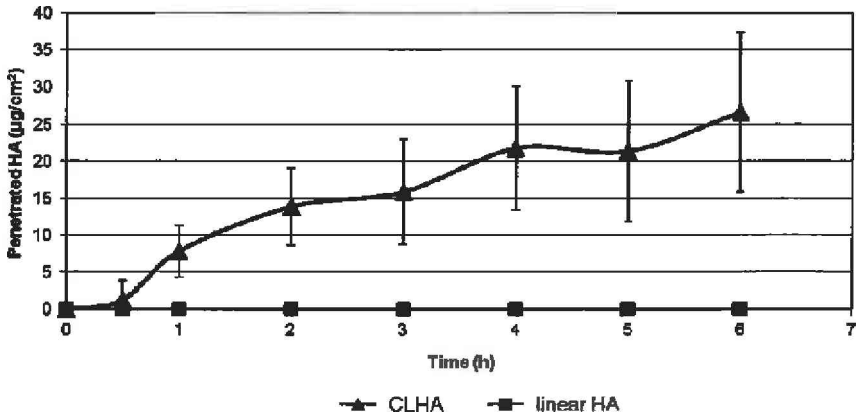

Figure 27. Cumulative amount of HA that penetrated through living animal skin

Similarly as in the *ex vivo* human epidermis study, there was no detectable penetration of linear HA. The quantity of CLHA that penetrated displayed a considerable elevation during the observation period; it increased steadily to about 26 μg/cm^2 by the end of the experiment.

4.2.4 Analysis of penetration

Penetration parameters (Table 6) were obtained from plots of the cumulative amount of HA penetrated per cm^2 (Q) versus time.

Table 6. Penetration parameters of CLHA. The data are the means (±SD) of six parallel measurements

	Comulative amount (%)	Q (μg/cm^2)	J (μg/cm^2/h)	K_p x 10^{-3} (cm/h)	T_{lag} (h)
Human epidermis	11.0±7.34	200±118	31.528	3.1528	0.12
Animal model	4.08±3.7	26.55±24	13.489	1.3489	0.49

The steady state flux (*J*) reflecting the absorption rate per unit area, and the lag time (T_{lag}) (symbolizing the duration of the delay between the first contact of the drug with the skin surface and the attainment of a steady state flux) were obtained from the slope and x intercept of the linear regression versus $t_{1/2}$, respectively. The permeability coefficient (K_p) was calculated according to Fick's first law of diffusion, based on the steady state flux and the applied drug concentration (C_d) of the donor phase: $K_p = J/C_d$ *(2)*

The absorption rate and permeability coefficient were about 3 times higher in the case of the human epidermis. The lower absorption rate and permeability coefficient and the longer lag time can be explained by the fact that the CLHA has to cross the epidermis, dermis and skin muscle to reach the acceptor phase, the penetration route therefore being much longer in the case of the animal model.

5 Summary

The primary aim of my Ph.D. work was to prepare and investigate a crosslinked HA.

- The nanoparticles obtained were spherical with a size in the nanometric scale. Their physico-chemical properties, including the transmittance of an aqueous system containing nanoparticles and the hydrodynamic size of the HA nanoparticles, were controlled by varying the cross-linking density, the concentration of native HA and the parameters of the media.
- The TEM and rheology results proved the existence of systems of well-dispersed spherical HA nanoparticles.

The manufacturing process was studied.

- The DLS, transmittance and TEM results demonstrated that increase of the concentration of the native HA (from 1 mg/ml to 3 mg/ml) resulted in smaller product particles.

  Comparisons of the particle sizes (TEM), particle size distributions (DLS) and molecular weight distributions in different phases of the technology led to the recognition of the loss of the smaller particles during the dialysis. The rheology results support the DLS and GPC results: the majority of the cross-linked nanoparticles are formed with a size less than 20 nm, but these particles can be lost during the purification.
- The electrical double layer and the measured HD were suppressed in media of higher conductivity. When the pH was increased, the HD displayed an increasing tendency. Narrower particle size range systems were observed at higher salinity, which did not change significantly when the pH was modified.
- The stability of these nanoparticles was not dependent on the medium and feed ratio (from 7 to 25%), and no aggregation was found after 3 weeks.

A semisolid HA-based nanoparticulate preparation was investigated in comparison with a hydrogel containing linear HA.

- This experimental work has revealed the advantages of CLHA over linear HA in dermal applications. The cross-linking of the linear HA molecule changes its

rheological parameters. The shear stress decreases in response to cross-linking. The dynamic rheological measurements proved that the specific elastoviscous property of the HA gel was slightly changed after the cross-linking procedure.

- The corneometric tests revealed that the hydration effect was preserved. There was no irritant effect of the CLHA molecule in TEWL tests.
- The diffusion and penetration study demonstrated that the cross-linking of HA resulted in better diffusion through a synthetic membrane and better penetration through the human epidermis and living animal skin than when linear HA was used, where no penetration was observed. The cross-linking of HA makes it suitable for transdermal applications, promoting hydration in deeper layers of the skin and giving the possibility of a signal effect for HA production. CLHA can lead to the development of an API carrier system for deep penetration into the skin.

REFERENCES

1 Peer,D., Karp,J.,M., Hong,S., Farokhzad,O.,C., Margalit,R., Langer,R. (2007) Nanocarriers as an emerging platform for cancer therapy. Nat. Nanotechnol., 2, 751–760.

2 Veiseh,O., Kievit,F.,M., Ellenbogen,R.,G., Zhang,M. (2011) Adv. Drug Delivery Reviews, 8, 582-596.

3 Laurent,U., Reed,R.,K. (1991) Turnover of hyaluronan in the tissues. Adv. Drug Delivery Reviews, V.7, 2, 237-256.

4 Ji,Y., Ghosh,K., Shu,X., Li,B., Sokolov,J., Prestwich,G.D., Clark,R., Rafailovich,M. (2006) Electrospun three-dimensional hyaluronic acid nanofibrous scaffolds. Biomaterials, 27, 3782–3792.

5 Almond,A., DeAngelis,P., Blundell,C. (2006) Hyaluronan: The Local Solution Conformation Determined by NMR and Computer Modeling is Close to a Contracted Left-handed 4-Fold Helix. J. Mol. Biol., 358, 1256–1269.

6 Robert,L., Robert,A.,M., Renard,G. (2010) Biological effects of hyaluronan in connective tissues, eye, skin, venous wall. Pat. Biologie, V58, 3, 187–198.

7 Witteveen,A., Sierevelt,I., Blankevoort,L., Kerkhoffs,G., Dijk,N. (2010) Intra-articular sodium hyaluronate injections in the osteoarthritic ankle joint: Effects, safety and dose dependency. Foot and Ankle Surg., V16, 4, 159–163.

8 Salk,R., Chang,T., D'Costa,W., Soomekh,D., Grogan,K. (2006) Sodium Hyaluronate in the Treatment of Osteoarthritis of the Ankle: A Controlled, Randomized, Double-Blind Pilot Study. J. Bone Joint. Surg. Am., 88, 295-302.

9 Strand,V., Conaghan,P., Lohmander,L., Koutsoukos,A., Hurley,F., Bird,H., Brooks,P., Day,R., Puhl,W., Band,P. (2006) An integrated analysis of five double-blind, randomized controlled trials evaluating the safety and efficacy of a hyaluronan product. OsteoArthritis and Cart., 14, 859-866.

10 Nakamura,M., Sato,N., Chikama,T., Hasegawa,Y., Nishida,T. (1997) Hyaluronan Facilitates Corneal Epithelial Wound Healing in Diabetic Rats, Exp. Eye Res., 64, 1043-1050.

11 Avila,L., Gianolio,D., Konowicz,P., Philbrook,M., Santos,M., Miller,R. (2008) Drug Delivery and Medical Applications of Chemically Modified Hyaluronan. Carboh. Chem., Biology and Medical Appl., Pages 333-357 .

12 Oh,E., Park,K., Kim,K., Kim,J., Yang,J., Kong,J., Lee, M., Hoffman,A., Hahn,S. (2010) Target specific and longacting delivery of protein, peptide, and nucleotide therapeutics using hyaluronic acid derivatives. J. Contr. Release, 141, 2-12.

13 Leach,J., Schmidt,C. (2005) Characterization of protein release from photocrosslinkable hyaluronic acid-polyethylene glycol hydrogel tissue engineering scaffolds. Biomaterials, 26, 125–135.

14 Kim,M., Park,T. (2002) Temperature-responsive and degradable hyaluronic acid /Pluronic composite hydrogels for controlled release of human growth hormone. J. of Cont. Release, 80, 69–77.

15 Li,H., Liu,Y., Shu,X., Gray,S., Glenn D. (2004) Prestwich, Synthesis and Biological Evaluation of a Cross-Linked Hyaluronan-Mitomycin C Hydrogel. Biomacr., 5, 895-902.

16 Choi,K., Lee,S., Park,K., Kim,K., Parka,J., Kwon,I., Seo Y. (2008) Preparation and characterization of hyaluronic acid-based hydrogel nanoparticles. J. of Physics and Chem. of Solids, 69, 1591–1595.

17 Segura,T., Chung,P., Shea,L. (2005) DNA delivery from hyaluronic acid-collagen hydrogels via a substrate-mediated approach. Biomaterials, 26, 1575–1584.

18 He,M., Zhao,Z., Yin,L., Tang,C., Yin,C. (2009) Hyaluronic acid coated poly(butyl cyanoacrylate) nanoparticles as anticancer drug carriers. Int. J. of Pharmaceutics, 373, 165–173.

19 Moriyama,K., Ooya,T., Yui,N., (1999) Hyaluronic acid grafted with poly(ethylene glycol) as a novel peptide formulation. J. of Cont. Release, 59, 77–86 .

20 Lee,H., Mok,H., Lee,S., Oh,Y., Park,T. (2007) Target-specific intracellular delivery of siRNA using degradable hyaluronic acid nanogels. J. of Contr. Release, 119, 245–252.

21 Luten,J., Nostrum,C., Smedt,S., Hennink,W. (2008) Biodegradable polymers as non-viral carriers for plasmid DNA delivery. J. of Contr. Release, 126, 97–110.

22 Kim,I., Mauck,R., Burdick,J. (2011) Hydrogel design for cartilage tissue engineering: A case study with hyaluronic acid. Biomaterials; 32, 8771-8782.

23 Pitarresi,G., Craparo,E., Palumbo,F., Carlisi,B., Giammona,G. (2007) Composite Nanoparticles Based on Hyaluronic Acid Chemically Cross-Linked with α,β-Polyaspartylhydrazide. Biomacrom., 8, 1890-1898.

24 Liu,Y., Shu,X., Prestwich,G. (2005) Biocompatibility and stability of disulfide-crosslinked hyaluronan films. Biomaterials, 26, 4737–4746.

25 Yamanlar,S., Sant,S., Boudou,T., Picart,C., Khademhosseini,A. (2011) Surface functionalization of hyaluronic acid hydrogels by polyelectrolyte multilayer films. Biomaterials; 32, 5590-5599.

26 Dulong,V., Lack,S., Cerf,D., Picton,J., Vannier,L., Muller,G. (2004) Hyaluronan-based hydrogels particles prepared by crosslinking with trisodium trimetaphosphate. Synthesis and characterization. Carb. Polymers, 57, 1–6.

27 Yeo,Y., Highley,C., Bellas,E., Ito,T., Marini,R., Langer,R., Kohane,D. (2006) In situ crosslinkable hyaluronic acid hydrogels prevent post-operative abdominal adhesions in a rabbit model. Biomaterials, 27, 4698-4705.

28 Choi,K., Min,K., Na,J., Kim,K., Park,J. (2009) Self-assembled hyaluronic acid nanoparticles as a potential drug carrier for cancer therapy: Synthesis, characterization, and in vivo biodistribution. J. of Materials Chem., 19, 4102–4107.

29 Benedetti,L., Topp,E., Stella,V. (1990) Microspheres of hyaluronic acid esters – Fabrication methods and in vitro hydrocortisone release. J. of Contr. Release, 13, 33–41.

30 Esposito,E., Menegatti,E., Cortesi,R. (2005) Hyaluronan-based microspheres as tools for drug delivery: A comparative study. Int. J. of Pharmaceutics, 288, 35–49.

31 Dehazya, P., Lu,C. (2002) Sodium hyaluronate microspheres.WO2002/041877.

32 Yun,Y., Goetz,D., Yellen,P., Chen,W. (2004) Hyaluronan microspheres for sustained gene delivery and site-specific targeting. Biomaterials, 25, 147–157.

33 Lai,J., Ma,D., Cheng,H., Sun,C., Huang,S., Li,Y. (2010) Ocular biocompatibility of carbodiimide cross-linked hyaluronic acid hydrogels for cell sheet delivery carriers. J. of Biomat. Science, 21, 359–376.

34 Yang,J., Yamato,M., Nishida,K., Ohki,T., Kanzaki,M., Sekine,H. (2006) Cell delivery in regenerative medicine: The cell sheet engineering approach. J. of Contr. Release, 116, 193–203.

35 Burns,J., Cox,S., Walts,A. (1991) Water insoluble derivatives of hyaluronic acid. US 5017229.

36 Cascone,M.,G., Sim,B., Sandra,D. (1995) Blends of synthetic and natural polymers as drug delivery systems for growth hormone. Biomaterials, 16, 569–574.

37 Antunes,J., Oliveira,J., Reis,R., Soria,J., Gomez-Ribelles,J., Mano,J. (2010) Novel poly(l-lactic acid)/hyaluronic acid macroporous hybrid scaffolds: Characterization and assessment of cytotoxicity. J. of Biom. Mat., 94, 856–869.

38 Borbely,J.; Rente,T.; Bodnar,M.; Schriffertne Denyicska,I. (2011) Hyaluronic acid-based cross-linked nanoparticles. US7,879,818

39 Bodnár,M., Daróczi,L., Batta,Gy., Bakó,J., Hartmann,J., Borbély,J. (2009) Preparation and characterization of cross-linked hyaluronan nanoparticles. Colloid. Polym. Sci., 287,991-1000.

40 Kvam,B., Atzori,M., Toffanin,R., Paoletti,S., Biviano,F. (1992) ^{1}H- and ^{13}C-NMR studies of solutions of hyaluronic acid esters and salts in methyl sulfoxide: comparison of hydrogen-bond patterns and conformational behaviour. Carbohydr. Res., 230,1.

41 Scott,J.E., HeatleyF. (1999) Hyaluronan forms specific stable tertiary structures in aqueous solution: A ^{13}C NMR study. Proc. Natl. Acad. Sci., 96, 4850.

42 Ambrosio,L., Borzacchiello,A., Netti,P.,A., Nicolais,L. (1999) Rheological study on hyaluronic acid and its derivative solutions. J. of Macrom. Sci., 36, 991–1000.

43 Schafer,H., Redelmeier,T., E. (1997) Skin barrier: Principles of percutaneous absorption. Arch. Dermatol., 133-924.

44 Lee,J.H., Lee,Y.J., Kim,J.S., Yoon,M.K., Choi,Y.,W. (2005) Formulation of microemulsion systems for transdermal delivery of aceclofenac. Archives of Pharm. Research, 28, 1097–1102.

45 Souto,E.B., Muller,R.,H. (2008) Cosmetic features and applications of lipid nanoparticles (SLN®, NLC®). Int. J. of Cosmetic Sci., 30,157–165.

46 Contreras,L., Elizabeth,J. (2007). Human skin drug delivery using biodegradable PLGA-nanoparticles. Saarbrucken, Germany: Saarland University. Open Access Server SciDok: Scientific documents from Saarland University. Available from URL: http://scidok.sulb.uni-saarland.de/volltexte/2007/1118/.html.

47 Bouwstra,J., Pilgram,G., Gooris,G., Korten,H., Ponec,M. (2001) New aspects of the skin barrier organisation. Skin Pharmacology and Applied Skin Physiology, 14, 52–62.

48 Mahmoud,M. (2010) Radioimmunoassay and radiochemical procedure for determination of cutaneous uptake and metabolism of sex steroid hormones. Berlin, Germany: Freie Universitat Berlin. University Library: Dissertation Online. Available from URL: http://www.diss.fu-berlin.de/diss/ servlets/MCRFileNodeServlet/FUDISS derivate 000000001647/?lang=en.html.

49 Potts,R.,O., Bommannan,D.,B., Guy,R.,H. (1992) Percutaneous absorption. Pharmacology of the skin. Boca Raton, CRC Press, 14–26

50 Sznitowska,M., Janicki,S., Williams,A.,C. (1998) Intracellular or intercellular localization of the polar pathway of penetration across stratum corneum. J. of Pharm. Sci., 87, 1109–1114.

51 Kuchler,S., Radowski,M.,R., Blaschke,T., Dathe,M., Plendl,J., Haag,R., Schafer-Korting, M., Kramer,K.D. (2009) Nanoparticles for skin penetration enhancement – A comparison of a dendritic core-multishell-nanotransporter and solid lipid nanoparticles. Eur. J. of Pharm. and Biopharmaceutics, 71, 243–250.

52 Vauthier,C., Dubernet,C., Fattal,E., Pinto-Alphandary,H., Couvreur,P. (2003). Poly(alkylcyanoacrylates) as biodegradable materials for biomedical applications. Adv. Drug Delivery Rev., 55, 519–548.

53 Langer, R. (2004) Transdermal drug delivery: Past, progress, current status and future prospects. Adv. Drug Delivery Rev., 56, 557–558.

54 Schiller,J., Volpi,N., Hrabárová,E., Soltés,L., Hyaluronic Acid: A Natural Biopolymer. In:. Biopolymers: Biomedical and Environmental Applications. Kalia S, Avérous L. John Wiley & Sons, Inc., Hoboken, NJ, USA, 2011. p. 3-34.

55 Girish,K., Kemparaju,K. (2007) The magic glue hyaluronan and its eraser hyaluronidase. A biological overview. Life Sci., 80, 1921-43.

56 Anilkumar,T., Jaseer,M., Anumol,J., Arun,J., Mohanan,P., Krishnan,L. (2011) Advantage of hyaluronic acid as a component of fibrin sheet for care of acute wound. Biologicals, 39, 81-88.

57 Romagnoli,M., Belmontesi,M., Hyaluronic acid-based fillers: theory and practice. Clinics in Dermatology 2008; 26: 123-159.

58 Price,R., Berry,M., Navsaria,H. (2007) Hyaluronic acid: the scientific and clinical evidence. J. Plast. Reconstr. Aesthetic Surg., 60, 1110-1119.

59 Kong,M., Chen,X., Kweon,D., Park,H. (2011) Investigation on skin permeation of hyaluronic acid based nanoemulsions as transdermal carrier. Carb. Polymer, 86, 837-843.

60 Brown,M., Hanpanitcharoen,M., Martin,G. (2001) An in vitro investigation into the effect of glycosaminoglycans on the skin partitioning and deposition of NSAIDs. Intl. J. Pharm., 225, 113-121.

61 Masters,K., Shah,D., Leinwand,L., Anseth,K. (2005) Crosslinked hyaluronan scaffolds as a biologically active carrier for valvular interstitial cells. Biomaterials, 26, 2517-2525.

62 Lim,H., Cho,E., Lee,J., Kim,J. (2012) A novel approach for the use of hyaluronic acid-based hydrogel nanoparticles as effective carriers for transdermal delivery systems. Physicochem. Eng. Aspects, 402, 80-87.

63 Ilgin,P., Avci,G., Silan,C., Ekici,S., Aktas,N., Ayyala,R., John,V., Sahiner,N. (2010) Colloidal drug carriers from (sub)micron hyaluronic acid hydrogel particles with tunable properties for biomedical applications. Carbohydr. Polymer, 82, 997-1003.

64 Schanté,C., Zuber,G., Herlin,C., Vandamme,T.,F. (2011) Chemical modifications of hyaluronic acid for synthesis of derivatives for broad range of biomedical applications. Carbohydr. Polymer, 85, 469-489.

65 Banerji,S., Wright,A., Noble,M., Mahoney,D., Campbell,I., Day,A., (2007) Structures of the Cd44-hyaluronan complex provide insight into a fundamental carbohydrate–protein interaction. Nat. Structural and Molecular Biology, 14, 234–239.

66 Alkrad,J., Mrestani,Y., Neubert,R. (2003) The release profiles of intact and enzymatically digested hyaluronic acid from semisolid formulations using multi-layer membrane system. Eur. J. Pharm. Biopharm, 56, 37-41.

67 Hadgraft,J. (2001) Skin, the final frontier Int. J. Pharm., 224, 1–18

68 Kanitakis,J. (2002) Anatomy, histology and immunohistochemistry of normal human skin. Eur. J. Dermatol., 12, 390–397.

69 Trommer,H., Neubert, R.,H. (2006) Overcoming the stratum corneum: the modulation of skin penetration Skin Pharmacol. Appl. Skin Physiol., 19, 106–121.

70 Netzlaff,F., Schaefer,U.,F., Lehr,C.,M., Meiers,P., Stahl,J., Kietzmann,M., Niedorf,F. (2006) Comparison of bovine udder skin with human and porcine skin in percutaneous permeation experiments. Altern. Lab. Anim., 34, 499–513.

71 Bouwstra,J.,A., Ponec,M. (2006) The skin barrier in healthy and diseased state. Biochim. Biophys. Acta, 1758, 2080–2095.

72 Norlen L. (2001) Skin barrier structure and function: the single gel phase model. J. Invest. Dermatol., 117, 830–836.

73 Friend,D.,R. (1992) *In vitro* skin permeation techniques. J. Control. Release, 18, 235–248

74 Gray,G.,M., Yardley,H.,J. (1975) Lipid compositions of cells isolated from pig, human, and rat epidermis, J. Lipid Res., 16, 434–440.

75 Jacobi,U., Kaiser,M., Toll,R., Mangelsdorf,S., Audring,H., Otberg,N., Sterry,W. (2007) Lademann Porcine ear skin: an *in vitro* model for human skin. Skin Res. Technol., 13, 19–24.

76 Holbrook,K.,A., Odland,G.,F. (1974) Regional differences in the thickness (cell layers) of the human stratum corneum: an ultrastructural analysis. J. Invest. Dermatol., 62, 415–422.

77 Sandby-Moller,J., Poulsen,T., Wulf,H.,C. (2003) Epidermal thickness at different body sites: relationship to age, gender, pigmentation, blood content, skin type and smoking habits, Acta Derm.-Venereol., 83, 410–413.

78 Simon,G.,A., Maibach,H.,I. (2000) The pig as an experimental animal model of percutaneous permeation in man: qualitative and quantitative observations—an overview, Skin Pharmacol. Appl. Skin Physiol., 13, 229–234.

79 Simon,G.,A., Maibach,H.,I. (1998) Relevance of hairless mouse as an experimental model of percutaneous penetration in man, Skin Pharmacol. Appl. Skin Physiol., 11, 80–86.

80 Wester,R.,C., Maibach,H.,I. In vivo methods for percutaneous absorption measurements, R.L. Brounaugh, H.I. Maibach (1989) Percutaneous absorption: mechanisms-methodology-drug delivery (2nd edition), Marcel Dekker Inc., 215–237.

81 Sato,K., Sugibayashi,K., Morimoto,Y. (1991) Species differences in percutaneous absorption of nicorandil. J. Pharm. Sci., 80,104–107.

82 Lin,S.,Y., Hou,S.,J., Hsu,T.,H., Yeh,F.,L. (1992) Comparisons of different animal skins with human skin in drug percutaneous penetration studies, Methods Find. Exp. Clin. Pharmacol., 14, 645–654.

83 Moser,K., Kriwet,K., Naik,A., Kalia,Y., Guy R.H. (2001) Passive skin penetration enhancement and its quantification in vitro. Eur. J. Pharm. Biopharm., 52, 103-112.

84 Barry,B.W. (1987) Mode of action of penetration enhancers in human skin. Control. Rel., 6, 85-97.

85 http://www.ancient-minerals.com/transdermal-magnesium/how-topical/

86 Cevc,G., Vierl,U. (2010) Nanotechnology and the transdermal route: A state of the art review and critical appraisal. Control. Release, 141, 277-299.

87 Siewert,M., Dressman,J., Brown,C., Shah,V., (2003) FIP/AAPS Guidelines to Dissolution/in Vitro Release Testing of Novel/Special Dosage Forms. AAPS Pharm. Sci. Tech. 4, 1-10.

88 OECD. (2004). Skin Absorption: In Vitro Method. OECD,

89 Borgia,S., Schlupp,P., Mehnert,W., Schäfer-Korting,M. (2008) In vitro skin absorption and drug release – A comparison of six commercial prednicarbate preparations for topical use. Eur. J. of Pharmaceutics and Biopharmaceutics, 68, 380–389.

90 Laschke,M., Strohe,A., Scheuer,C., Eglin,D., Verrier,S., Alini,M., Pohlemann,T., Menger,M. (2009) In vivo biocompatibility and vascularization of biodegradable porous polyurethane scaffolds for tissue engineering. Acta Biomater, 5, 1991-2001.

91 Sckell A., Leunig MSckell,A., Leunig,M. (2009) Dorsal skinfold chamber preparation in mice : studying angiogenesis by intravital microscopy. Mol. Biol., 467, 305-317.

92 Sorg,H., Krueger,C., Vollmar,B., (2007) Extending the scope out of the chamber: Intravital insights in skin wound healing. J. Anat., 211 810-818.

93 Erős,G., Hartmann,P., Berkó,S., Csizmazia,E., Csányi,E., Sztojkov-Ivanov,A., Németh,I., Szabó-Révész,P., Zupkó,I., Kemény,L., (2012) A novel murine model for the in vivo study of transdermal drug penetration. The Scientific Word Journal 2012, 1-9.

94 Kligman,A., Christophers,E. (1963) Preparation of isolated sheets of human stratum corneum. Arch Dermatol; 88, 702-705.

95 Cowman,MK, Matsuoka,S. (2005) Experimental approaches to hyaluronan structure. Carbohydr. Res., 340, 791–809.

96 Balazs EA. (1974) The physical properties of synovial fluid and the special role of hyaluronic acid. In: Helfet A, editor. Disorders of the knee. Philadelphia: T. B. Lippincott Company, 63–75.

ACKNOWLEDGEMENTS

I would like to thank
Professor Piroska Szabó-Révész
Head of the Department of Pharmaceutical Technology
and present Head of the Ph.D. programme Pharmaceutical Technology
for providing me with the opportunity to work in this department and to complete my work under her guidance.

I would like to express my warmest thanks to my supervisor
Associate Professor Dr. Erzsébet Csányi
for her guidance, encouragement and numerous advices during my Ph.D. work.

I would like to express my most grateful thanks to
Dr. János Borbély and Dr. Magdolna Bodnár
for chance to reach my dream and numerous advices during my Ph.D work.

I am very grateful to **all of my co-authors** for their kind collaboration.

I thank **all members** of Department of Pharmaceutical Technology and **all members** of BBS Biochemicals LLC for their help and friendship.

I owe my thanks to my **family** for their encouragement, support understanding and for giving me a peaceful background.

ANNEX

I.

Carbohydrate Polymers 83 (2011) 1322–1329

Contents lists available at ScienceDirect

Carbohydrate Polymers

journal homepage: www.elsevier.com/locate/carbpol

Preparation and investigation of a cross-linked hyaluronan nanoparticles system

Mónika Maroda[a,b], Magdolna Bodnár[a], Szilvia Berkó[b], József Bakó[a], Gábor Erős[c], Erzsébet Csányi[b], Piroska Szabó-Révész[b], John F. Hartmann[d], Lajos Kemény[c], János Borbély[a,*]

[a] BBS Biochemicals LLC, Kiserdo 4, H-4225 Debrecen, Hungary
[b] Department of Pharmaceutical Technology, University of Szeged, Eötvös 6, H-6720 Szeged, Hungary
[c] Department of Dermatology and Allergology, University of Szeged, Korányi fasor 6-8, H-6720 Szeged, Hungary
[d] ElizaNor Polymer LLC, Princeton, NJ 08550, USA

ARTICLE INFO

Article history:
Received 6 April 2010
Received in revised form 26 July 2010
Accepted 23 September 2010
Available online 29 September 2010

Keywords:
Hyaluronic acid
Nanoparticle
Nanosphere
Cross-linking

ABSTRACT

The present paper describes the preparation and characterization of hydrophilic hyaluronan nanoparticles formed by cross-linking of hyaluronic acid (HA) with 2,2′(ethylenedioxy)bis(ethylamine) in the presence of water-soluble carbodiimide (CDI) in aqueous media. The particle size of cross-linked nanosystems was measured by dynamic light scattering (DLS) and transmission electron microscopy (TEM), transmittance by UV–VIS spectrophotometry, gel permeation chromatography (GPC) and rheology to characterize the physico-chemical properties.

The aqueous nanosystems prepared were stable, transparent or mildly opalescent with values of transmittance above 91%. It was observed, that a fraction of particles with size less than 20 nm, has been released during the purification by diafiltration. It was established that the hydrodynamic size of cross-linked HA nanoparticles can be controlled by variation of the reaction conditions such as concentration of HA, salt concentration of media, ratio of cross-linker and the final pH of the reaction mixture.

1. Introduction

Hyaluronic acid (HA) is a non-sulphated glycosaminoglycan that is an unbranched polysaccharide consisting of repetitive disaccharide units with reactive carboxyl groups. It is a biodegradable, biocompatible, non-toxic, non-immunogenic and non-inflammatory biomaterial; therefore, it has been used for several medical applications.

HA can be found in all tissues and body fluids of living creatures and most abundantly in the soft connective tissues. The total amount of HA in the adult human has been estimated to be 11–17 g (Laurent & Reed, 1991). The HA nanofibrous scaffold was successfully fabricated to mimic the architecture of natural extracellular matrix (Almond, DeAngelis, & Blundell, 2006; Ji et al., 2006).

The excellent water-binding capacity of HA is responsible for retaining moisture in eyes, joints, and skin tissues (Robert, Robert, & Renard, 2010). The solution of HA is highly viscous with unique viscoelastic properties which enables its use for orthopedy (Witteveen, Sierevelt, Blankevoort, Kerkhoffs, & van Dijk, in press). Many studies have been performed to create HA as an injectable form (Salk, Chang, D'Costa, Soomekh, & Grogan, 2006), which is used to treat osteoarthritis of the knee. (Strand et al., 2006).

HA can be used as an eye-treating solution (Nakamura, Sato, Chikama, Hasegawa, & Nishida, 1997). Oral application of HA has been lately suggested, although its effectiveness needs to be demonstrated.

Several HA derivatives have been developed for drug delivery. HA has potential as a biodegradable carrier for transdermal drug delivery (Avila et al., 2008). HA has also been used as a novel depot system (Oh et al., 2010). HA in the forms of physically and chemically cross-linked hydrogels (Kim & Park, 2002; Leach & Schmidt, 2005; Li, Liu, Shu, Gray, & Prestwich, 2004) has been developed as nano- and micro particulate systems (Choi et al., 2008; Segura, Chung, & Shea, 2005) for various protein, drug (He, Zhao, Yin, Tang, & Yin, 2009), peptide (Moriyama, Ooya, & Yui, 1999) or gene (Lee, Mok, Lee, Oh, & Park, 2007; Luten, van Nostrum, De Smedt, & Hennink, 2008) delivery.

Various methods have been developed to produce cross-linked hyaluronic acid, as hydrogels (Crescenzi, Francescangeli, Taglienti, Capitani, & Mannina, 2003; Masters, Shah, Leinwand, & Anseth, 2005), films (Liu, Shu, & Prestwich, 2005), or particulate systems (Dulong et al., 2004; Pitarresi, Craparo, Palumbo, Carlisi, & Giammona, 2007). Particulate systems are usually formed in emulsion, in which the size of droplets can control the size of particles. Solvent evaporation (Lim, Forbes, Berry, Martin, & Brown, 2002), spray-drying (Esposito, Menegatti, & Cortesi, 2005) and coacervation (Vasiliu, Popa, & Rinaudo, 2005) are also well-known techniques to produce micro- or nano-sized particulate systems.

* Corresponding author. Tel.: +36 52 542 743; fax: +36 52 541 742.
E-mail address: j.borbely50@gmail.com (J. Borbély).

0144-8617/$ – see front matter © 2010 Elsevier Ltd. All rights reserved.
doi:10.1016/j.carbpol.2010.09.039

Table 1
Reaction conditions of matrix products prepared in pure water.

Name	Medium	HA (mg)	Concentration of HA (mg/ml)	Stoichiometric ratio of cross-linking (%)	Quantity of diamin (1.0%, v/v) (μl)	Quantity of CDI (mg)
A_1_25	Water	50	1	25	228	9.3
A_2_25	Water	100	2	25	456	18.5
A_3_25	Water	150	3	25	684	27.8
A_3_12	Water	150	3	12	328	13.3
A_3_7	Water	150	3	7	191	7.8

In this work, preparation of stable cross-linked HA nanoparticles is described. The particulate systems were obtained by covalently cross-linking of carboxyl groups of HA linear chain with a 2,2′(ethylenedioxy)bis (ethylamine) in the presence of water-soluble carbodiimide (CDI) in aqueous media, as described earlier (Bodnár et al., 2009). The purpose of the present study was to investigate the effect of the reaction conditions on the formation of HA nanoparticles. It was observed that the salt and HA concentrations in the reaction mixture have significant effect on the size of particles formed.

The results based on TEM, DLS and rheology experiments reveal that well-dispersed HA nanoparticles systems with spherical shape were obtained. It was found that the particle sizes and size distribution can be influenced by the concentration of HA and the salt concentration of the media.

Intra and intermolecular cross-linking processes were formed and nanosystems with broad size distribution were produced, however, the smaller particles were lost during the dialysis.

2. Experimental

2.1. Materials

The HA sodium salt (M_W = 4350 kDa) was obtained from Gedeon Richter Ltd., Hungary. Quality of the sodium hyaluronate met the European Pharmacopoeia (Ph. Eur.) requirements. 2,2′(Ethylenedioxy)bis(ethylamine) and 1-[3-(dimethylamino) propyl]-3-ethylcarbodiimide methiodide (CDI) were purchased from Sigma–Aldrich, Co. The pH was adjusted with NaOH and HCl solutions as required. All other chemicals were analytical grade. Millipore-filtered water was used throughout the study.

2.2. Reaction conditions

2.2.1. Preparation of cross-linked hyaluronan nanoparticles

Cross-linked HA nanoparticles were prepared according to the procedure first reported by Bodnár et al. (2009). Briefly, HA (M_W = 4350 kDa) was dissolved in aqueous media to produce a clear solution, and then adjusted to pH 5.5. The diamine solution (1.0 v/v% in water, pH = 5.5) was added to the HA solution and mixed for 30 min at room temperature. The water-soluble CDI solution was added dropwise, and the reaction was stirred for 24 h. The solution containing hyaluronan nanoparticles was purified by dialysis and freeze-dried. The yield of HA nanoparticles was between 76% and 94%. The reaction conditions of cross-linked HA nanoparticles are summarized in Table 1, and synthesis scheme of cross-linking reaction is represented in Fig. 1.

2.2.2. Media

Aqueous media were used for the preparation of nanoparticles. The cross-linking reaction of HA was carried out in three different media such as pure water (designated with letter "A"), NaCl (c = 0.09%, w/w, and c = 0.9%, w/w) solutions (designated with letter "B" and "C", respectively). The water was purified by deionization, and reverse osmosis (Milli-Q-Plus instrument).

2.2.3. Matrix and matrix products

Matrix products are the end-products of the reactions which were synthesised under different reaction conditions, as medium applied, concentration of HA and the ratio of cross-linking. The nanoparticles obtained are identified by a three notation system as follows: the first letter means the media, the second notation is a number representing the concentration of HA (mg/ml), and the third notation stands for the stoichiometric ratio of cross-linking. For instance, A_1_25 notation means: the media is pure water (designated with letter "A"), concentration of HA is 1 mg/ml and the ratio of cross-linking is 25%.

A summary of the HA nanoparticles that have been prepared with their notations is shown in Table 2.

2.3. Characterization of the nanoparticles

2.3.1. Transmittance

Transmittances of cross-linked hyaluronan nanosystems were measured using an HP-8453 UV–VIS spectrophotometer at an operating wavelength of λ = 500 nm in optically homogeneous quartz cuvettes at 25 °C.

2.3.2. Dynamic light scattering (DLS)

Hydrodynamic diameter and size distribution of cross-linked hyaluronan nanosystems were measured using a Zetasizer Nano ZS instruments (Malvern Instruments Ltd., Worcestershire, UK), at an operating wavelength of λ_o = 532 nm. Measurements of size distribution and the Z-average size of nanoparticles were performed at 25 °C with an angle detection of 173° in optically homogeneous polystyrene cuvettes.

The samples were taken from the reaction mixture. Each sample was measured five times and average serial data were calculated.

The pH of the matrix products was adjusted by the addition of NaOH (c = 0.1 M) or HCl (c = 0.1 M) solutions.

2.3.3. Transmission electron microscopy (TEM)

Size and morphology of the dried hyaluronan nanoparticles were gauged by JEOL2000 FX-II transmission electron microscope.

For TEM observation, the hyaluronan nanoparticles were prepared from the reaction mixture at a concentration of 0.2 mg/ml. The pH of diluted colloid systems containing nanoparticles was adjusted to pH 10. The sample for TEM analysis was obtained by placing a drop (V = 10 μl) of the colloid dispersion onto a carbon-coated copper grid. The samples were dried at room temperature and then examined using a TEM without any further modification or coating.

The particle size distribution was obtained from measured particles visualized by TEM images and then analyzed using the Microsoft Office Excel 2007 program file.

Table 2
Matrix products of parallel reactions prepared in pure water.

A_1_25	A_2_25	A_3_25
A_1_12	A_2_12	A_3_12
A_1_7	A_2_7	A_3_7

2.3.4. Gel permeation chromatography (GPC)

GPC analysis of HA and that of cross-linked particles was performed on a Waters HPLC system using BioSuite 450 HR column. The effluent was monitored at 210 nm. The mobile phase was a mixture of 0.05 M NaOAc, 0.2 M NaCl and water–methanol with a ratio of 8:2 and the flow rate was 0.7 ml/min. Samples were dissolved in water, and filtered with a 5 μm pre-column sieve.

2.3.5. Rheology

Rheological measurements were carried out with a Physica MCR101 rheometer (Anton Paar, Austria). A cone-plate measuring device was used in which the cone angle was 1°, and the thickness of the sample was 0.046 mm in the middle of the cone. The measurements were performed at 25 °C. The pH was adjusted to 6.3 ± 0.2. Flow curves of the different samples were also determined. The

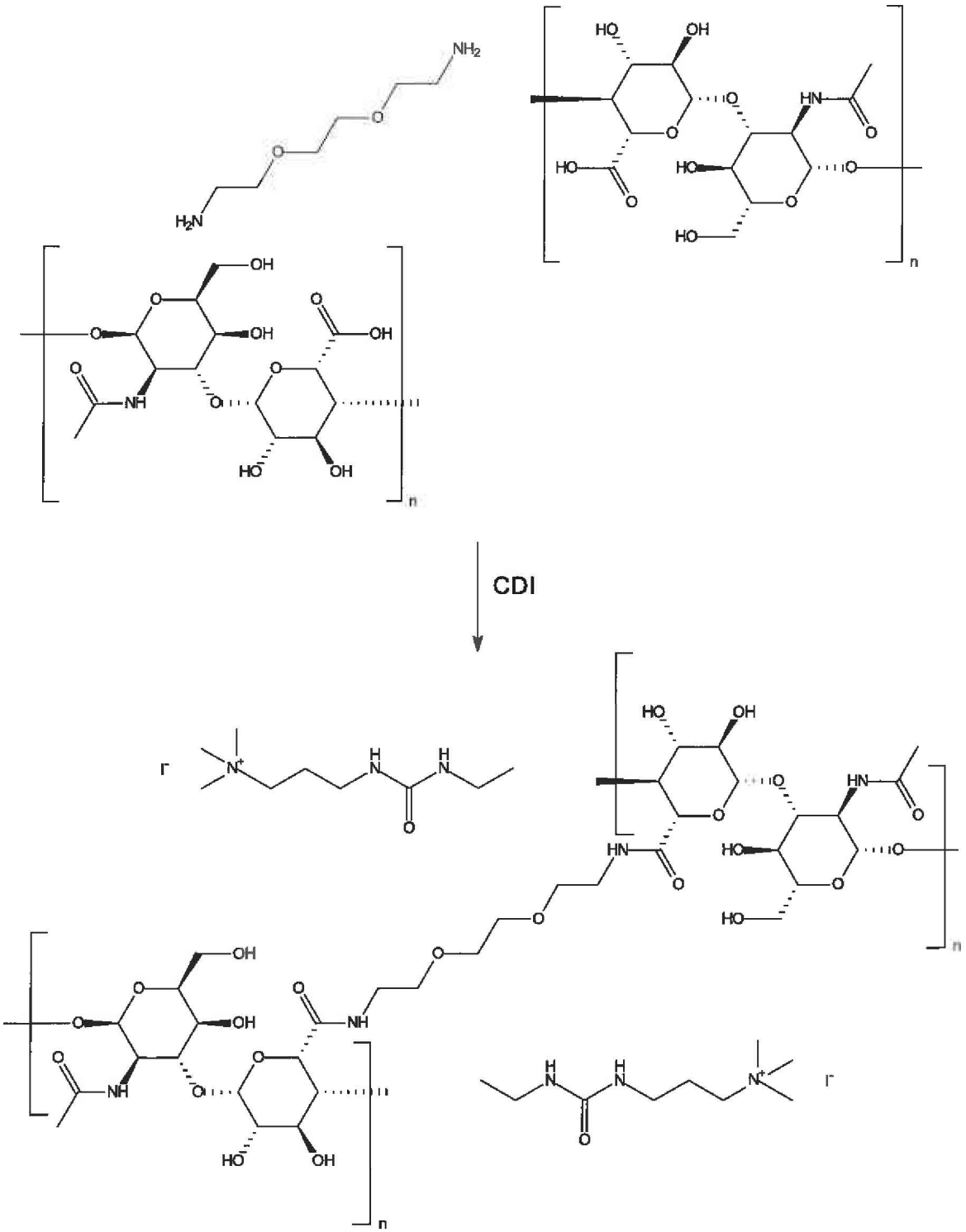

Fig. 1. Schematic representation of the synthesis of cross-linked HA derivatives.

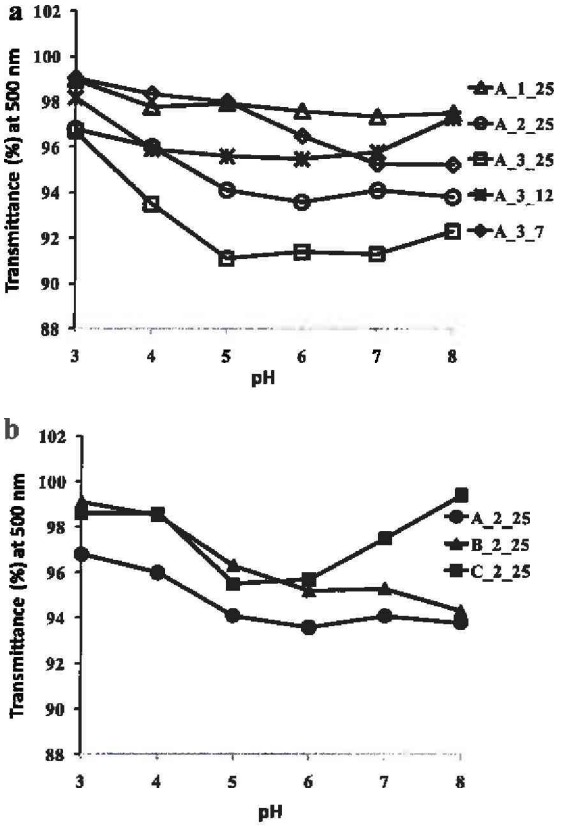

Fig. 2. (a) Effect of concentration of HA, the ratio of cross-linking and the pH of the environment on the transmittance of cross-linked hyaluronan nanoparticles. (b) Effect of pH and salt concentration of the media on the transmittance values of hyaluronan nanoparticles

shear rate was increased from 0.1 to 150 1/s (up curve), and then decreased from 150 to 0.1 1/s (down curve) in the CR mode. The shearing time was 300 s in case of both segments.

3. Results and discussion

3.1. Transmittance results

The transmittance values were measured from the reaction mixtures containing different cross-linked hyaluronan nanoparticles. These colloid dispersions were transparent or mildly opalescent systems in aqueous media. The transmittance values were between 91% and 99%.

The general trend that appears in Fig. 2a is in accordance with the Bouguer–Lambert–Beer law that transmittance values decrease due to the increasing concentrations of HA. The transmittance values were very high in wide pH range because of solvation of the cross-linked HA nanoparticles in aqueous media.

It was observed that the pH was not a factor for transmittance values of the aqueous systems. Stable colloid particles were formed over a wide pH range independently of the media (Fig. 2b) and ratio of cross-linking (from 7% to 25%, Fig. 2a).

3.2. DLS results

Samples were taken from the reaction mixture before and after dialysis. The pH of the samples was adjusted by sodium-hydroxide or hydrochloric acid solutions.

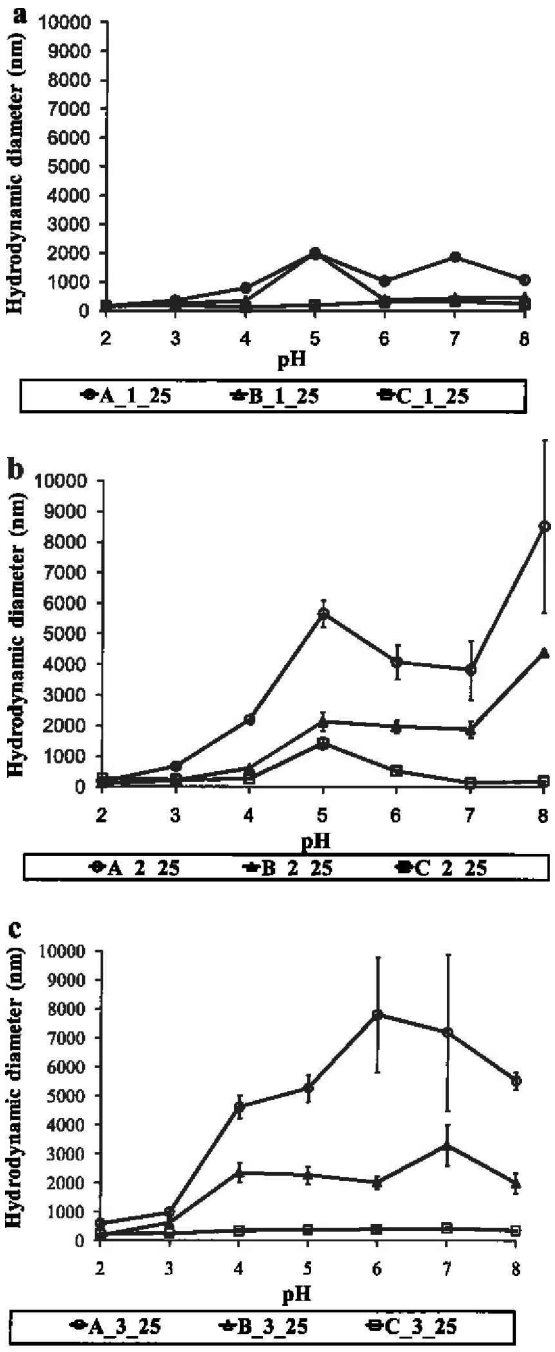

Fig. 3. Effect of pH and salt concentration of the medium on the *Z*-average hydrodynamic diameter of hyaluronan nanoparticles cross-linked at 25%, at the indicated HA concentration. (a) c_{HA} = 1 mg/ml; (b) c_{HA} = 2 mg/ml; and (c) c_{HA} = 3 mg/ml.

3.2.1. Hydrodynamic diameter

The cross-linking process of HA can result in intramolecular and intermolecular cross-linking. One part of cross-linked hyaluronan nanoparticles was formed as small, individual particles; however, large particles were also produced. The large particles can be aggregates, associations caused by secondary interactions or intermolecular cross-linked particles. Therefore, the hydrodynamic diameter of nanoparticles from reaction mixtures was not monomodal, so the *Z*-average size was used to compare hydrodynamic size.

Analysis of the *Z*-average size of nanoparticles (Fig. 3) revealed that the hydrodynamic diameter of nanoparticles decreases when the salt concentration of the media was increased.

Hydrodynamic size of swelled particles was calculated from the translational diffusion coefficient using the Stokes–Einstein equation: $d(H) = kT/3\pi\eta D$, where: $d(H)$ = hydrodynamic diameter, D = translational diffusion coefficient, k = Boltzmann's constant, T = absolute temperature, and η = viscosity. The translational diffusion coefficient depends both on the size of the particle and on the surface structure, as well as the salt concentration of the medium.

Low conductivity of the medium eventuates an extended double layer of ions around the particle, reducing the diffusion speed and

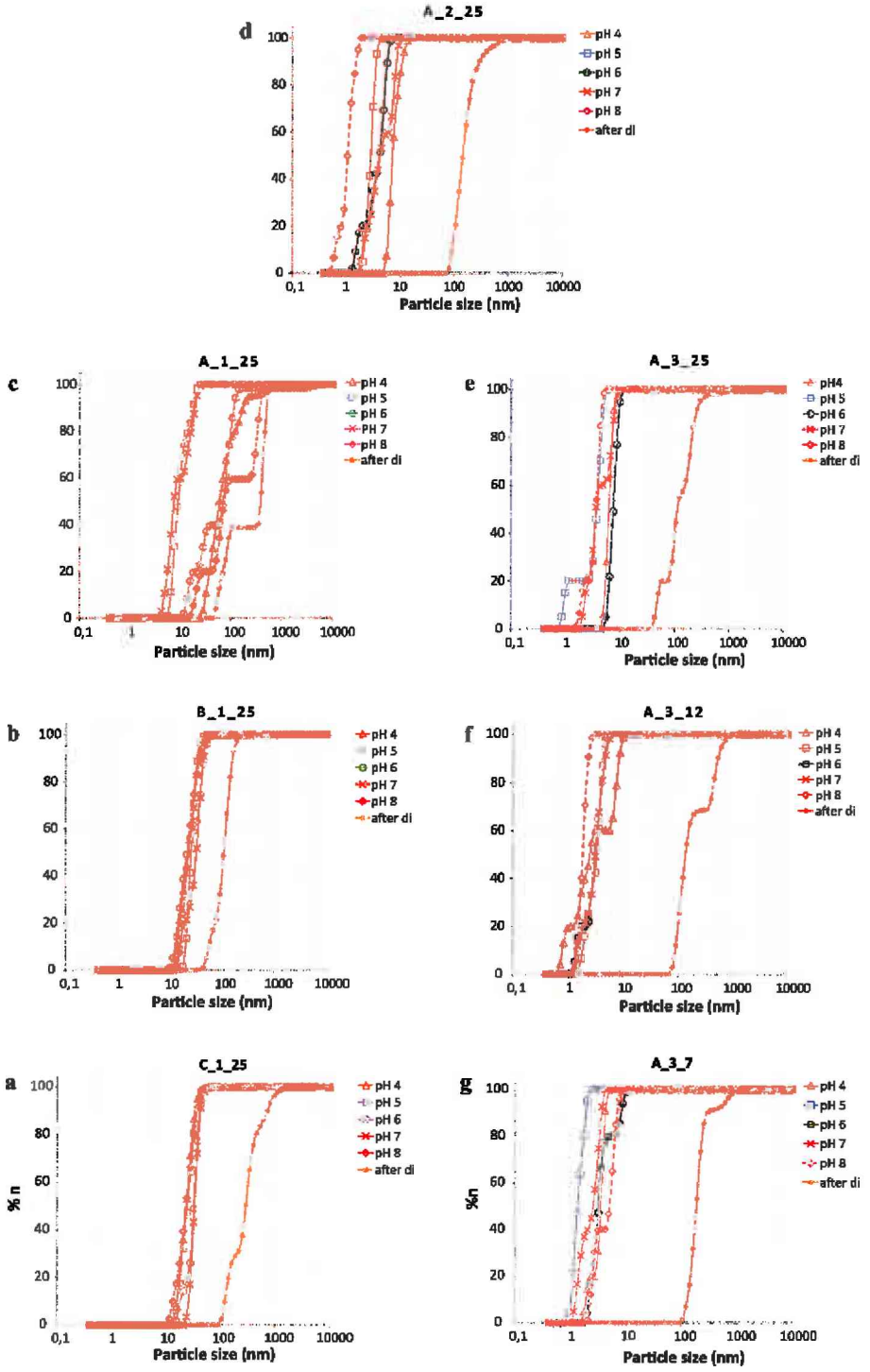

Fig. 4. Effect of pH and purification on the particle size distribution of cross-linked hyaluronan particles at the indicated reaction conditions: (a) c_{HA} = 1 mg/ml, ratio of cross-linking: 25%, c_{NaCl} = 0.9 m/m%; (b) c_{HA} = 1 mg/ml, ratio of cross-linking: 25%, c_{NaCl} = 0.09 m/m%; (c) c_{HA} = 1 mg/ml, ratio of cross-linking: 25%, prepared in water; (d) c_{HA} = 2 mg/ml, ratio of cross-linking: 25%, prepared in water; (e) c_{HA} = 3 mg/ml, ratio of cross-linking: 25%, prepared in pure water; (f) c_{HA} = 3 mg/ml, ratio of cross-linking: 12%, prepared in pure water; and (g) c_{HA} = 3 mg/ml, ratio of cross-linking: 7%, prepared in pure water.

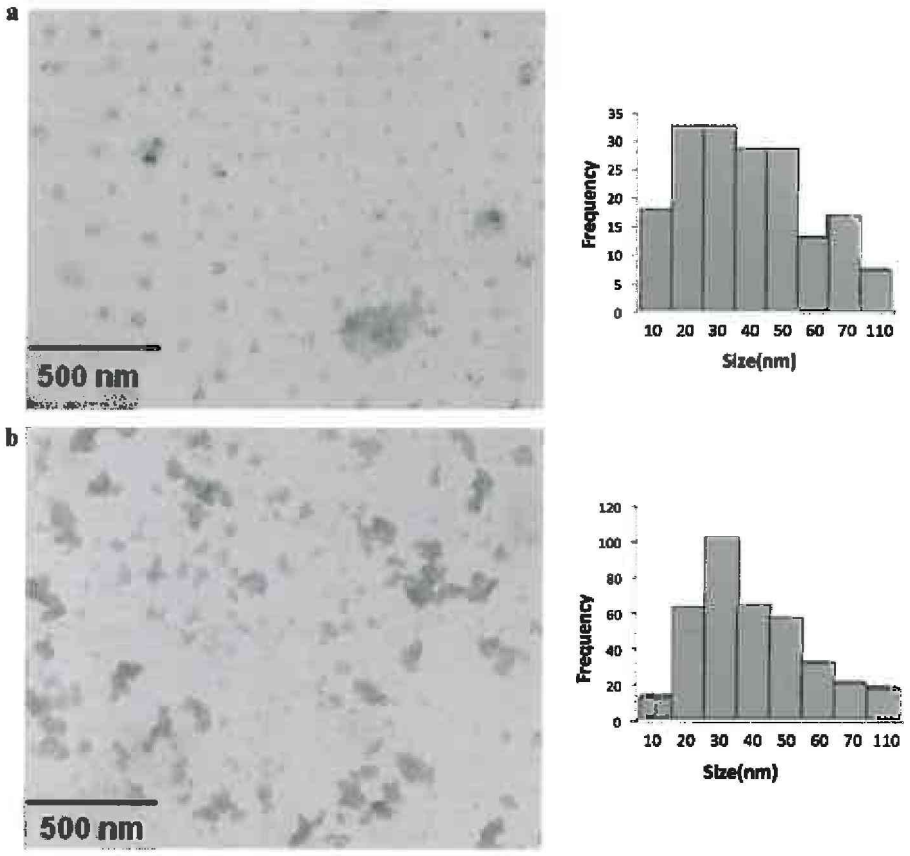

Fig. 5. TEM images and size distributions of cross-linked hyaluronan particles. (a) A_1_25 (c_{HA} = 1 mg/ml, at a cross-linking stoichiometric ratio of 25%, prepared in pure water) and (b) A_3_7 (c_{HA} = 3 mg/ml, at a cross-linking stoichiometric ratio of 7%, prepared in pure water).

resulting in a larger, apparent hydrodynamic diameter than using other media of higher conductivity.

Fig. 3 shows the effect of pH on the hydrodynamic size. It can be seen that by increasing the pH, the average size increased in all cases. This tendency increased as the initial concentration of HA increased and the salt concentration of medium decreased. The residual carboxyl groups of HA can be deprotonated, and the repulsive interactions between the negatively charged functional groups increase the size of particles.

To all appearances, the cross-linked hyaluronan particles can swell in aqueous media, the hydrodynamic size of particles depends on the pH and the salt concentration of the environment.

3.2.2. *Particle size distribution (PSD)*

Fig. 4 shows the particle size distribution of aqueous colloid systems containing cross-linked hyaluronan particles. Fig. 4c–e shows that the end point of number distribution profiles of the reaction mixtures shifts to the smaller particles by increasing the concentration of HA at the same 25% ratio of cross-linking. Namely, the HA formed smaller nanoparticles by increasing the concentration of HA a result independent of the pH.

The effect of cross-linking ratio on the hydrodynamic size was also studied.

Based on Fig. 4e–g it can be established that nano-sized particles with narrow size distribution can be obtained using lower (7% or 12%) cross-linking ratios. The size of nanoparticles in these systems was below 10 nm, and the pH was not a factor.

The effect of salt concentration on the size of the particles was also determined. Fig. 4a–c represents that by increasing the salinity of reaction mixtures, cross-linked particles with narrower size distribution were produced. Change in pH was without effect. Nevertheless, no significant correlations were established between the hydrodynamic diameters of swelled particles and the physicochemical parameters of the reactions; the size and size distribution of all hyaluronan particles were below 20 nm.

However, significant differences were observed between the PSD values of reaction mixtures and PSDs adopted for the dialyzed samples. The later mentioned profiles were indicated as 'after dial' text shown in Fig. 4. Considering that PSD for all of tested dialyzed matrix products showed a shift to the larger particle sizes, it became apparent that dialysis caused a loss of smaller particles. This was confirmed by GPC and rheology. The tested reaction mixtures contain larger particles, which make up all of the particles after dialysis.

In summary, the size and size distribution measurements indicate that intra- and intermolecular cross-linking processes did occur and nanosystems with broad size distribution were produced.

3.3. *TEM results*

TEM micrographs showed (Fig. 5) that the cross-linked nanoparticles were separated into spherical particles. TEM micrographs confirmed the nano-size of dried hyaluronan particles and showed the distribution of these derivatives. These results support the existence of the small nanoparticles ($d \sim 10$ nm) not only in the A_1_25 reaction mixture but also in A_3_7 where the HA concentration was higher and the ratio of cross-linking was lower. Based on the size distribution of histograms, it can be established that the sizes of the dried particles did not exceed 110 nm.

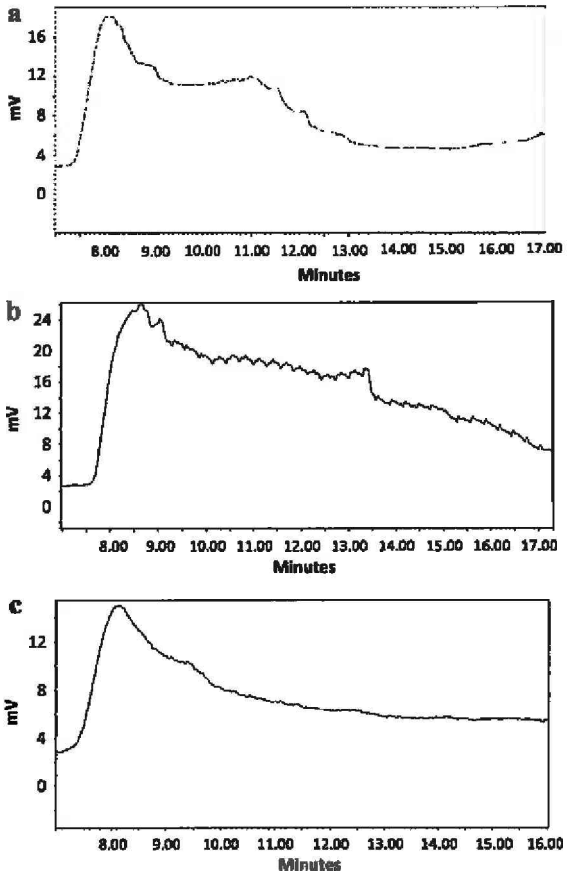

Fig. 6. GPC chromatograms of (a) HA (c_{HA} = 3 mg/ml); (b) the reaction mixture of the A_3_7 (c_{HA} = 3 mg/ml, at a cross-linking stoichiometric ratio of 25%, prepared in pure water); and (c) the purified A_3_7.

3.4. GPC results

Fig. 6a shows the GPC trace of HA. It implies the broad size distribution of linear biopolymer. Cross-linking modification of HA produced nanoparticles. Fig. 6b and c represents the GPC chromatograms of HA nanoparticles before and after dialysis. Reaction mixture containing HA nanoparticles (Fig. 6b) demonstrates that a unimodal nanoparticulate system was obtained with broad size distribution. Nevertheless, the retention time values for HA nanoparticles increased, smaller particles were formed during the cross-linking reaction.

Reaction mixture was purified by dialysis using cellulose dialysis tubes (MWCO = 12,000 Da). Fig. 6c shows the GPC chromatogram of the purified reaction mixture. This result suggests that the smaller particles were formed during the cross-linking reaction, and these particles diffuse through the membrane tube therefore they were lost during the dialysis.

3.5. Rheology

Viscosity is an important property of colloid systems, which is related to the nature, the extent of intermolecular interactions, and entanglements of polymer chains. Colloid systems containing cross-linked hyaluronan nanoparticles are colloid dispersions. The shear stress vs. shear rate graphs ("flow curves") indicate shear thinning, referring to a fact that the macromolecular systems behave as pseudoplastic materials. HA is a linear biopolymer, but the cross-linking reactions result in smaller particles. Fig. 7 shows

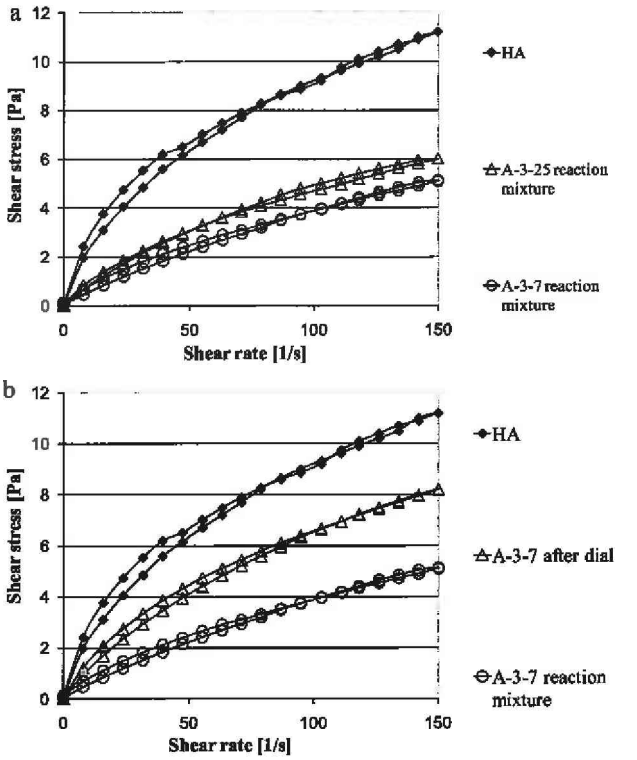

Fig. 7. (a) Shear rate dependence of the shear stress for the systems of HA and its cross-linked derivatives at the indicated cross-linking ratios. (b) Effect of purification on the rheological properties of cross-linked hyaluronan nanoparticles (c_{HA} = 3 mg/ml, pH = 6.3 ± 0.2).

the dependence of the shear rate on the shear stress of HA and hyaluronan nanoparticles at different ratios of cross-linking.

The flow curves of the nano-particulate systems were lower than flow curve of the linear HA, which is consistent with successful cross-linking and the formation of smaller particles.

Fig. 7a shows the effect of cross-linking ratio of HA on the rheological properties. It can be concluded that the curves of nanoparticles in this figure with no significant difference produced by the degree of cross-linking. In contrast, Fig. 7b shows the effects of dialysis on rheological measurements. The data demonstrates that dialysis increases shear stress.

These measurements are in agreement with the DLS and GPS results indicating that due to cross-linking small particles are formed and these diffuse through the membrane during dialysis. Therefore, HA nanoparticles possess a higher molecular weight and their spherical shape results in a lower viscosity than that exhibited by linear HA.

4. Conclusions

In this paper, we have shown that nano-sized particles based on HA have been successfully prepared by amidation with a bifunctional amine as a cross-linking agent in the presence of carbodiimide. Transparent or mildly opalescent colloid systems were fabricated in aqueous media at room temperature.

Physico-chemical properties, including transmittance of aqueous system containing HA nanoparticles, hydrodynamic size and size distribution of hyaluronan nanoparticles were controlled by varying the ratio of cross-linking, concentration of HA and parameters of media.

TEM and rheology results proved the existence of the well-dispersed HA nanoparticles systems with spherical shape.

Comparison of the particle sizes and size distribution at different phases of the technology leads to recognition of loss of the smaller particles during the dialysis.

DLS results indicate that the concentration of HA and the salt concentration of the media affect the hydrodynamic size of cross-linked nanoparticles, but the ratio of cross-linking did not.

The stability of these nanoparticles was not dependent on the media and feed ratio (from 7 to 25%), and no aggregation was found after several weeks.

The rheological measurements support the DLS and GPS results such as one part of cross-linked nanoparticles is formed with size less than 20 nm, but these particles can be lost during the purification.

Acknowledgements

Authors thank Lajos Daróczi for TEM micrographs. The study was supported by the TAMOP 4.2.2-08/1 and GOP-2.1.1-09/A-2009-2848 and Innocsekk Plusz grants.

References

Almond, A., DeAngelis, P. L., & Blundell, C. D. (2006). Hyaluronan: The local solution conformation determined by NMR and computer modeling is close to a contracted left-handed 4-fold helix. *Journal of Molecular Biology, 358*, 1256–1269.

Avila, L. Z., Gianolio, D. A., Konowicz, P. A., Philbrook, M., Santos, M. R., & Miller, R. J. (2008). Drug delivery and medical applications of chemically modified hyaluronan. *Carbohydrate Chemistry, Biology and Medical Applications*, 333–357.

Bodnár, M., Daróczi, L., Batta, G., Bakó, J., Hartmann, J. F., & Borbély, J. (2009). Preparation and characterization of cross-linked hyaluronan nanoparticles. *Colloid and Polymer Science, 287*, 991–1000.

Choi, K. Y., Lee, S., Park, K., Kim, K., Parka, J. H., Kwon, I. C., et al. (2008). Preparation and characterization of hyaluronic acid-based hydrogel nanoparticles. *Journal of Physics and Chemistry of Solids, 69*, 1591–1595.

Crescenzi, V., Francescangeli, A., Taglienti, A., Capitani, D., & Mannina, L. (2003). Synthesis and partial characterization of hydrogels obtained via glutaraldehyde crosslinking of acetylated chitosan and of hyaluronan derivatives. *Biomacromolecules, 4*, 1045–1054.

Dulong, V., Lack, S., Le Cerf, D., Picton, L., Vannier, J. P., & Muller, G. (2004). Hyaluronan-based hydrogels particles prepared by crosslinking with trisodium trimetaphosphate. Synthesis and characterization. *Carbohydrate Polymers, 57*, 1–6.

Esposito, E., Menegatti, E., & Cortesi, R. (2005). Hyaluronan-based microspheres as tools for drug delivery: A comparative study. *International Journal of Pharmaceutics, 288*, 35–49.

He, M., Zhao, Z., Yin, L., Tang, C., & Yin, C. (2009). Hyaluronic acid coated poly(butyl cyanoacrylate) nanoparticles as anticancer drug carriers. *International Journal of Pharmaceutics, 373*, 165–173.

Ji, Y., Ghosh, K., Shu, X. Z., Li, B., Sokolov, J. C., Prestwich, G. D., et al. (2006). Electrospun three-dimensional hyaluronic acid nanofibrous scaffolds. *Biomaterials, 27*, 3782–3792.

Kim, M. R., & Park, T. G. (2002). Temperature-responsive and degradable hyaluronic acid/pluronic composite hydrogels for controlled release of human growth hormone. *Journal of Controlled Release, 80*, 69–77.

Laurent, U. B. G., & Reed, R. K. (1991). Turnover of hyaluronan in the tissues. *Advanced Drug Delivery Reviews, 7*(2), 237–256.

Leach, J. B., & Schmidt, C. E. (2005). Characterization of protein release from photocrosslinkable hyaluronic acid-polyethylene glycol hydrogel tissue engineering scaffolds. *Biomaterials, 26*, 125–135.

Lee, H., Mok, H., Lee, S., Oh, Y.-K., & Park, T. G. (2007). Target-specific intracellular delivery of siRNA using degradable hyaluronic acid nanogels. *Journal of Controlled Release, 119*, 245–252.

Li, H., Liu, Y., Shu, X. Z., Gray, S. D., & Prestwich, G. D. (2004). Synthesis and biological evaluation of a cross-linked hyaluronan–mitomycin C hydrogel. *Biomacromolecules, 5*, 895–902.

Lim, S. T., Forbes, B., Berry, D. J., Martin, G. P., & Brown, M. B. (2002). In vivo evaluation of novel hyaluronan/chitosan microparticulate delivery systems for the nasal delivery of gentamicin in rabbits. *International Journal of Pharmaceutics, 231*, 73–82.

Liu, Y., Shu, X. Z., & Prestwich, G. D. (2005). Biocompatibility and stability of disulfide-crosslinked hyaluronan films. *Biomaterials, 26*, 4737–4746.

Luten, J., van Nostrum, C. F., De Smedt, S. C., & Hennink, W. E. (2008). Biodegradable polymers as non-viral carriers for plasmid DNA delivery. *Journal of Controlled Release, 126*, 97–110.

Masters, K. S., Shah, D. N., Leinwand, L. A., & Anseth, K. S. (2005). Crosslinked hyaluronan scaffolds as a biologically active carrier for valvular interstitial cells. *Biomaterials, 26*, 2517–2525.

Moriyama, K., Ooya, T., & Yui, N. (1999). Hyaluronic acid grafted with poly(ethylene glycol) as a novel peptide formulation. *Journal of Controlled Release, 59*, 77–86.

Nakamura, M., Sato, N., Chikama, T.-I., Hasegawa, Y., & Nishida, T. (1997). Hyaluronan facilitates corneal epithelial wound healing in diabetic rats. *Experimental Eye Research, 64*, 1043–1050.

Oh, E. J., Park, K., Kim, K. S., Kim, J., Yang, J.-A., Kong, J.-H., et al. (2010). Target specific and long-acting delivery of protein, peptide, and nucleotide therapeutics using hyaluronic acid derivatives. *Journal of Controlled Release, 141*(1), 2–12.

Pitarresi, G., Craparo, E. F., Palumbo, F. S., Carlisi, B., & Giammona, G. (2007). Composite nanoparticles based on hyaluronic acid chemically cross-linked with α,β-polyaspartylhydrazide. *Biomacromolecules, 8*, 1890–1898.

Robert, L., Robert, A.-M., & Renard, G. (2010). Biological effects of hyaluronan in connective tissues, eye, skin, venous wall. *Pathologie Biologie, 58*(3), 187–198.

Salk, R. S., Chang, T. J., D'Costa, W. F., Soomekh, D. J., & Grogan, K. A. (2006). Sodium hyaluronate in the treatment of osteoarthritis of the ankle: A controlled, randomized, double-blind pilot study. *Journal of Bone and Joint Surgery, 88*, 295–302.

Segura, T., Chung, P. H., & Shea, L. D. (2005). DNA delivery from hyaluronic acid-collagen hydrogels via a substrate-mediated approach. *Biomaterials, 26*, 1575–1584.

Strand, V., Conaghan, P. G., Lohmander, L. S., Koutsoukos, A. D., Hurley, F. L., Bird, H., et al. (2006). An integrated analysis of five double-blind, randomized controlled trials evaluating the safety and efficacy of a hyaluronan product for intra-articular injection in osteoarthritis of the knee. *OsteoArthritis and Cartilage, 14*, 859–866.

Vasiliu, S., Popa, M., & Rinaudo, M. (2005). Polyelectrolyte capsules made of two biocompatible natural polymers. *European Polymer Journal, 41*, 923–932.

Witteveen, A. G. H., Sierevelt, I. N., Blankevoort, L., Kerkhoffs, G. M. M. J., & van Dijk, C. N. (in press). Intra-articular sodium hyaluronate injections in the osteoarthritic ankle joint: Effects, safety and dose dependency. *Foot and Ankle Surgery*.

II.

Acta Pharmaceutica Hungarica 82. 15-22 2012.

A bőrön keresztüli hatóanyag permeáció modellezése és penetrációfokozók hatásának vizsgálata

CSIZMAZIA ESZTER, BERKÓ SZILVIA, MARODA MÓNIKA, SZABÓNÉ RÉVÉSZ PIROSKA, CSÁNYI ERZSÉBET*

Szegedi Tudományegyetem, Gyógyszertechnológiai Intézet, Szeged, Eötvös u. 6. – 6720
**Levelezési cím. csanyi@pharm.u-szeged.hu*

Summary

Csizmazia, E., Berkó, Sz., Maroda, M., Szabó-Révész, P., Csányi, E.: ***Modelling of pecutaneous drug permeation and investigation of penetration enhancer effect***

Present study provides a short review concerning the applicable membranes for modelling the percutaneous drug permeation and about their importance. The theoretical introduction summarizes the transdermal drug permeation routes and enhancement strategies. Two penetration enhancers are presented, the Transcutol and a sucrose ester, the Sucrose laurate which can offer an interesting possibility. Various recently applied and tested membranes (synthetic membrane, human, animal and artificial skin) are shown, which can be used for modelling dermal drug permeation. Furthermore two investigation methods are demonstrated for examining the drug diffusion, penetration and permeation, the vertical Franz diffusion cell and the ATR-FTIR spectroscopy, which can offer possibility for studying the skin at molecular level, too. Our previous in vitro, ex vivo and in vivo experimental results support, that choosing the appropriate model membrane is of primary importance. Examining the drug permeation through the skin is indispensable to get information about the interactions between the drug, the penetration enhancers and the skin as well, and to study also the drug accumulation in the skin.

Keywords: *Franz cell, FTIR, Human epidermis, Penetration enhance*

Összefoglaló

Jelen tanulmány a bőrön keresztüli hatóanyag permeáció modellezésére alkalmazható membránokról kíván rövid áttekintést nyújtani és jelentőségükre rávilágítani. Az elméleti bevezető a perkután hatóanyag permeáció útjait és a penetrációfokozás lehetőségeit foglalja össze. Két ígéretes penetrációfokozó anyagot mutat be, a Transcutolt és a cukorészterek csoportjába tartozó Szacharóz-laurátot. Valamint bemutatásra kerülnek a napjainkban alkalmazott és kipróbálás alatt álló különböző membránok (szintetikus membrán, humán, állati és mesterséges bőr), melyek hatóanyagok dermális permeációjának modellezésére használhatók. Továbbá ismertetni kívántuk a hatóanyag diffúzió, penetráció és permeáció vizsgálatára szolgáló módszerek közül a vertikális Franz diffúziós cellát és az ATR-FTIR spektroszkópiát, mely lehetőséget nyújt a bőr molekuláris szinten történő tanulmányozására is. Korábbi in vitro, ex vivo és in vivo kísérletes eredményeinkkel pedig azt kívántuk alátámasztani, hogy a permeációs vizsgálatok során alapvető fontosságú a célnak leginkább megfelelő modell membrán kiválasztása. A bőrön keresztüli hatóanyag permeációs vizsgálatok elvégzése ugyanis elengedhetetlen ahhoz, hogy információt kapjunk arról is, hogy a hatóanyag és penetrációfokozók kölcsönhatásba lépnek-e a bőrrel, akkumulálódnak-e benne.

Kulcsszavak: *Franz cella, FTIR, humán epidermisz, penetrációfokozás.*

Bevezetés

Napjainkban egyre inkább előtérbe kerül a gyógyszerek bőrön keresztüli alkalmazása, ami számos hatóanyag esetében előnyt jelenthet az orális bevitellel szemben. Népszerűségének legfőbb oka, hogy elkerülhető vele a máj metabolizáló hatása, ezáltal a hatóanyag jobb biohasznosíthatóságát eredményezheti. Továbbá csökken az orális alkalmazás esetén tapasztalható plazma csúcskoncentráció, így a mellékhatások is mérséklődnek [1].

A fő probléma azonban az alternatív kapukon keresztüli hatóanyag bevitellel, hogy csak kevés hatóanyag képes leküzdeni a szervezet védő barrierjeit, melyek közül az egyik legjelentősebb a bőr. A bőr barrier funkciójáért a legkülső rétege, a stratum corneum (SC) felelős. Ezen rétegre az úgynevezett „téglafal-szerkezet" jellemző, ahol a „téglákat" elszarusodott, sejtmag nélküli corneocyták felelnek meg. Közöttük pedig lipid- és vízrétegek helyezkednek el (*1. ábra*).

A SC alapvető funkciója, hogy barriert képezzen az idegen anyagok és a párolgó víz számára. A szigorúan rendezett struktúrájának és kitűnő diffúziós ellenállásának köszönhetően azonban számos hatóanyag bejuttatását megnehezíti, olykor lehetetlenné teszi. A bőrön keresztüli diffúziós folyamatok megértése elengedhetetlen a transzdermális gyógyszerhordozó rendszerek fejlesztéséhez [2].

A perkután hatóanyag permeáció magába foglalja a bőrfüggelékeken (szőrtüsző, verejtékmirigy)

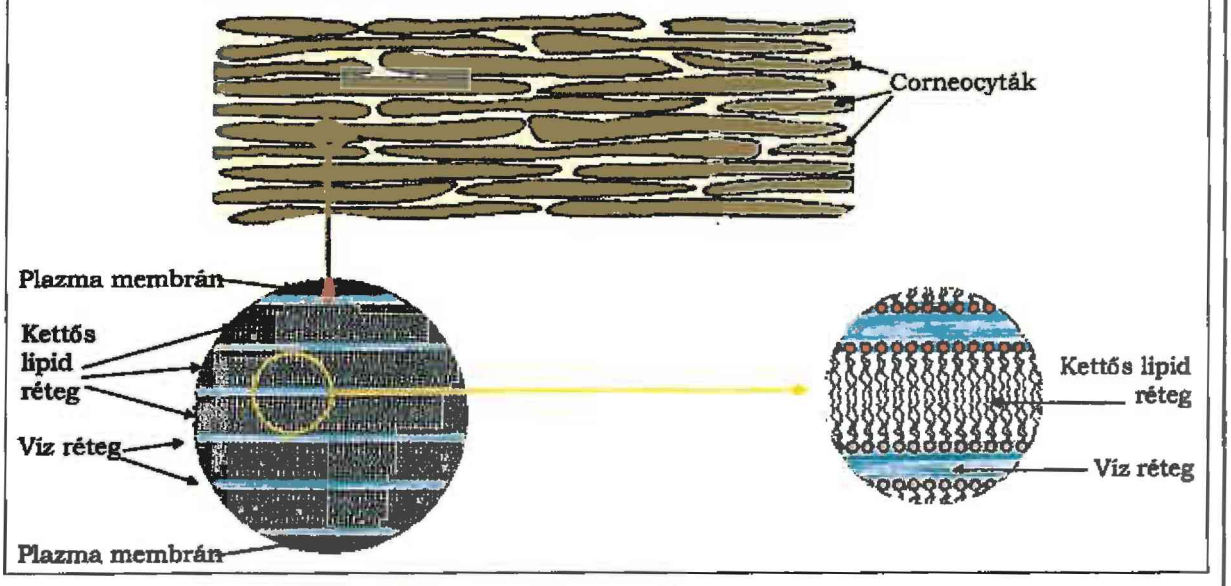

1. ábra: A stratum corneum „téglafal-szerkezete"

és az intakt epidermiszen keresztüli diffúziót. Az intakt epidermiszen keresztül transzcelluláris úton, a corneocytákon és a köztük levő lipideken keresztül, valamint intercelluláris úton, a corneocyták közötti járatokban diffundálhat a hatóanyag (*2. ábra*) [3].

Leggyakrabban a hatóanyag intercelluláris úton történő permeációja valósul meg. A kettős lipid szerkezetből adódik, hogy ez az út a hidrofil és a lipofil karakterű hatóanyagok számára egyaránt lehetőséget biztosít. Általánosan elfogadott tény, hogy a transzdermális hatóanyag bevitelhez olyan nemionos anyagok a legalkalmasabb jelöltek, melyek alacsony olvadáspontúak (< 200 °C), alacsony molekulatömegűek (< 500 Da), és megfelelő oldékonysággal (logP: 1–4) rendelkeznek a SC lipofil régiójában ahhoz, hogy átdiffundáljanak, és még kellően hidrofil karakterűek ahhoz, hogy az élő epidermiszben képesek legyenek megoszlani [4]. Az ezen kritériumoknak megfelelő hatóanyagok száma meglehetősen kevés. Penetrációfokozó technikák alkalmazásával azonban javítható a hatóanyagok perkután permeációja [5]. A penetrációfokozás leggyakrabban alkalmazott stratégiáit az *I. táblázat* foglalja össze [6].

A cél, hogy a különböző technikák közül meg-

I. táblázat

Transzdermális penetrációfokozási stratégiák

Hatóanyag-hordozó kölcsönhatása	• Megfelelő hatóanyag/prodrug • Kémiai potenciál • Ionpár/koacervátumok • Eutektikus rendszerek
Hordozók és részecskék	• Liposzómák, nioszómák, transzferoszómák, mikroemulziók és nanoemulziók, solid lipid nanopartikulumok • Nagy sebességű részecskék
Stratum corneum módosítása	• Hidratáció • **Kémiai penetrációfokozók**
Stratum corneum elkerülése vagy eltávolítása	• Mikrotűk alkalmazása • SC eltávolítása • Hatóanyag szőrtüszőn keresztüli szállítása
Elektromosságon alapuló módszerek	• Ultrahang • Iontoforézis • Elektroporáció (elekropermeábilizáció) • Magnetoforézis • Fotomechanikus hullámok

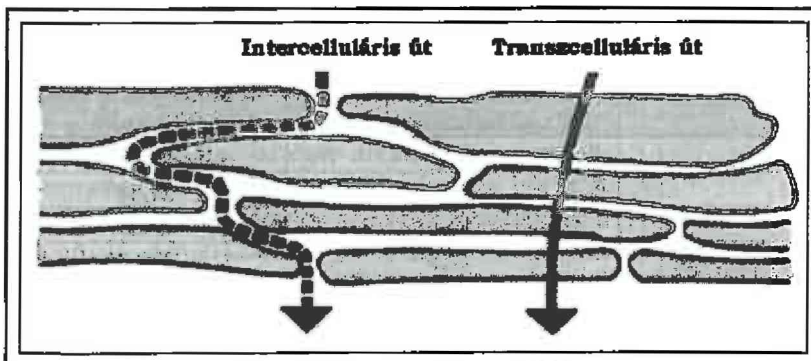

2. ábra: A bőrön keresztüli penetrációs utak

találjuk a leghatékonyabb és emellett a legbiztonságosabb módszert, mely nem okoz a SC szerkezetében irreverzibilis károsodást. A rendelkezésre álló módszerek közül a SC módosításán alapuló lehetőségek közül azon kémiai penetrációfokozó anyagok alkalmazása különösen fontos, melyekkel reverzibilisen lehet megnyitni a SC szigorúan rendezett szerkezetét, felfüggeszteni a bőr barrier funkcióját, ezáltal lehetővé téve az egyébként gyengén penetrálódó hatóanyagok bejutását a mélyebb rétegekbe [6]. A kémiai anyagok (Azone, terpének, zsírsavak, alkoholok stb.) megbonthatják a SC rendezett lipid struktúráját, permeábilisabbá téve ezzel azt. Az ionos felületaktív anyagok (pl. decil-metil-szulfoxid, DMSO) a corneocyták keratin tartalmával lépnek kölcsönhatásba, és a protein struktúrát bontják meg. Számos oldószer (propilénglikol) pedig a kémiai környezet megváltoztatásával módosítja a hatóanyag oldékonysági tulajdonságait, és növeli a megoszlását a szaruretegben [6, 7].

Ígéretes penetrációfokozó anyag lehet a *Transcutol®*, amely hatékony szolubilizáló közeg számos hatóanyag számára, mivel poláris és apoláris oldószerekkel egyaránt elegyedik. Továbbá előnyös tulajdonsága, hogy nem toxikus, biokompatibilis a bőrrel, és humektáns hatással is rendelkezik [8, 9]. Képes vizet abszorbeálni a bőr mélyebb rétegeiből, így növeli a SC víztartalmát, mely ezáltal megduzzad, az intercelluláris lipidek szerkezetük megváltozása nélkül képesek eltávolodni egymástól, és csökken a diffúziós rezisztencia [10, 11, 12].

A *cukorészterek* a nemionos felületaktív anyagok legújabb generációjába tartoznak, és szintén ígéretes penetrációfokozók. A szacharóz észterek hidrofil részként szacharózt, lipofil részként zsírsavakat tartalmaznak. A szacharóz 8 hidroxil csoportja 8 zsírsavval észteresíthető. Minél nagyobb az észterezettség foka, és minél hosszabb a zsírsavlánc a cukorészterben, annál kisebb a HLB érték. Kedvező tulajdonságaik közé sorolható, hogy nem toxikusak, nem irritálják a bőrt és biodegradábilisek [13]. Így használhatók dermális és transzdermális készítményekben. Irodalmi adatok alapján hatékony abszorpció- és penetrációfokozó tulajdonságúak [14, 15]. A 12 szénatomszámú alkil lánc mutatja a leghatékonyabb membrán permeábilitást, mivel a C12-es lánc közepes olaj/víz oldékonysága révén képes penetrálni a kettős lipid rétegbe [16].

A bőrön keresztüli hatóanyag permeáció modellezésére alkalmazható membránok

A bőrön keresztüli permeáció modellezésére a szintetikus membránok mellett humán és állati bőrmembránok is alkalmazhatók. A leggyakrabban használt transzdermális hatóanyag permeációs membrán modelleket az *3. ábra* foglalja össze.

Ezen vizsgálatok leggyakrabban *szintetikus membránon* keresztül történnek *in vitro*. Általánosságban elmondható, hogy ez a membrán a biológiai membránokhoz képest permeábilisabb, így hatóanyag felszabadulási és diffúziós vizsgálatokhoz használják. Napjainkban azonban egyre gyakrabban helyettesítik különféle biológiai membránokkal [17]. A transzdermális készítmények fejlesztése során ugyanis nem elegendő membrán diffúziós vizsgálatokat végezni, melyek az átdiffundált hatóanyag mennyiségét mutatják. Elengedhetetlen a biológiai közegen keresztüli permeációs vizsgála-

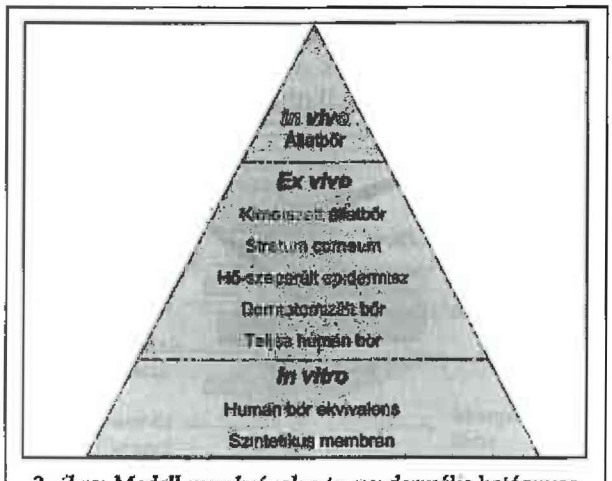

3. ábra: Modell membránok a transzdermális hatóanyag permeációs vizsgálatokhoz

II. táblázat

Bőrfelszíni lipidek mennyisége és a SC vastagsága néhány fajban

Fajok	*Stratum corneum* vastagsága (μm)	Lipidek mennyisége (μg/cm²)
Ember	***18,2***	***60,5***
Szőrtelen egér	8,8	212,4
Szőrtelen patkány	15,4	273,3
Sertés	17,5	130,0
Tengerimalac	18,6	224,7
Kutya	19,9	*NK*
Marha	30,9	*NK*
Birka	31,4	*NK*

NK: nem közölt adat

tok beiktatása is, hiszen a hatóanyag kölcsönhatása a bőrrel és a SC esetleges rezervoár funkciója csak ilyen módon tanulmányozható.

Az *ex vivo* vizsgálatokhoz használható kadáver bőr, de általában redukciós plasztikai műtétek során kimetszett bőrt alkalmaznak. A kísérletek végezhetők *teljes humán bőrön*, ami a SC-ból, az élő epidermiszből és a dermiszből áll (2000-3000 μm). Figyelembe kell azonban venni, hogy a permeálódó molekula fiziológiás körülmények között nem minden esetben halad át a teljes dermiszen, a mikrokeringés elszállíthatja.

Ennek a problémának a leküzdésére használható *dermatomizált bőr*, melyet egy speciális, dermatomizációs technikával metszenek, és a SC-on valamint az epidermiszen kívül a dermisznek csak egy részét tartalmazza (400-500 μm) [18].

A dermisz teljes eltávolítására számos mechanikai, termikus és kémiai módszer létezik. A legáltalánosabban alkalmazott technika az epidermisz és dermisz elválasztására a hő-szeparációs eljárás (*4b-c ábra*), mely a szubkután zsírszövet eltávolítását követően végezhető (*4a ábra*) [19]. A *hő-szeparált epidermisz* vastagsága mindössze 20-200 μm.

Néhány esetben csak a *stratum corneum* (10-15 μm) szükséges a vizsgálathoz. Ez az elszarusodott bőrréteg tripszint használva enzimes emésztéssel izolálható az élő epidermisztől. A művelet során teljes humán bőrt vagy hő-szeparált epidermiszt 37 °C-on 24 órán keresztül tripszin oldatban inkubálnak. Az inkubációs idő elteltével az oldatban csupán az elhalt sejteket tartalmazó SC marad vissza [5].

A humán bőr a legrelevánsabb modell a permeációs vizsgálatokhoz, az elérhetősége azonban limitált. A transzdermális készítmények biohasznosíthatóságának vizsgálatai és a komponensek kockázat értékelése egyre több ilyen jellegű vizsgálatot igényel, így újabb modellek bevonása szükséges. Az irodalom számos *állati bőrt* javasol ezen vizsgálatok elvégzéséhez a humán bőr kiváltására. Patkány, szőrtelen patkány, szőrtelen egér, sertés és tengerimalac kimetszett bőrét használják a leggyakrabban *ex vivo* modellként, hogy a humán perkután penetrációt modellezzék. Az állatok bőrének szarurétege azonban különbözik az emberitől vastagságában, a corneocyta rétegek számában, a szőrtüszők sűrűsége tekintetében, és eltérő lehet a bőrük víztartalma, a lipidek aránya és morfológiája is (*II. táblázat*) [21, 22]. A majom [23] és a sertés [24] bőrének permeábilitása áll legközelebb az emberi bőréhez. De ezen állatok be-

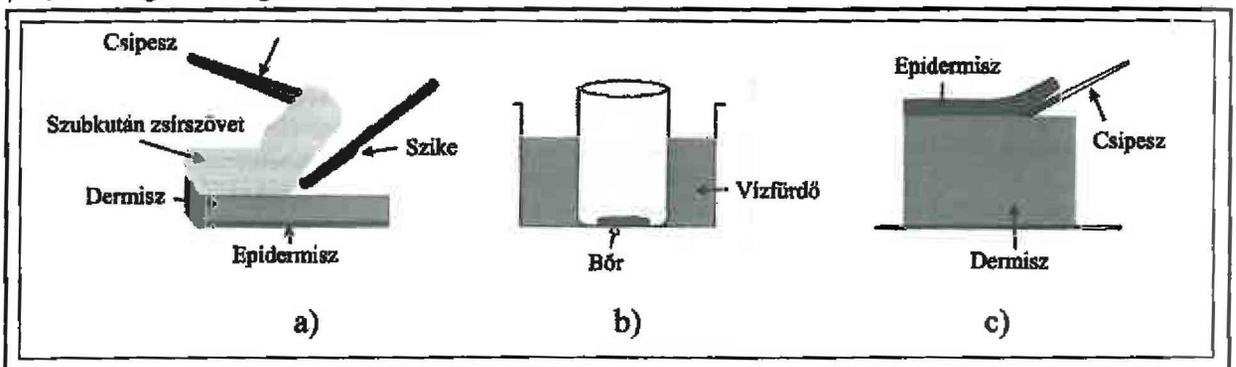

4. ábra a-c): Humán bőrpreparátum készítése hő-szeparációs eljárással

szerzése drágább és nehezebben megoldható, mint a kisebb laboratóriumi állatoké. Így a legszélesebb körben rágcsálók bőrét használják. A szőr hiánya és a csökkent szőrtüszőszám miatt szőrtelen patkány, tengerimalac és egér alkalmazása javasolt, hiszen ezek bőre jobban hasonlít a humán bőrre. A szőrtüszők ugyanis fontos szerepet játszhatnak a hatóanyag penetrációban, és a szőrös állatokon végzett vizsgálat félrevezető eredményt adhat [25].

Az utóbbi években komoly törekvések folynak különféle alternatív modellek kidolgozására. Ez alapvető fontosságú a humán bőr nehéz elérhetősége és a világszerte növekvő állatkísérletek elleni tiltakozások miatt. A jövőben a *humán bőr ekvivalensek* nyújthatnak megoldást. Ezeket a mesterséges bőröket transzplantációhoz, klinikai sebgyógyításhoz és kémiai anyagok toxikológiai teszteléséhez már használják, de számos típusuk áll vizsgálat alatt, hogy alkalmas modellt biztosítsanak bőr permeációs vizsgálatok során is. Az *Epiderm™*-et (MatTek, USA) és a *Skinethic*-et (Skinethik, Franciaország) közömbös szűrőmembránon növesztik, míg az *Episkin®* (L'Oreal, Franciaország) egyrétegű kollagénen tenyésztett bőr [26, 27]. Ezek a szintetikus bőrök élő sejteket tartalmaznak, melyek metabolikusan aktívak, de a legtöbb esetben jóval nagyobb permeábilitást mutatnak, mint a humán epidermisz.

A *5. ábra* egy rekonstruált bőr ekvivalens (*5d ábra*) mikroszkópos metszetét mutatja természetes humán bőr modellekhez (*5a-c ábra*) hasonlítva [28].

Hatóanyag diffúziós és permeációs vizsgálatok Franz cellával

A hatóanyag vivőanyagból való felszabadulásának, bőrbe jutásának, illetve membránon keresztüli diffúziójának modellezésére a vertikális Franz diffúziós cella (Hanson Microette TM Topical & Transdermal Diffusion Cell System, Hanson Research Corporation, USA) tekintendő a legelterjedtebb és elfogadottabb módszernek [28].

A donor és az akceptor fázist egy membrán (mesterséges, állati vagy humán) választja el egymástól. Akceptor fázisként 37 °C-ra termosztált foszfát puffer (PBS pH=7,4) alkalmazható, mellyel a fiziológiás keringési körülmények modellezhetők (*6. ábra*).

A membránon négyzetcentiméterenként átjutott kumulatív hatóanyag mennyiség (Q) idő függvényében ábrázolható. Ennek segítségével meghatározhatók a különböző permeációs paraméterek.

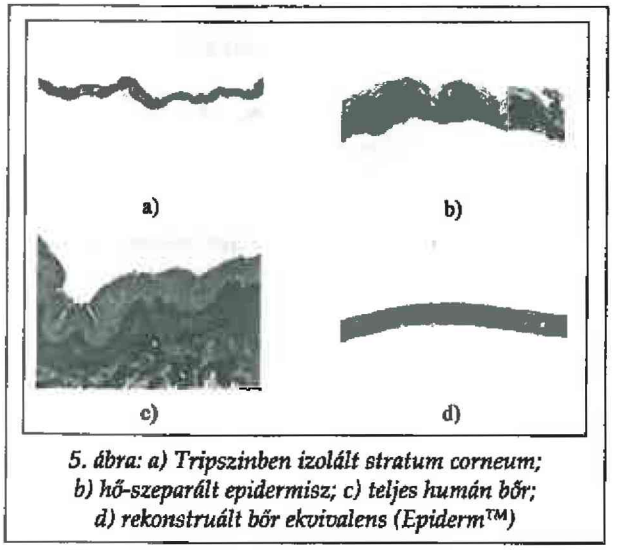

5. ábra: a) Tripszinben izolált stratum corneum; b) hő-szeparált epidermisz; c) teljes humán bőr; d) rekonstruált bőr ekvivalens (Epiderm™)

Az idő és az átjutott anyag mennyiségének kapcsolata több fázissal jellemezhető. A *lag time* (T_{lag}) azt a késedelmi időt jelenti, mely a hatóanyag bőrrel történő első kontaktusától a diffúziós egyensúly (*steady state flux*: J) eléréséig eltelik, és a görbe egyenes szakaszának az X tengellyel való metszéspontja adja.

„J" az abszorpciós rátát jellemzi egységnyi felületen, mely a görbe egyenes szakaszának meredekségéből határozható meg. A permeábilitási koefficiens (K_p) Fick első törvénye alapján a diffúziós sebesség és a donor fázisban alkalmazott hatóanyag koncentráció (C_d) segítségével az alábbi módon számolható ki [29].

$$K_p = J/C_d \qquad \text{1. egyenlet}$$

A penetrációfokozók hatásának jellemzésére az ún. *enhancer index* (EI) szolgál, mely a penetrációfokozót tartalmazó és az anélküli készítmény permeábilitási koefficienséből számítható ki [30].

$$EI = K_{p(\text{penetrációfokozóval})} / K_{p(\text{penetrációfokozó nélkül})} \qquad \text{2. egyenlet}$$

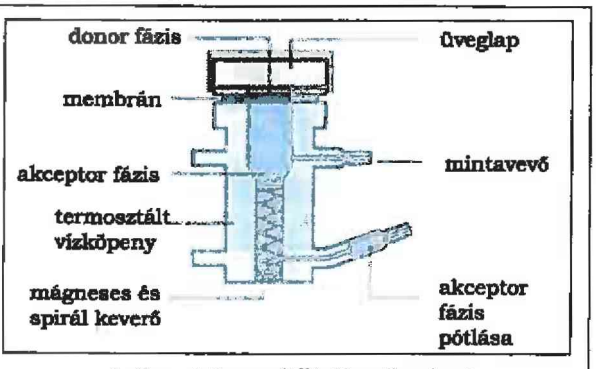

6. ábra: A Franz diffúziós cella részei

Hatóanyag penetrációs vizsgálatok ATR-FTIR spektroszkópiával

Az ATR-FTIR (Attenuated Total Reflectance – Fourier Transform Infrared) spektroszkópia egy hatékony nem-invazív *in vivo* módszer a SC biofizikai szerkezetének molekuláris szinten történő tanulmányozására. Mérési elve az infravörös sugarak bőrben való elnyelődése. Jellemezhető vele a bőr víz, lipid és protein tartalma, tanulmányozható a stratum corneum szerkezetének rendezettsége, nyomon követhető a hatóanyag penetráció, és alkalmas penetrációfokozó segédanyagok hatásmechanizmusának tisztázására. Nagy előnye ennek a technikának, hogy magyarázatot adhat az *in vivo* perkután penetrációfokozás mértékére és mechanizmusára is [31-33].

Az ún. *tape stripping* módszerrel kombinálva pedig nemcsak a SC legfelső rétege jellemezhető, hanem a mélyebb régiókról is információt kaphatunk [34-37]. Egy adhezív tapasz (D-Squame® Skin sampling discs, CuDerm Corporation, USA) segítségével minta gyűjthető a bőr egymás alatti rétegeiből, majd a tapaszt a készülék ZnSe kristályára helyezve, infravörös sugárzással vizsgálható a SC összetétele (*7. ábra*).

A *8. ábrán* a bőr spektruma látható. 3200-3600 cm^{-1} közötti hullámszám tartományban a víz O-H kötéseinek sávjai detektálhatók. Ha ebben a hullámszám tartományban intenzívebb és szélesebb csúcs mutatkozik kezelés hatására, akkor az a bőr hidratálódására utal. A 2920 cm^{-1}-es és a 2850 cm^{-1}-es hullámszámnál a metilén csoportok sávjai ($-CH_2$) jelennek meg, amik a SC lipidjeinek a szénhidrogén láncait jelölik. Ebben a régióban figyelhetjük meg, hogy a bőrön alkalmazott anyagok megbontották-e a SC-ra jellemző szabályos rendezett struktúrát, illetve vontak-e ki lipideket a bőrből. Az amid I illetve amid II abszorpciós csúcsok az 1650 cm-es és az 1550 cm^{-1}-es hullámszámnál a fehérje kötések jelenlétére utalnak. Ezek a frekvenciák érzékenyek a SC proteinjeinek konformáció változására. A különböző penetrációfokozó segédanyagok és a hidratáció hatására bekövetkező lipidstruktúrabeli változások jól követhetők a színképen. Ilyenkor vagy lecsökken a lipidek mennyisége a bőrben a kivonás hatására, vagy megnő a lipid láncok rendezetlensége. A kivonást a csúcsok magasságának és szélességének csökkenése mutatja. Ha a lipidek fluiditása következik be, akkor a csúcs magasabb frekvencia felé tolódik el, a csúcsok kiszélesedéséből pedig a láncok rotációs szabadságának megnövekedésére következtethetünk [38].

A hatóanyag penetráció vizsgálatára szolgáló membrán kiválasztásának jelentősége

Az SZTE Gyógyszertechnológiai Intézetében a nem-szteroid gyulladáscsökkentők közül az Ibuprofen transzdermális permeációját illetve penetrációjának növelési lehetőségeit vizsgáltuk szintetikus membránon keresztül *in vitro*, valamint humán epidermiszen keresztül *ex vivo* [39] és szőrtelen egér bőrén *in vivo* [40]. Tanulmányoztuk a hatóanyag felszabadulását egy penetrációfokozót nem tartalmazó hidrogélből, valamint Transcutol illetve egy cukorészter (Szacharóz-laurát) tartalmú készítményből.

A szintetikus membránon végzett hatóanyag diffúziós vizsgálatok eredményéből megállapítottuk, hogy a Transcutol hatékonyan fokozta az Ibuprofen diffúzióját. A Szacharóz-laurát viszont inkább gátolta a diffúziós folyamatot. Az epidermiszen történő vizsgálatoknál azonban éppen ellenkező eredményre jutottunk. A cukorészter szignifikánsan fokozta a penetrációt, a Transcutol viszont inkább csökkentette [39].

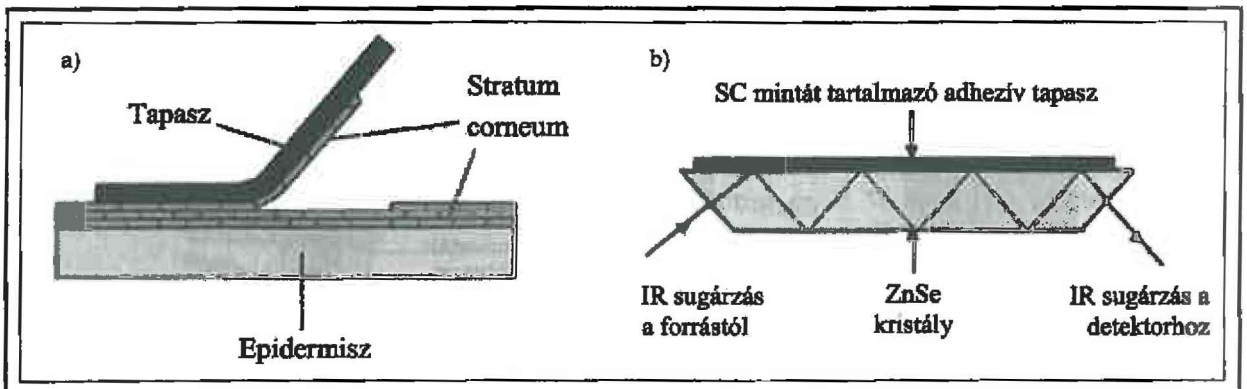

7. ábra: a) Mintavétel az adhezív tapasszal; b) A SC-ot tartalmazó tapasz vizsgálata a ZnSe kristályon

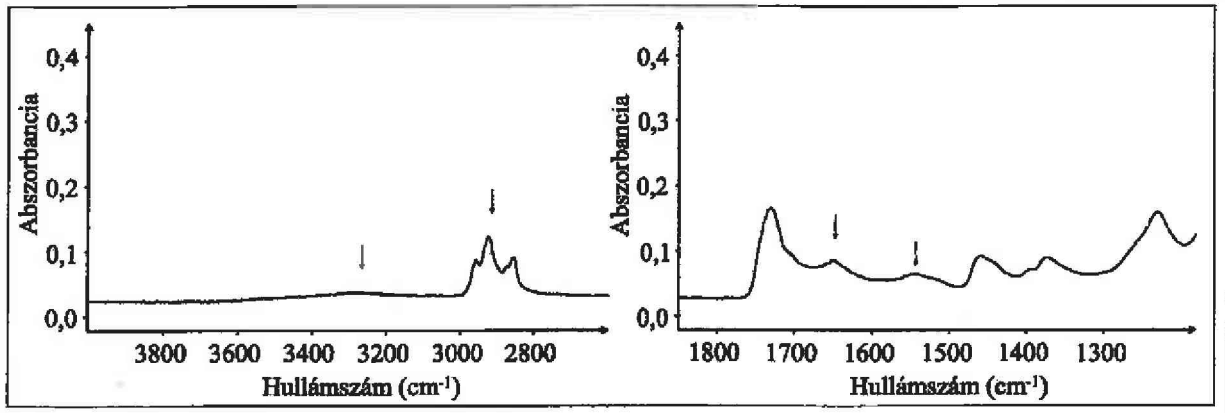

8. ábra: A bőr infravörös színképe

Ez az érdekes vizsgálati eredmény a két penetrációfokozó eltérő hatásmechanizmusából adódik. A Szacharóz-laurát a bőr szerkezetében okoz enyhe változásokat, a hosszú szénhidrogén láncai kölcsönhatásba léphetnek a SC lipidjeivel, csökkentve a barrier funkciót [41]. Ez az oka annak, hogy *ex vivo*, humán epidermiszen befolyásolja a bőrpenetrációt, szintetikus membránon keresztül *in vitro* azonban nincs hatása. A Transcutol a hatóanyag barrierben való oldékonyságát fokozza. Ezenkívül humektáns hatással is rendelkezik, megnöveli a bőr és a donor fázis víztartalmát, és a donor kompartment változása befolyásolhatja az oldékonyságot és a hatóanyag termodinamikai aktivitását [42]. A Transcutolról azonban azt is leírták, hogy megnöveli némely helyileg alkalmazott hatóanyag akkumulációját a bőrben, így nem minden esetben fokozza a transzdermális permeációt. Az általunk tapasztalt csökkent permeáció oka is ez a depó képződés lehet. A SC intercelluláris lipidjei megduzzadnak anélkül, hogy változást idéznének elő a bőr speciális kettős lipid szerkezetében, és ezek a megduzzadt lipidek tartják vissza elsősorban a lipofil karakterű hatóanyagokat. Ezáltal az Ibuprofen is felhalmozódik a SC-ban, és csökkent transzdermális permeációt eredményez *ex vivo* [44].

Az *in vivo* FTIR analízist a permeációs vizsgálatokban tapasztaltak alátámasztására végeztük [43]. A Transcutol tartalmú gélnél kiemelkedően magas értéket találunk a SC legfelső rétegében, ami alátámasztja azon feltételezésünket, miszerint a hatóanyag a bőrben akkumulálódik és depót képez. A vizsgálatok eredménye továbbá azt mutatta, hogy a Szacharóz-laurát tartalmú készítménnyel jelentős mértékű bőrhidratációt és hatóanyag penetráció növekedést tudtunk elérni, jelentősebb irreverzibilis bőrszerkezeti változás nélkül [40].

Összegzés

Vizsgálati eredményeink egyértelműen mutatják, hogy a dermális készítmények fejlesztése során a célnak megfelelő membrán megválasztás alapvető fontosságú. Ha a készítmények fejlesztése során alkalmazott segédanyagok az epidermisz szerkezeti elemeivel kölcsönhatásba lépve fejtik ki penetrációfokozó hatásukat, akkor a szintetikus membrán nem elegendő a hatóanyag permeációs vizsgálatok elvégzéséhez. Ezen vizsgálatok során tájékoztató információt kaphatunk a hatóanyag hordozóból történő felszabadulásának kinetikájáról, és a diffúzió sebességéről, de elengedhetetlen a bőrön keresztüli vizsgálatok elvégzése is, hogy informálódjunk arról is, hogy a hatóanyag és a segédanyagok kölcsönhatásba lépnek-e a bőrrel, akkumulálódnak-e benne, valamint a penetrációfokozó segédanyagok hatásmechanizmusát is fel tudjuk deríteni. A penetrációs vizsgálatok oki hátterének megvilágítására az FTIR technika alkalmas módszer.

Köszönetnyilvánítás

A munka a TÁMOP-4.2.1/B-09/1/KONV-2010-0005 azonosító számú, „Kutatóegyetemi Kiválósági Központ létrehozása a Szegedi Tudományegyetemen" című projekt és az NKTH - A*STAR <Hungarian - Singaporean> Bilateral S&T International Co-operation (BIOSPONA) TeT-08-SG-STAR támogatásával készült.

IRODALOM

1. *Cevc, G.*: Expert. Opin. Inv. Drug *6*, 1887-1937 *(1997)*.
2. *Schäfer-Korting, M., Mehnert, W., Korting, H-Ch.*: Adv. Drug Deliver. Rev. *59*, 427-443 *(2007)*.
3. *Moser, K., Kriwet, K., Naik, A., Kalia, Y.N., Guy, R.H.*: Eur. J. Pharm. Biopharm. *52*, 103-112 *(2001)*.

4. *Benson, H.A.E.:* Curr. Drug Deliv. 2, 23-33 *(2005).*
5. *Carsten Ehrhardt and Kwang-Jin Kim:* Drug Absorption Studies In Situ, In Vitro and In Silico Models, Springer, New York *Ulrich F. Schaefer, Steffi Hansen, Marc Schneider, Javiana Luengo Contreras, and Claus-Michael Lehr:* Models for Skin Absorption and Skin Toxicity Testing *(2008).*
6. *Barry, B.W.:* Eur. J. Pharm. Sci. *14,* 101-114 *(2001).*
7. *Thong, H.-Y., Zhai, H., Maibach, H.I.:* Skin Pharmacol. Phys. *20,* 272–282 *(2007).*
8. *Mura, P., Faucci, M.T., Bramanti, G., Corti, P.:* Eur. J. Pharm. Sci. *9,* 365-372 *(2000).*
9. *Mura, S., Manconi, M., Sinico, Ch., Valenti, D., Fadda, A.M.:* Int. J. Pharm. *380,* 72-79 *(2009).*
10. *Ganem-Quintanar, A., Lafforgue, C., Falson-Rieg, F., Buri, P.:* Int. J. Pharm. *147,* 165-171 *(1997).*
11. *D'Arpino, S., Corbrion-Archer, V., Marty, J.-P., Lantieri, L., Vincent, C.-M., Astier, A., Paul, M.:* Drug Develop. Res. *58,* 283-290 *(2003).*
12. *Harrison, J.E., Watkinson, A.C., Green, D.M., Hadgraft, J., Brain, K.:* Pharm. Res. *13,* 542-546 *(1996).*
13. *Csóka, G., Marton, S., Zelko, R., Otomo, N., Antal, I.:* Eur. J. Pharm. Biopharm. *65,* 233-237 *(2007).*
14. *Lehmann, L., Keipert, S., Gloor, M.:* Eur. J. Pharm. Biopharm. *52,* 129-136 *(2001)*
15. *Ganem-Quintanar, A., Quintanar-Guerrero, D., Falson-Rieg, F., Buri, P.:* Int. J. Pharm. *173,* 203-210 *(1998).*
16. *Ayala-Bravo, H.A., Quintanar-Guerrero, D., Naik, A., Kalia, Y.N., Cornejo-Bravo, J.M., Ganem-Quintanar, A.:* Pharm. Res. *20,* 1267-1273 *(2003).*
17. *Haigh, J.M., Smith, E.W.:* Eur. J. Pharm. Sci. *2,* 311-330 *(1994).*
18. *Franz, T. J., Lehman, P. A., Raney, S. G., Cetero.* www.aapsj.org/abstracts/AM_2008/AAPS2008-003071.PDF
19. *Kligman, A.E., Christophers, E.:* Arch. Dermatol. *88,* 702-705 *(1963).*
20. *El Maghraby, G.M., Barry, B.W., Williams, A.C.:* Eur. J. Pharm. Sci. *34,* 203-222 *(2008).*
21. *Magnusson, B.M., Walters, K.A., Roberts, M.S.:* Adv. Drug Deliver. Rev. *50,* 205-227 *(2001).*
22. *Wester, R.C., Noonan, P.K., Maibach, H.I.:* Arch. Dermatol. Res. *267,* 229-235 *(1980).*
23. *Reifenrath, W.G., Chellquist, E.M., Shipwash, E.A., Jederberg, W.W.:* Fundam. Appl. Toxicol. *4,* S224-S230 *(1984).*
24. *Nolan, L.M.A., Corish, J., Corrigan, O.I., Fitzpatrick, D.* Int. J. Pharm. *341,* 114-124 *(2007).*
25. *Netzlaff, F., Kaca, M., Bock, U., Haltner-Ukomadu, E., Meiers, P., Lehr, C.-M., Schaefer, U.F.:* Eur. J. Pharm. Biopharm. *66,* 127–134 *(2007).*
26. *Rai, V., Ghosh, I., Bose, S., Silva, S.M.C., Chandra, P., Michniak-Kohn, B.:* J. Drug Deliv. Sci. Tec. *20,* 75-87 *(2010).*
27. *Wagner, H., Kostka, K.-H., Lehr, C.-M., Schaefer, U.F.:* J. Control. Release *75,* 283-295 *(2001).*
28. *Siewert, M., Dressman, J., Brown, C.K., Shah, V.P.:* FIP/AAPS Guidelines to Dissolution/in Vitro Release Testing of Novel/Special Dosage Forms. AAPS Pharm. Sci. Tech. *4, 1-10 (2003).*
29. *Schroeder, I.Z., Franke, P., Schaefer, U.F., Lehr, C.-M.:* J. Control. Release *118,* 196-203 *(2007).*
30. *Vaddi, H.K., Ho, P.C., Chan, Y.W., Chan, S.Y.:* J. Control. Release *81,* 121-133 *(2002).*
31. *Bernard, G., Auger, M., Soucy, J., Pouliot, R.:* Biochim. Biophys. Acta *1770,* 1317–1323 *(2007)*
32. *Boncheva, M., Damien, F., Normand, V.:* Biochim. Biophys. Acta *1778,* 1344–1355 *(2008)*
33. *Dias, M., Naik, A., Guy, R.H., Hadgraft, J., Lane, M.E.:* Eur. J. Pharm. Biopharm. *69,* 1171–1175 *(2008)*
34. *Bommannan, D., Potts, R.O., Guy, R.H.:* J. Invest. Dermatol. 95, 403–408 (1990)
35. *Brancaleon, L., Bamberg, M.P., Sakamaki, T., Kollias, N.:* J. Invest. Dermatol. *116,* 380-386 *(2001)*
36. *Hahn, T., Hansen, S., Neumann, D., Kostka, K.-H., Lehr, C.-M., Muys, L., Schafer, U.F.:* Skin Pharmacol. Physiol. *23,*183–192 *(2010)*
37. *Thiele, J.J., Traber, M.G., Packer, L.:* J. Invest. Dermatol. *110,* 756–761 *(1998)*
38. *Gremlich, H.U., Yan, B.:* New York: Marcel Dekker *42, (2001)*
39. *Csizmazia, E., Erős, G., Berkesi, O., Berkó, Sz., Szabó-Révész, P., Csányi, E.:* J. Drug Deliv. Sci. Tec. *21,* 411-415 *(2011)*
40. *Csizmazia, E., Erős, G., Berkesi, O., Berkó, Sz., Szabó-Révész, P., Csányi, E.:* Pharm. Dev. Technol. *17,* 125-128 *(2012)*
41. *Bolzinger, M.A., Thevenin, Carduner, C., Poelman, M.C.:* Int. J. Pharm. *176,* 39-45 *(1998).*
42. *Ganem-Quintanar, A., Lafforgue, C., Falson-Rieg, F., Buri, P.:* Int. J. Pharm. *147,* 165-171 *(1997).*
43. *Godwin, D.A., Kim, N.-H., Felton, L.A.:* Eur. J. Pharm. Biopharm. *53,* 2327 *(2002).*

Érkezett: 2012. február 15.

III.

European Polymer Journal 49 (2013) 2511–2517

Contents lists available at SciVerse ScienceDirect

European Polymer Journal

journal homepage: www.elsevier.com/locate/europolj

Advantages of cross-linked versus linear hyaluronic acid for semisolid skin delivery systems

Szilvia Berkó [a,*], Mónika Maroda [b], Magdolna Bodnár [c], Gábor Erős [d], Petra Hartmann [e], Kinga Szentner [d], Piroska Szabó-Révész [a], Lajos Kemény [d], János Borbély [c], Erzsébet Csányi [a]

[a] Department of Pharmaceutical Technology, University of Szeged, Eötvös u. 6, 6720 Szeged, Hungary
[b] TEVA Pharmaceuticals Ltd., Pallagi u. 13, 4042 Debrecen, Hungary
[c] BBS Biochemicals LLC, Kiserdő u. 4, 4225 Debrecen, Hungary
[d] Department of Dermatology and Allergology, University of Szeged, Korányi fasor 6-8, 6720 Szeged, Hungary
[e] Institute of Surgical Research, University of Szeged, Pécsi u. 6, 6720 Szeged, Hungary

ARTICLE INFO

Article history:
Received 12 July 2012
Received in revised form 25 March 2013
Accepted 2 April 2013
Available online 15 April 2013

Keywords:
Cross-linking
Hyaluronic acid
Skin penetration
Skin hydration

ABSTRACT

Cross-linking of the hyaluronic acid (hyaluronan, HA) molecule may be a possible chemical modification via which to improve the problem of the penetration of HA. The successful preparation and characterization of stable nanoparticulate systems based on HA were described and discussed previously. The purpose of the present study is to compare hydrogels based on linear or cross-linked HA as potential semisolid drug delivery forms from the aspects of deep HA penetration through the skin. The rheological properties, hydration, irritation effect, *in vitro* and *in vivo* skin penetration were studied. The hydration effect was kept and the rheological parameters were slightly changed after the cross-linking procedure. Diffusion and penetration studies demonstrated that the formation of smaller particles of HA by means of cross-linking resulted in better diffusion through a synthetic membrane and better penetration through the human epidermis and living animal skin as compared with linear HA, which did not penetrate.

1. Introduction

Hyaluronic acid (HA) also known as hyaluronan and sometimes presented as a hyaluronate (poly)anion from a chemical/structural aspects, is a non-sulfated glycosaminoglycan. In aqueous solution at physiological pH, HA exists as negatively charged hyaluronate macromolecules with an extended conformation. In a polyanionic form, the functional groups of HA make the biopolymer so hydrophilic that its binds 1000 times more water than might be predicted from its molar mass. HA is present in almost all biological fluids and tissues of the vertebrates, the highest amount being found in the extracellular matrix of the soft connective tissue. The skin contains slightly more than 50% of the total HA content present within the human body [1]. After the age of 20 years, the amount of HA continuously decreases.

Thanks to its versatile properties, such as its biocompatibility, non-immunogenicity, biodegradability and viscoelasticity, HA is an ideal biomaterial for cosmetic, medical and pharmaceutical applications. It is widely utilized for the treatment of osteoarthritis, vesico-urethral reflux and urinary incontinence. HA is incorporated in many moisturizing creams and wound-healing dressings, and it is also applied in ophthalmology [2–6]. However, with the exception of the vitreous body, where its half-life is 20–70 days, the turnover of HA in most tissues in the body is surprisingly rapid. The typical half-life in the human skin is 2–5 days, in the joints and pleura it is 0.5–1 day, and in the anterior chamber of the eye it is merely 1–2 h [1]. A novel approach is the use of HA-based nanoparticles as an effective carrier in transdermal drug delivery [7–11]. In view of the problem of the enzymatic degradation of HA, a number of research studies

* Corresponding author. Tel.: +36 62 545573; fax: +36 62 545571.
E-mail address: berko@pharm.u-szeged.hu (S. Berkó).

0014-3057/$ - see front matter © 2013 Elsevier Ltd. All rights reserved.
http://dx.doi.org/10.1016/j.eurpolymj.2013.04.001

have been made with the aim of elongating the presence of HA in the body [12]. Another problem in the application of HA is the administration route. In most cases, HA is injected, which is a painful application procedure and sometimes causes inflammatory complications and bacterial infections. HA exhibits good gelling properties and leads to a hydration effect in the uppermost layer of the stratum corneum following dermal application, which in most cases promotes penetration of the drug. The water may cause the compact structure of the horny layer to swell and open up, leading to an increase in the extent of penetration. However, the penetration of HA into the deeper layers of the skin is very slow or may be inhibited, depending on the molecular weight of the HA [13].

Cross-linking of the HA molecule may be a possible mode of chemical modification with the aims of preventing the degradation and improving the penetration of HA [12]. Various methods have been developed for the production of cross-linked HA systems for potential use in hydrogels [9,14,15], films [16,17] or particulate systems [10,18,19]. Several attempts have also been made to produce cross-linked HA particles through a carbodiimide technique in aqueous media [20–22]. This procedure has the advantage that stable colloid systems may be obtained in water without the use of any surfactant or other solvent.

We earlier [23,24] described and discussed the successful preparation and characterization of stable nanoparticulate systems based on HA. Covalent cross-linking through the carboxyl functional groups of HA was carried out with a diamine via a carbodiimide technique in aqueous media at room temperature. The effects of the molecular weight of HA, the cross-linking ratio and the environmental conditions were investigated. It was established that cross-linked HA particulate systems could be prepared which can form stable colloid systems in aqueous media.

In the present work, a stable cross-linked HA-based nanoparticulate semisolid preparation was investigated in comparison with a hydrogel containing linear HA. The rheological properties, hydration, irritation effect, *in vitro* and *in vivo* skin penetration abilities were studied.

2. Experimental part

2.1. Materials

The sodium salt of HA (M_W = 4350 kDa) was obtained from Gedeon Richter Ltd., Hungary. Its quality met the European Pharmacopoeia (Ph. Eur. 6) requirements. For the cross-linking reaction, 2,2-(ethylenedioxy)bis(ethylamine) and 1-[3-(dimethylamino)propyl]-3-ethylcarbodiimide methiodide (CDI) were purchased from Sigma–Aldrich, Co. Transcutol® and Labrasol® were from S & D Chemicals Ltd., Hungary, and glycerol 85% was from Molar Chemicals Kft, Hungary. All other chemicals were of analytical grade.

2.2. Preparation of cross-linked HA nanoparticles

Cross-linked HA nanoparticles were prepared according to the procedure described earlier [23,24]. Briefly, the sodium salt of HA was dissolved in water to produce a clear solution with a concentration of 1 mg/ml. The pH of the solution was adjusted to 5.5. The diamine solution (1.0 v/v% in water, pH = 5.5) was added to the HA solution and mixed for 30 min at room temperature. A CDI solution was next added dropwise, and the reaction mixture was stirred at room temperature for 24 h. The aqueous system containing cross-linked HA nanoparticles was subsequently purified by dialysis for 7 days against distilled water and freeze-dried. The cross-linking ratio was 25%.

2.3. Semisolid gel formulation

Glycerol 85%, and purified water as solvents, with Transcutol® and Labrasol® as penetration enhancers comprised the hydrophilic base of the gel. 1% of either the cross-linked or the linear HA was dispersed into this base. The gels were stirred at intervals until complete dissolution was attained.

2.4. Rheological measurements

Rheological measurements were carried out with a Physica MCR101 rheometer (Anton Paar, Austria). A cone-plate measuring device was used in which the cone angle was 1°, and the thickness of the sample in the middle of the cone was 0.046 mm. Flow curves of the different samples were also determined. The shear rate was increased from 0.1 to 100 1/s (up-curve), and then decreased from 100 to 0.1 1/s (down-curve) in the CR mode. The shearing time in both segments was 300 s. Oscillation measurements were used to analyze both storage modulus (G') and loss modulus (G'') for frequencies between 0.01 and 100 Hz in the linear viscoelastic region. The measurements were performed at 32 °C.

2.5. Hydration and irritation tests

The Corneometer® CM 825 (Courage and Khazaka Electronic GmbH, Cologne, Germany) is the instrument commonly used worldwide to determine the level of hydration of the skin surface, mainly the stratum corneum [25,26]. The investigation is based on measurement of the capacitance of a dielectric medium. The Tewameter® TM 300 (Courage and Khazaka Electronic GmbH, Cologne, Germany) is the most generally accepted measuring device for the assessment of transepidermal water loss (TEWL). This is the most important parameter for evaluation of the barrier function of the stratum corneum. High TEWL values indicate a greater of water loss and are consistent with increased damage to the barrier function of the stratum corneum, such as may occur during irritant exposure. The probe indirectly measures the density gradient of water evaporation from the skin via the two pairs of sensors inside the hollow cylinder [27,28].

Six hairless mice strain (SKH-1) without any dermatological disease or allergy were used in the experiment. All interventions were in full accordance with the NIH guidelines relating to experimentation with animals. The procedures and protocols of all animal experiments in the present study were approved in advance by the Ethical Committee for the Protection of Animals in Scientific Re-

search at the University of Szeged. Promote the attainment of standard circumstances, all the skin tests were performed after the adaptation of the animals to room conditions (30 min at 23–25 °C and 40–50% RH). During the experiment, test samples were applied to the skin of the dorsal region in all animals. The measured values were compared with those on the non-treated skin. The changes in moisturizing and TEWL levels were expressed as percentages.

2.6. In vitro HA diffusion and skin penetration measurements

Membrane diffusion and permeability studies were performed with a vertical Franz diffusion cell system (Hanson Microette TM Topical and Transdermal Diffusion Cell System, Hanson Research Corporation, Chatsworth, CA, USA). 0.30 g of sample was placed as a donor phase on a Porafil membrane filter (cellulose acetate; pore diameter 0.45 μm) or on human epidermis supported on Porafil membrane filter. The effective diffusion surface area was 1.767 cm^2. Phosphate buffer solution (PBS; pH = 7.4) was used as an acceptor phase to ensure sink conditions. The rotation of the magnetic stirbar was set to 450 rpm. Experiments were performed at 37 ± 0.5 °C for 24 h in the case of the synthetic membrane, for 48 h with the human epidermis. Samples of 0.8 ml were taken from the acceptor phase by the autosampler (Hanson Microette Autosampling System, Hanson Research Corporation, Chatsworth, CA, USA) and replaced with fresh receiving medium. The quantitative measurements of linear and cross-linked HA were carried out by means of gel permeation chromatography (GPC).

2.7. Preparation of human epidermis by a heat-separated technique

Excised human skin from Caucasian female patients who had undergone abdominal plastic surgery was used. This was approved by the Ethical Committee of the University of Szeged, Albert Szent-Györgyi Clinical Centre (Human Investigation Review Board). Immediately after excision, the subcutaneous fatty tissue was removed and the skin was stored frozen at −20 °C. For the permeation study, the skin was thawed, and the epidermis was separated from the underlying dermis through use of a heat separation technique based on a procedure reported by Kligman and Christophers [29]. Individual portions were immersed in water at 60 °C for 90 s. Following removal of skin from the water, it was placed stratum corneum side up on a filter paper, and the epidermis (comprising the stratum corneum and viable epidermis) was gently removed from the underlying dermis with the use of forceps. The dermis was discarded and the epidermal membrane was floated on the surface of PBS (pH = 7.4) for at least 20 min, after which it and it was placed on a supporting Porafil membrane.

2.8. In vivo animal study

The modified skinfold chamber model that we developed unites the advantages of *in vitro* and *in vivo* methods, i.e. the possibility of frequent sample-taking in order to describe the penetration kinetics of the drug and the use of intact, living skin [30]. Moreover, the detection of local side-effects, skin irritation or other types of alteration in the skin is possible. The experiments were performed on 15-week-old male hairless mice of strain SKH-1. The full skin was removed from one side of the skinfold. Another side of the skinfold the skin comprised complete epidermis dermis and skin muscle. The gel (0.1 g) was applied to the intact site, and the stainless steel cylinder with 1 ml of acceptor phase (PBS, pH = 7.4) was fixed into the wounded site of the skinfold. The effective diffusion surface area was 1.539 cm^2. The drug had to penetrate through the complete living skin to reach the acceptor phase, where the presence of the drug was detected. Experiments were performed for 6 h. The total acceptor phase was changed every hour. HA was determined by GPC.

2.9. GPC method

The GPC analysis of linear HA and cross-linked HA particles was performed on a Waters HPLC system with an Ultrahydrogel-Linear column. The eluent was monitored at 220 nm. The mobile phase was a mixture of 140 mM

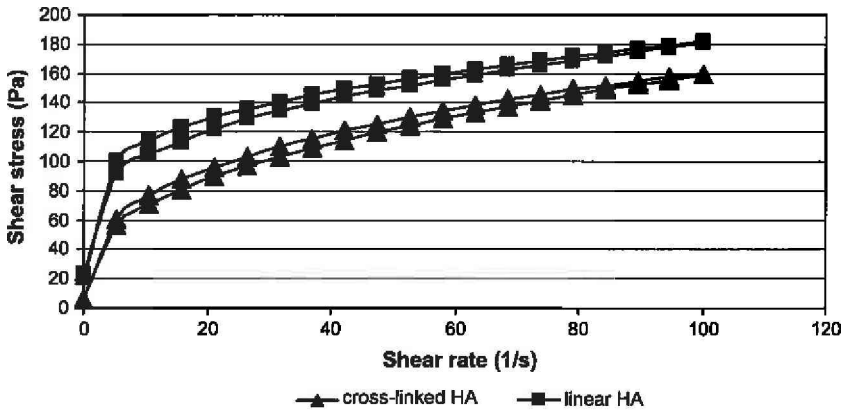

Fig. 1. Flow curves of semisolid preparations containing linear or cross-linked HA.

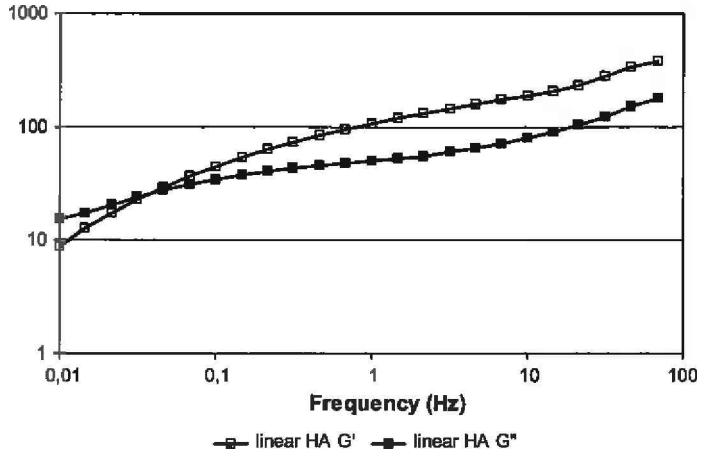

Fig. 2. The storage modulus (G') and the loss modulus (G'') of linear HA.

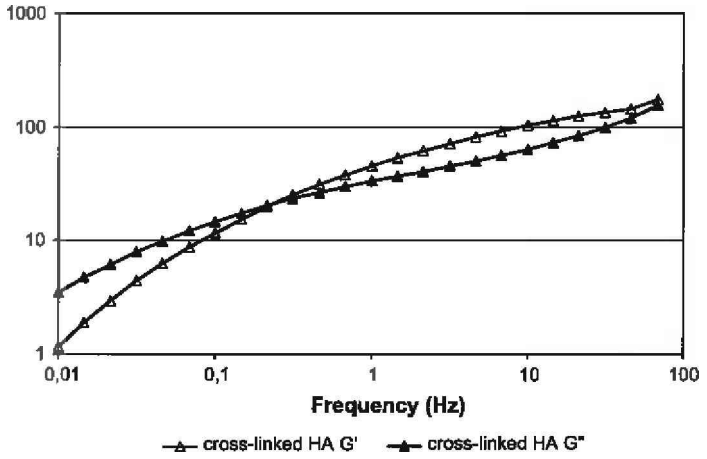

Fig. 3. The storage modulus (G') and the loss modulus (G'') of cross-linked HA.

NaCl, 7.5 mM Na_2HPO_4, 2 mM NaH_2PO_4 and 2.7 mM KCl, pH 7.4 (PBS); the flow rate was 1 ml/min. The analysis time was 20 min/sample. Samples were dissolved in PBS, and filtered through a 5 μm pre-column sieve.

2.10. Statistical analysis

The results were evaluated and analyzed statistically with Student's *t*-test. The data are the averages of the results of six parallel experiments ± SD ($p < 0.05^*$).

3. Results and discussion

3.1. Results of rheological measurements

Rheological characteristics are important properties of colloid systems, related to the nature and extent of the intermolecular interactions and the entanglements of the polymer chains. The produced cross-linked nanoparticles

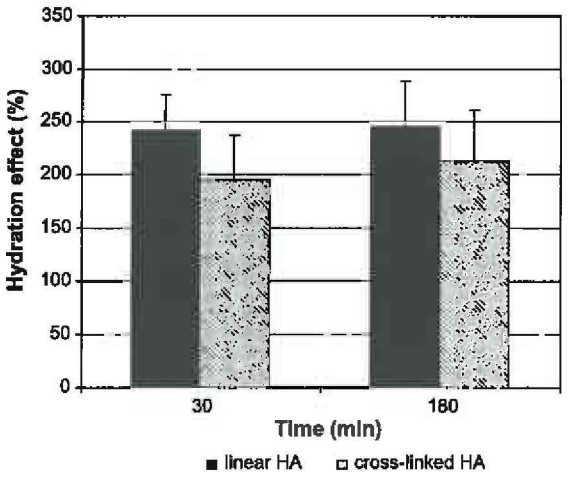

Fig. 4. Hydration effects of linear and cross-linked HA.

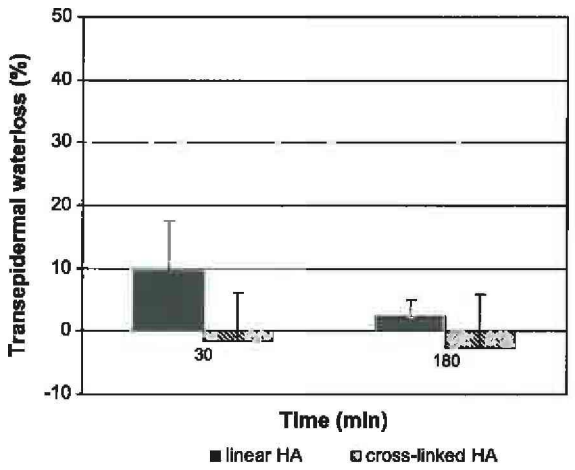

Fig. 5. Transepidermal water loss of linear and cross-linked HA.

have lower viscosity than the parent linear biopolymer because of the contraction of linear chains in connection with intrachain cross-linking and the absence of entanglement coupling [23]. Fig. 1 shows the flow curves of cross-linked and linear HA. Both the gel exhibited slight thixotropy. The shear stress of the cross-linked HA was a little lower than that of the linear HA, which confirmed the successful cross-linking and the formation of smaller particles.

The elastoviscous nature of linear HA has been studied quite extensively. At lower frequencies the HA gel behaves as a viscous solution, at higher frequencies it behaves elastically [31,32]. These properties are shown by the changes of the elastic storage modulus (G'), and the viscous loss modulus (G''), as a function of frequency (Fig. 2). The transition from viscous to elastic behavior is marked by the crossover point of the two curves. This specific elastoviscous property appears in cross-linked HA curves, too (Fig. 3). However, it requires higher frequency to rich the crossover point, which results in the elastic property of the preparation containing cross-linked HA. The elasticity (G' values) of the gel is decreased, thanks to the modification of the molecule.

3.2. Results of hydration and irritation tests

Corneometry determines the water content of the skin surface, and mainly the stratum corneum. It was found that there were no differences in the hydration effects of the cross-linked HA and linear HA. Linear HA is known to hydrate the skin surface; after the chemical modification, the cross-linked HA retained the hydration effect (Fig. 4). In this study the cross-linking ratio was 25%, which did not influence the hydration effect significantly. TEWL proved to be decreased after the application of the cross-linked HA gel, which means that it undergoes longer hydration with no irritation effect on the skin (Fig. 5).

3.3. In vitro diffusion, penetration and in vivo studies

Fig. 6 depicts the rate of accumulation per unit area of linear and cross-linked HA that diffused through the synthetic membrane. It is clear that the diffusion of the cross-linked HA was more intensive, at 1028 μg/cm^2. After 10 h a steady state was seen. The linear HA also diffused through the synthetic membrane, but more slowly, and the amount diffused was significantly less, at 739 μg/cm^2. The better diffusion of the cross-linked HA may be explained by the lower viscosity and the smaller particle size caused by the cross-linking [23]. The penetration through the human epidermis is illustrated in Fig. 7. There was no detectable penetration of linear HA during the observation period, whereas the level of penetration of cross-linked HA was 200 μg/cm^2. Fig. 8 demonstrates the penetration of the cross-linked and linear HA as a function of time through living animal skin. Similarly as in the *in vitro* human epidermis study, there was no detectable penetration of linear HA. The quantity of cross-linked HA that penetrated displayed a considerable elevation during the observation period increased steadily, to about 26 μg/cm^2 by the end of the experiment.

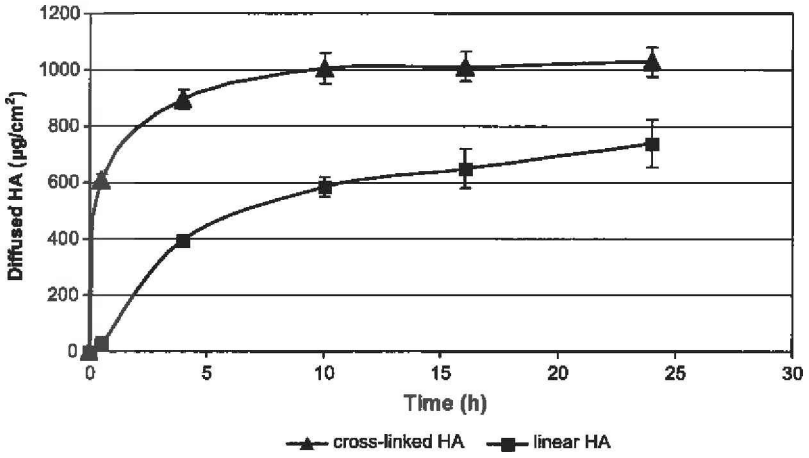

Fig. 6. Cumulative amount of HA that diffused through a synthetic membrane.

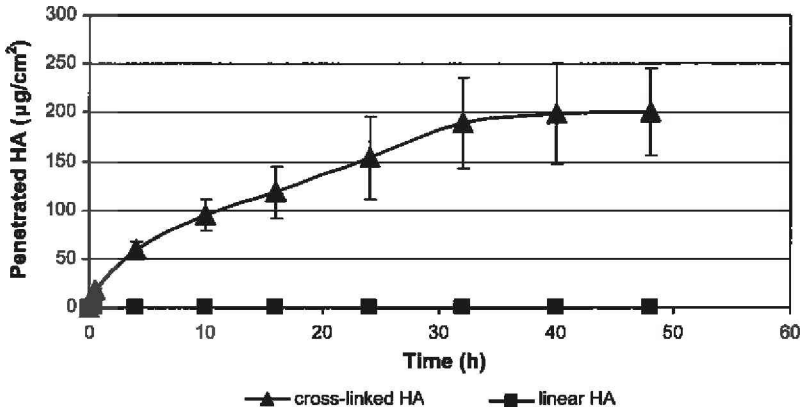

Fig. 7. Cumulative amount of HA that penetrated through the human epidermis.

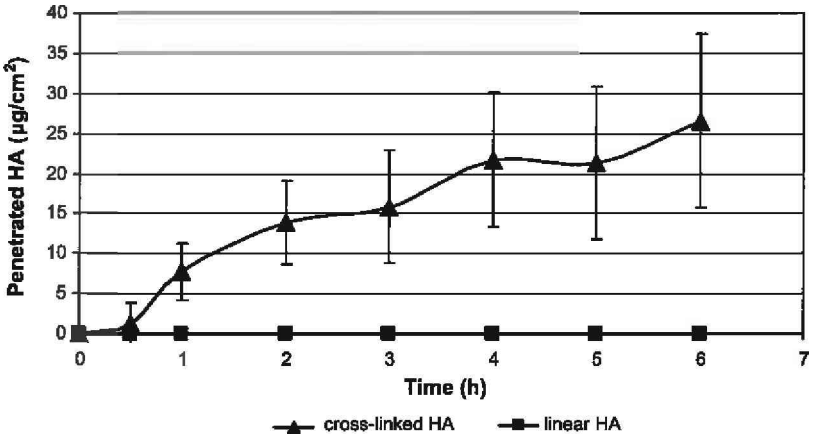

Fig. 8. Cumulative amount of HA that penetrated through living animal skin.

Table 1
Penetration parameters of cross-linked HA. The data are the means (±SD) of six parallel measurements.

	Cumulative amount (%)	Q (ug/cm²)	J (ug/cm²/h)	$K_p \times 10^{-3}$ (cm/h)	T_{lag} (h)
Human epidermis	11.0 ± 7.34	200 ± 118	31.528	3.1528	0.12
Animal model	4.08 ± 3.7	26.55 ± 24	13.489	1.3489	0.49

3.4. Analysis of penetration

Penetration parameters (Table 1) were obtained from plots of the cumulative amount of HA penetrated per cm^2 (Q) versus time. The steady state flux (J) reflecting the absorption rate per unit area, and the lag time (T_{lag}) (symbolizing the duration of the delay between the first contact of the drug with the skin surface and the attainment of a steady state flux) were obtained from the slope and x intercept of the linear regression versus $t^{1/2}$, respectively. The permeability coefficient (K_p) was calculated according to Fick's first law of diffusion, based on the steady state flux and the applied drug concentration (C_d) of the donor phase [33]:

$$K_p = J/C_d \quad (1)$$

The absorption rate and permeability coefficient were about three times higher in the case of the human epidermis. The lower absorption rate and permeability coefficient and the longer lag time can be explained by the fact that the cross-linked HA has to cross the epidermis dermis and skin muscle to reach the acceptor phase, the penetration route therefore being much longer in the case of the animal model.

4. Conclusions

This experimental work has revealed the advantages of cross-linked HA versus linear HA in dermal applications. The cross-linking of the linear HA molecule changes its rheological parameters. The shear stress decreases in re-

sponse to cross-linking. The dynamic rheological measurements proved that the specific elastoviscous property of HA gel was slightly changed after the cross-linking procedure. The corneometry tests showed that the hydration effect was preserved. There was no irritant effect of the cross-linked molecule in TEWL tests. The diffusion and penetration study demonstrated that the cross-linking of HA resulted in better diffusion through a synthetic membrane and penetration through the human epidermis and living animal skin than when linear HA was used, when penetration was no observed. The cross-linking of HA makes it suitable for transdermal applications, promoting to make hydration in deeper layers of the skin and giving the possibility of a signal effect for HA production. The cross-linked HA can lead to the development of drug carrier system for the deep penetration of the skin.

Acknowledgements

The authors are grateful to József Bakó for GPC measurement, and to S & D Chemicals Ltd., Hungary for providing samples Transcutol® and Labrasol®.

The study was supported by the NKTH—A*STAR (Hungarian-Singaporean) Bilateral S & T International Cooperation (BIOSPONA) and TÁMOP 4.2.1/B-09/1/KONV-2010-0005.

References

[1] Schiller J, Volpi N, Hrabárová E, Soltés L. Hyaluronic acid: a natural biopolymer. In: Kalia S, Avérous L, editors. Biopolymers: biomedical and environmental applications. Hoboken (NJ, USA): John Wiley & Sons, Inc.; 2011. p. 3–34.
[2] Girish KS, Kemparaju K. The magic glue hyaluronan and its eraser hyaluronidase. A biological overview. Life Sci 2007;80:1921–43.
[3] Anilkumar TV, Jaseer M, Anumol J, Arun J, Mohanan PV, Krishnan LK. Advantage of hyaluronic acid as a component of fibrin sheet for care of acute wound. Biologicals 2011;39:81–8.
[4] Robert L, Robert AM, Renard G. Biological effect of hyaluronan in connective tissues, eye, skin, venous wall. Role in aging. Pathol Biol 2010;58:187–98.
[5] Romagnoli M, Belmontesi M. Hyaluronic acid-based fillers: theory and practice. Clin Dermatol 2008;26:123–59.
[6] Price RD, Berry MG, Navsaria HA. Hyaluronic acid: the scientific and clinical evidence. J Plast Reconstr Aesthet Surg 2007;60:1110–9.
[7] Kong M, Chen XG, Kweon DK, Park HJ. Investigation on skin permeation of hyaluronic acid based nanoemulsions as transdermal carrier. Carbohydr Polym 2011;86:837–43.
[8] Brown MB, Hanpanitcharoen M, Martin GP. An in vitro investigation into the effect of glycosaminoglycans on the skin partitioning and deposition of NSAIDs. Int J Pharm 2001;225:113–21.
[9] Masters KS, Shah DN, Leinwand LA, Anseth KS. Crosslinked hyaluronan scaffolds as a biologically active carrier for valvular interstitial cells. Biomaterials 2005;26:2517–25.
[10] Lim HJ, Cho EC, Lee JA, Kim J. A novel approach for the use of hyaluronic acid-based hydrogel nanoparticles as effective carriers for transdermal delivery systems. Colloids Surf A: Physicochem Eng Aspects 2012:1. http://dx.doi.org/10.1016/j.colsurfa.2012.03.02.
[11] Ilgin P, Avci G, Silan C, Ekici S, Aktas N, Ayyala RS, et al. Colloidal drug carriers from (sub)micron hyaluronic acid hydrogel particles with tunable properties for biomedical applications. Carbohydr Polym 2010;82:997–1003.
[12] Schanté CE, Zuber G, Herlin C, Vandamme TF. Chemical modifications of hyaluronic acid for synthesis of derivatives for broad range of biomedical applications. Carbohydr Polym 2011;85:469–89.
[13] Alkrad JA, Mrestani Y, Neubert RHH. The release profiles of intact and enzymatically digested hyaluronic acid from semisolid formulations using multi-layer membrane system. Eur J Pharm Biopharm 2003;56:37–41.
[14] Kim IL, Mauck RL, Burdick JA. Hydrogel design for cartilage tissue engineering: a case study with hyaluronic acid. Biomaterials 2011;32:8771–82.
[15] Pitarresi G, Palumbo FS, Tripodo G, Cavallaro G, Giammona G. Preparation and characterization of new hydrogel based on hyaluronic acid and, β-polyaspartylhydrazide. Eur Polym J 2007;43:3953–62.
[16] Liu Y, Shu XZ, Prestwich GD. Biocompatibility and stability of disulfide crosslinked hyaluronan films. Biomaterials 2005;26:4737–46.
[17] Yamanlar S, Sant S, Boudou T, Picart C, Khademhosseini A. Surface functionalization of hyaluronic acid hydrogels by polyelectrolyte multilayer films. Biomaterials 2011;32:5590–9.
[18] Dulong V, Lack S, Le Cerf D, Picton L, Vannier JP, Muller G. Hyaluronan-based hydrogels particles prepared by crosslinking with trisodium trimetaphosphate. Synthesis and characterization. Carbohydr Polym 2004;57:1–6.
[19] Pitarresi G, Craparo EF, Palumbo FS, Carlisi B, Giammona G. Composite nanoparticles based on hyaluronic acid chemically cross-linked with α, β-polyaspartylhydrazide. Biomacromolecules 2007;8:1890–8.
[20] Choi KY, Lee S, Park K, Kim K, Parka JH, Kwon IC, et al. Preparation and characterization of hyaluronic acid-based hydrogel nanoparticles. J Phys Chem Solid 2008;69:1591–5.
[21] Yeo Y, Highley CB, Bellas E, Ito T, Marini R, Langer R, et al. In situ cross-linkable hyaluronic acid hydrogels prevent post-operative abdominal adhesions in a rabbit model. Biomaterials 2006;27:4698–705.
[22] Oh EJ, Park K, Kim KS, Kim J, Yang JA, Kong JH, et al. Target specific and longacting delivery of protein, peptide, and nucleotide therapeutics using hyaluronic acid derivatives. J Controlled Release 2010;141(1):2–12.
[23] Bodnár M, Daróczi L, Batta Gy, Bakó J, Hartmann JF, Borbély J. Preparation and characterization of cross-linked hyaluronan nanoparticles. Colloid Polym Sci 2009;287:991–1000.
[24] Maroda M, Bodnár M, Berkó Sz, Bakó J, Erős G, Csányi E, et al. Preparation and investigation of a cross-linked hyaluronan nanoparticles system. Carbohydr Polym 2011;83:1322–9.
[25] Gönüllü Ü, Yener G, Üner M, Incegül T. Moisturizing potentials of ascorbyl palmitate and calcium ascorbate in various topical formulations. Int J Cosmetic Sci 2004;26:31–6.
[26] Yilmaz E, Borchert HH. Effect of lipid-containing, positively charged nanoemulsions on skin hydration, elasticity and erythema—an in vivo study. Int J Pharm 2006;307:232–8.
[27] Gloor M, Senger B, Langenauer M, Fluhr JW. On the course of the irritant reaction after irritation with sodium lauryl sulphate. Skin Res Techn 2004;10:144–8.
[28] Jensen JM, Schütze S, Neumann C, Proksch EJ. Impaired cutaneous permeability barrier function, skin hydration, and sphingomyelinase activity in keratin 10 deficient mice. J Invest Dermatol 2000;115:708–13.
[29] Kligman AE, Christophers E. Preparation of isolated sheets of human stratum corneum. Arch Dermatol 1963;88:702–5.
[30] Erős G, Hartmann P, Berkó Sz, Csizmazia E, Csányi E, Sztojkov-Ivanov A, et al. A novel murine model for the in vivo study of transdermal drug penetration. Sci World J 2012. 9p, [Article ID 543536].
[31] Cowman MK, Matsuoka S. Experimental approaches to hyaluronan structure. Carbohydr Res 2005;340:791–809.
[32] Balazs EA. The physical properties of synovial fluid and the special role of hyaluronic acid. In: Helfet A, editor. Disorders of the knee. Philadelphia: T. B. Lippincott Company; 1974. p. 63–75.
[33] Wagner H, Kostka KH, Lehr CM, Schaefer UF. Interrelation of permeation and penetration parameters obtained from *in vitro* experiments with human skin and skin equivalents. J Control Release 2001;75:283–95.